UNIVERSIDADE FEDERAL DE SANTA MARIA
CENTRO DE CIÊNCIAS DA SAÚDE
PROGRAMA DE PÓS-GRADUAÇÃO EM CIÊNCIAS ODONTOLÓGICAS

Ana Carolina Cadore Rodrigues

COMPORTAMENTO MECÂNICO SOB FADIGA DE ZIRCÔNIA POLICRISTALINA: EFEITO DO DESGASTE POR BROCAS PARA USINAGEM EM CAD/CAM E TRATAMENTOS DE SUPERFÍCIE

Santa Maria, RS
2022

Ana Carolina Cadore Rodrigues

COMPORTAMENTO MECÂNICO SOB FADIGA DE ZIRCÔNIA POLICRISTALINA: EFEITO DO DESGASTE POR BROCAS PARA USINAGEM EM CAD/CAM E TRATAMENTOS DE SUPERFÍCIE

Tese apresentada ao Curso de Doutorado do Programa de Pós-Graduação em Ciências Odontológicas, da Universidade Federal de Santa Maria (UFSM, RS), como requisito parcial para a obtenção do título de **Doutor em Ciências Odontológicas.**

Orientador: Prof. Dr. Luiz Felipe Valandro
Coorientador: Prof. Dr. Cornelis Johannes Kleverlaan

Santa Maria, RS
2022

Ana Carolina Cadore Rodrigues

COMPORTAMENTO MECÂNICO SOB FADIGA DE ZIRCÔNIA POLICRISTALINA: EFEITO DO DESGASTE POR BROCAS PARA USINAGEM EM CAD/CAM E TRATAMENTOS DE SUPERFÍCIE

Tese apresentada ao Curso de Doutorado do Programa de Pós-Graduação em Ciências Odontológicas, da Universidade Federal de Santa Maria (UFSM, RS), como requisito parcial para a obtenção do título de **Doutor em Ciências Odontológicas**.

Aprovada em 16 de setembro de 2022

____

Luiz Felipe Valandro, Dr. (UFSM)
(Presidente/Orientador)

____

Cornelis Johannes Kleverlaan, Dr. (ACTA)
(Coorientador)

____

Amanda Maria de Oliveira Dal Piva, Dra. (ACTA)

____

Camila da Silva Rodrigues, Dra. (UNESP)

____

Catina Prochnow, Dra. (HPG)

____

Sara Fraga, Dra. (UFRGS)

Santa Maria, RS
2022

Dedico à Deus, à minha família e ao meu amor Rodrigo

AGRADECIMENTOS

A **Deus**, por guiar meus passos e iluminar o meu caminho. Obrigada pela minha vida, pela minha família e pelas pessoas maravilhosas que colocastes em meu caminho.

Aos meus pais, **Maristela Cadore Rodrigues** e **Paulo Cesar Rodrigues**, todo o meu amor e minha gratidão. Vocês são meus exemplos de caráter e dedicação. Obrigada por todo amor e carinho. Obrigada por terem me dado a vida e nunca medirem esforços em me ajudar. Obrigada por toda a dedicação, por me incentivarem a sempre melhorar, por todo apoio e suporte. Por serem meu porto seguro e por estarem sempre ao meu lado me ajudando a vencer. Agradeço a Deus por ter feito de vocês meus pais. Amo muito vocês.

Ao meu amor, **Rodrigo da Cunha Rossignollo Tavares**. Obrigada por todo amor e dedicação. Por ser a pessoa que és, amorosa, dedicada, companheira e por estar ao meu lado em todos os momentos. Obrigada por sempre me incentivar a melhorar e acreditar em mim mesma. Por todo o apoio e suporte de sempre. Obrigada também por me ajudar a vencer os meus medos e a realizar os meus sonhos. Agradeço todos os dias por ter você em minha vida. Te amo.

Aos meus irmãos, **Ana Paula Cadore Rodrigues** e **Gabriel Cadore Rodrigues**, meus melhores amigos. Obrigada por todo o amor e companheirismo de vocês. Obrigada por sempre estarem ao meu lado e por me ajudarem sempre que preciso. Por acreditarem em mim, por terem me dado forças para superar os meus medos e saber que jamais estarei sozinha. Vocês são essenciais em minha vida, amo vocês.

À **Mia**, minha irmã felina. Obrigada por todo amor que você nos dedica. Amo você.

Aos meus avós, **Sady Rodrigues**, **Joanita Moscatelli Rodrigues**, **Luiz João Cadore** e **Rosalina Marin Cadore**. Obrigada por todo amor, carinho e dedicação. Agradeço a Deus por ter tido a oportunidade de conviver com vocês que são grandes exemplos em minha vida. Aos meus avós, **Joanita**, **Luiz** e **Rosalina**, a saudade é eterna e os amarei para sempre. *"Nenhuma árvore alcança os céus sem a força de suas raízes (Bert Hellinger)"*

Aos meus **familiares**, **tios(as)** e **primos(as)**, e a **família do meu namorado**, muito obrigada por toda torcida e apoio.

Ao meu orientador, **Luiz Felipe Valandro**. És um exemplo de pessoa pela qual me espelho por seus valores pessoais e pela sua dedicação profissional. Muito obrigada por todas as oportunidades que me foram dadas, por estar sempre disposto em me ajudar e por todos os ensinamentos transmitidos ao longo desses anos. *"Habilidade e personalidade podem abrir portas, mas é o caráter que as mantém abertas (Frank Sherman Land)"*

To Professor **Cornelis Johannes Kleverlaan**. Thank you for the opportunity and for opening doors for me. Thank you so much for all the help and learning. I loved meeting and working with you.

Ao Professor **Gabriel Kalil Rocha Pereira**. Muito obrigada por estar sempre disposto e não medir esforços em me ajudar. Por toda a tua dedicação e empenho em transmitir teus ensinamentos. Muito obrigada também por todo apoio e incentivo. Tu és um exemplo de pessoa e profissional íntegro e tens toda minha admiração.

À Professora **Marília Pivetta Rippe**, todo meu carinho, respeito e admiração. Obrigada por me ajudar sempre que precisei. Tu és com certeza uma das pessoas responsáveis por eu ter escolhido a área de Prótese dentária. Muito obrigada por ter me ajudado desde o início e me incentivado a seguir esse caminho. Obrigada pela amizade, pelo carinho, por ser essa pessoa dedicada, integrada e possuidora de um coração imenso.

Aos amigos do **Grupo de Pesquisa em Prótese Dentária** e **demais amigos da Pós-Graduação**. Muito obrigada pelos momentos de convívio, troca de conhecimentos e amizade.

Ao **Pablo Soares Machado**. Obrigada pela amizade que vem desde a graduação, mas que principalmente se consolidou na Pós-Graduação. Obrigada pelos momentos de convívio e descontração. Por compartilhar diversos momentos de dúvidas, mas também de conquistas. Obrigada também por todo apoio e por toda a ajuda nos momentos que precisei.

Ao **Renan Vaz Machry**. Obrigada pela amizade, pelo companheirismo e convívio. Por compartilhar diversos momentos desde as disciplinas, trabalhos e momentos de descontração. Muito obrigada também por toda a ajuda de sempre, mas principalmente durante o período sanduíche, foi muito importante para mim.

Aos amigos **Jessica Klöckner Knorst**, **Renan Vaz Machry** e **Kiara Serafini Dapieve**. Obrigada por todo apoio e suporte nos momentos que precisei e claro pelos momentos inesquecíveis que compartilhamos. O meu período em Amsterdã foi mais feliz com vocês.

Aos amigos, **Ana Paula Pereira Reiniger**, **Gustavo Figueira Andrade** e **Fernando Ceolin Ferigollo**. Obrigada pela amizade, companheirismo e apoio em todos os momentos. Agradeço por tê-los como amigos. "Quem caminha sozinho pode até chegar mais rápido, mas aquele que vai acompanhado, com certeza vai mais longe (Clarice Lispector)"

Aos amigos, **Ana Clara Cassanti**, **Paulo Cezar Rocha**, **Lucas Bonaldi**, **Amanda Dal Piva** e **João Paulo Tribst**. Muito obrigada pela amizade e companheirismo. Sou muito grata por ter conhecido e convivido com vocês durante o meu período em Amsterdã. Obrigada por todo apoio e suporte, mas principalmente pelos momentos que compartilhamos.

À dona **Vanir**, **Márcio** e **Colomby**. Muito obrigada pela amizade e por todo apoio e suporte de sempre.

Aos professores da comissão examinadora: **Amanda Dal Piva**, **Camila Rodrigues**, **Catina Prochnow**, **Sara Fraga**, **Liliana May** e **Atais Bacchi**. Obrigada pela disponibilidade em contribuir para o aprimoramento dessa tese.

À **Universidade Federal de Santa Maria (UFSM)** e ao **Programa de Pós-Graduação em Ciências Odontológicas (PPGCO)**, pelo ensino de qualidade e todas as oportunidades de qualificação pessoal. Sou grata e tenho orgulho de ter realizado toda minha formação profissional nessa instituição.

Aos **Professores do PPGCO**, por contribuírem com a minha formação acadêmica e pessoal.

À **CAPES** (Coordenação de Aperfeiçoamento de Pessoal de Nível Superior), pelo auxílio em minha formação profissional com a concessão de bolsa de estudos durante o meu período de Pós-Graduação, incluindo período sanduíche.

“Na vida, não vale tanto o que temos, nem tanto importa o que somos. Vale o que realizamos com aquilo que possuímos e, acima de tudo importa o que fazemos de nós”

Francisco Cândido Xavier

RESUMO

COMPORTAMENTO MECÂNICO SOB FADIGA DE ZIRCÔNIA POLICRISTALINA: EFEITO DO DESGASTE POR BROCAS PARA USINAGEM EM CAD/CAM E TRATAMENTOS DE SUPERFÍCIE

AUTORA: Ana Carolina Cadore Rodrigues
ORIENTADOR: Luiz Felipe Valandro
COORIENTADOR: Cornelis Johannes Kleverlaan

Três estudos compõe o presente trabalho. O primeiro avaliou o efeito de diferentes tratamentos de superfície interna no desempenho em fadiga (flexão biaxial) e características superficiais (topografia e rugosidade) de uma cerâmica de zircônia parcialmente estabilizada com 5 mol% de ítria (5YSZ). Para tal, discos cerâmicos (ISO 6872-2015) foram alocados considerando: Ctrl: sem tratamento; GLZ: glaze de baixa fusão; SNF: deposição de nanofilmes de sílica (5nm); AlOx: jateamento com óxido de alumínio; SiC: jateamento com AlOx revestido por sílica; 7%Si: jateamento com AlOx revestido por 7% de sílica. O teste de fadiga à flexão biaxial foi realizado (configuração piston-on-three-balls), assim como análises de topografia, conteúdo cristalino, rugosidade e fractografia. De acordo com o resultado, o GLZ melhora a performance em fadiga da 5YSZ, enquanto a deposição de filmes de sílica não afeta as propriedades mecânicas da mesma. Entre os jateamentos, AlOx diminui o comportamento em fadiga da cerâmica. O segundo avaliou o efeito de diferentes tratamentos na superfície interna de restaurações simplificadas de uma zircônia estabilizada com 5 mol% de óxido de ítrio no comportamento em fadiga mecânica antes e após envelhecimento. Discos cerâmicos (Ø= 10mm; espessura= 1mm) foram alocados considerando: “tratamentos de superfície” (Ctrl: sem tratamento; PM: primer; GLZ: glaze; SNF: deposição de nanofilmes de sílica (5nm); AlOx: jateamento com AlOx; SiC: jateamento com AlOx revestido por sílica; 7%Si: jateamento com AlOx revestido por 7% de sílica) e “envelhecimento” (baseline: 24h (37°C); envelhecido: 90 dias (37°C) + 12,000 ciclos térmicos). Os discos foram tratados, cimentados com cimento resinoso em análogo de dentina, submetidos ou não ao envelhecimento e subsequentemente ao teste de fadiga step-stress. Análises de fractografia, topografia, rugosidade, ângulo de contato e microscopia de força atômica foram realizadas. Como conclusão, tratamentos de superfície interna da zircônia são obrigatórios para estabilidade do comportamento à fadiga após o envelhecimento do conjunto restaurador, enquanto o não tratamento induz resultados instáveis. O terceiro avaliou o efeito da simulação em laboratório do desgaste do CAD/CAM e tratamentos de superfície interna nas características superficiais (topografia e rugosidade) e comportamento em fadiga de uma zircônia parcialmente estabilizada com 4 mol% de óxido de ítrio (4YSZ) cimentada adesivamente a um análogo de dentina. Discos cerâmicos (Ø= 10mm; espessura= 1mm) foram alocados considerando: “simulação em laboratório do desgaste do CAD/CAM” (desgastado; polido) e “tratamentos de superfície” (Ctrl: sem tratamento; AlOx: jateamento com AlOx; GLZ: glaze), e posteriormente cimentados com cimento resinoso em análogo de dentina e submetidos ao teste de fadiga step-stress. Foi realizada análise complementar para verificar a capacidade de infiltração do GLZ em defeitos superficiais no aumento da resistência flexural (RF) da 4YSZ. Para isso, espécimes em barras foram confeccionados considerando os grupos N-ID: sem indentação; ID: indentação; ID-GLZ: indentação+GLZ, e testados no ensaio de RF. Análises de rugosidade, topografia e fractografia foram realizadas. Como conclusão, a simulação em laboratório do desgaste do CAD/CAM promoveu um efeito prejudicial no comportamento em fadiga da 4YSZ e o GLZ induziu melhor performance em comparação ao jateamento. Além disso, o GLZ aumentou a resistência flexural das barras após indentação. Ademais, existe uma relação inversa entre rugosidade e carga para falha em fadiga da 4YSZ, quanto maior a rugosidade pior o comportamento mecânico do conjunto.

Palavras-chave: Desenho e fabricação auxiliados por computador. Fadiga. Resistência flexural. Tratamentos de superfície. Zircônia translúcida.

ABSTRACT

MECHANICAL BEHAVIOR UNDER FATIGUE OF POLYCRYSTALLINE ZIRCONIA: EFFECT OF GRINDING BUR FOR CAD/CAM MACHINING AND SURFACE TREATMENTS

AUTHOR: Ana Carolina Cadore Rodrigues
ADVISOR: Luiz Felipe Valandro
CO-ADVISOR: Cornelis Johannes Kleverlaan

Three studies compose the present study. The first one evaluated the effect of different intaglio surface treatments on fatigue behavior (biaxial flexural fatigue strength) and surface characteristics (topography and roughness) of a 5 mol% partially stabilized zirconia ceramic (5YSZ). For that, ceramic discs (ISO 6872-2015) were allocated considering: Ctrl: no-treatment; GLZ: low-fusing porcelain glaze; SNF: SiO_2 nanofilm deposition (5nm); AlOx: air-abrasion with aluminum oxide; SiC: air-abrasion with silica-coated AlOx; 7%Si: air-abrasion with 7% silica-coated AlOx. The biaxial flexural fatigue strength tests were performed (piston-on-three-balls assembly), besides topographic, surface roughness, fractographic and phase analysis. According to the results, low-fusing porcelain glaze enhances the fatigue performance of 5YSZ, while the deposition of silica nanofilms does not affect its mechanical properties. Among air-abrasions, the AlOx decreased the fatigue behavior of ceramic. The second study evaluated the distinct conditioning effect of the intaglio surface of bonded 5 mol% stabilized zirconia simplified restorations on the mechanical fatigue behavior of the set, prior to and after aging. Ceramic discs (Ø= 10mm; thick= 1mm) were allocated considering "surface treatments" (Ctrl: no-treatment; PM: primer; GLZ: glaze; SNF: SiO_2 nanofilm deposition (5 nm); AlOx: air-abrasion with AlOx; SiC: air-abrasion with silica-coated AlOx; 7%Si: air-abrasion with 7% silica-coated AlOx; and "aging" (baseline: 24h (37°C); aged: 90 days (37°C) + 12,000 thermal cycles). The discs were treated, luted with resin cement onto the dentin analogue, subjected to aging or not, and subsequently tested under a step-stress fatigue test. Fractography, topography, surface roughness, contact angle, and atomic force microscopy were performed. In conclusion, conditioning the intaglio surface of zirconia is mandatory for fatigue behavior stability after aging of the set, while non-treatment induces unstable results. The third study evaluated the effect of in-lab simulation of CAD/CAM grinding and intaglio surface treatments on the surface characteristics (topography and roughness) and fatigue behavior of adhesively luted 4 mol% yttria-stabilized zirconia (4YSZ) simplified restorations. Ceramic discs (Ø= 10mm; thick= 1mm) were allocated considering "In-lab simulation of CAD/CAM grinding" (ground; polished) and "surface treatments" (Ctrl: no treatment; AlOx: air abrasion with AlOx; GLZ: glaze), and posteriorly luted with resin cement onto a dentin analogue material and tested under a step-stress fatigue test. Complementary analysis was performed to verify the ability of GLZ infiltration in surface defects to increase the flexural strength (FS) of 4YSZ. For that, specimens in bars were confeccioned considering the groups N-ID: non-indented; ID: indented; ID-GLZ: indented + GLZ, and tested in the FS test. In conclusion, in-lab simulation of CAD/CAM grinding promoted deleterious fatigue behavior of 4YSZ and GLZ induced a better performance compared to air abrasion. In addition, GLZ increased the flexural strength of the bars after indentation. Furthermore, there is an inverse relationship between roughness and fatigue failure load of 4YSZ, the higher the surface roughness, the lower the fatigue behavior of the set.

Keywords: Computer-aided design and manufacturing. Fatigue. Flexural strength. Surface treatments. Translucent zirconia.

SUMÁRIO

1. INTRODUÇÃO

Próteses dentárias fixas totalmente cerâmicas são consideradas uma alternativa de tratamento as próteses metalocerâmicas devido a maior exigência por estética, aos avanços na tecnologia CAD/CAM (*Computer-aided design/Computer-aided manufacturing*) e desenvolvimento e aprimoramento de materiais cerâmicos mais resistentes (DENRY; KELLY, 2014). A tecnologia CAD/CAM destaca-se na confecção de restaurações dentais totalmente cerâmicas devido à viabilidade de fabricação em menor tempo, com menor sensibilidade técnica e maior precisão e eficiência (BLATZ; CONEJO, 2019).

De forma geral, o sistema CAD/CAM envolve três momentos: aquisição da imagem do preparo dentário e estruturas adjacentes por meio do uso de câmeras intraorais ou escaneamento do modelo de trabalho; desenho digital da restauração realizado em software específico; e confecção da restauração a partir de um processo aditivo ou subtrativo de usinagem com instrumentos diamantados de corte (ALGHAZZAWI, 2016; RITZBERGER et al., 2010; SULAIMAN, 2020). Para confecção da restauração pelo processo subtrativo de usinagem, blocos cerâmicos pré-fabricados são empregados, e devido a sua obtenção por um processo controlado e padronizado resultam em uma restauração com menos defeitos intrínsecos em comparação às restaurações confeccionadas pelas técnicas tradicionais e manuais (DA SILVA et al., 2017; GIORDANO, 2006).

O processo de usinagem para a confecção da restauração compreende primeiramente o contato entre a broca e a cerâmica gerando a indução de um campo de concentração de tensões; com subsequente acúmulo de energia e o início da formação de trincas nas regiões de alta concentração de tensão, levando a propagação das trincas com o progresso da usinagem; por fim, as múltiplas microtrincas se fundem levando a remoção do material. Assim, a usinagem modifica a superfície cerâmica levando a um aumento da rugosidade assim como danos superficiais e subsuperficiais (REKOW; THOMPSON, 2005; SINDEL et al., 1998; ZHANG; SATISH; KO, 1994).

Entre os materiais restauradores disponíveis para esse sistema, as cerâmicas à base de zircônia ganharam popularidade por possuírem excelentes propriedades mecânicas como alta resistência flexural e tenacidade à fratura, e excelente biocompatibilidade (PICONI; MACCAURO, 1999; STAWARCZYK et al., 2017). Além disso, as cerâmicas evoluíram ao longo dos anos e novas gerações de zircônia parcialmente estabilizadas com óxido de ítrio foram desenvolvidas para melhorar as características ópticas para seu uso em restaurações monolíticas (STAWARCZYK et al., 2017). No princípio, a primeira geração composta de zircônia tetragonal estabilizada por ítrio apresentava um alto índice de refração da luz, o que resultava em um caráter extremamente opaco do material, sendo principalmente indicada para infraestrutura de restaurações recobertas por porcelana (STAWARCZYK et al., 2017). Entretanto, um dos problemas relacionados a esse material era o lascamento da cerâmica de cobertura, o que poderia ser evitado com a confecção de restaurações monolíticas (material sem cerâmica de recobrimento) (SAILER et al., 2015). Assim, uma segunda geração de zircônia foi desenvolvida com composição semelhante à de primeira geração, sendo parcialmente estabilizada na fase tetragonal, mas apresentando uma redução no número e tamanho dos grãos de óxido de alumínio (Al_2O_3) permitindo maior passagem de luz e consequentemente maior translucidez, sendo considerada na fabricação de restaurações monolíticas (STAWARCZYK et al., 2017). Apesar disso, as zircônias de segunda geração ainda eram insuficientemente estéticas para uso na região anterior e apresentavam inferior translucidez comparada a cerâmicas vítreas, o que levou ao desenvolvimento da zircônia de terceira geração (STAWARCZYK et al., 2017).

Nesse sentido, a partir da zircônia parcialmente estabilizada com 3% mol de óxido de ítrio foi desenvolvida a zircônia de terceira geração com maior porcentagem de óxido de ítrio (≥4-5% mol), aumentando a quantidade de fase cúbica em sua microestrutura (STAWARCZYK et al., 2017). Os cristais cúbicos apresentam um volume maior comparado aos tetragonais permitindo que a dispersão de luz seja menos intensa nos limites dos grãos e, por conseguinte resulta em um aumento considerável na translucidez do material (STAWARCZYK et al., 2017). Entretanto, essa maior quantidade de fase cúbica leva a uma possibilidade reduzida de transformação de fase de tetragonal para monoclínica, o que dificulta ou previne o mecanismo de tenacificação por transformação do material (CHEN et al., 2020; KARLSEN; SCHRIWER; ØILO, 2020; KONSTANTINIDIS et al., 2018; PEREIRA et al., 2018; STAWARCZYK et al., 2017; SULAIMAN et al., 2017).

O processo mais utilizado para a fabricação de restaurações de zircônia é utilizando blocos parcialmente sinterizados (*soft machining*), pelo fato de que os blocos totalmente sinterizados (*hard machining*) são mais difíceis de usinar, despendendo mais tempo, o que diminui também a longevidade das brocas, além de introduzir mais defeitos superficiais (DENRY, 2013; DENRY; KELLY, 2008; MIYAZAKI; HOTTA, 2011; ZARONE; RUSSO; SORRENTINO, 2011). Os defeitos produzidos pelo CAD/CAM na superfície interna da coroa cerâmica são críticos pois estão localizados na superfície de cimentação que é submetida à concentração de tensões de tração, responsáveis pela iniciação e nucleação da trinca e posterior crescimento e propagação da mesma ao longo do material (KELLY et al., 1990, 2017; SCHERRER et al., 2017). Estudos na literatura apontam que a usinagem em CAD/CAM reduz significativamente a resistência da zircônia (CORAZZA et al., 2015; FRAGA et al., 2017; GUILARDI et al., 2020; WANG; ABOUSHELIB; FEILZER, 2008). Além disso, estudos que utilizaram diferentes métodos de simulação da usinagem (com brocas ou lixas de granulação) na fabricação de espécimes de zircônia, também verificaram redução na resistência do material (GUILARDI et al., 2020; ZUCUNI et al., 2017a).

Diversas condições clínicas podem ser consideradas preditoras do comportamento mecânico de restaurações cerâmicas por induzirem modificações topográficas da superfície, e consequentemente alterações da população de defeitos (KELLY et al., 2017; SCHERRER et al., 2017). Assim como o processo de usinagem (FRAGA et al., 2017; GUILARDI et al., 2020), tratamentos da superfície interna da restauração (CADORE-RODRIGUES et al., 2019, 2021; PROCHNOW et al., 2018) também são etapas importantes que podem gerar defeitos superficiais e são essenciais para uma adesão estável (CADORE-RODRIGUES et al., 2020b; ÖZCAN; BERNASCONI, 2015; ÖZCAN; VALLITTU, 2003). Além disso, a capacidade do cimento resinoso de se infiltrar adequadamente nos defeitos superficiais pode promover uma melhor distribuição de tensão no conjunto minimizando o impacto da população de defeitos, e consequentemente melhorando o comportamento mecânico do material (DE KOK et al., 2017; SPAZZIN et al., 2016, 2017).

Devido a microestrutura da zircônia possuir alto conteúdo cristalino com ausência de matriz vítrea, sua superfície não é susceptível/reativa a ação do ácido fluorídrico (tratamento clássico utilizado em cerâmicas vítreas para otimização de adesão) o que dificulta a união micromecânica resultante (ÖZCAN; VALLITTU, 2003). Logo, métodos de tratamento de superfície alternativos são necessários em busca de melhorar a adesão à zircônia. O método mais comumente aceito é o uso de jateamento com partículas de óxido de alumínio revestido ou não por sílica (KERN; WEGNER, 1998) que aumenta a rugosidade superficial, modifica a energia de superfície e a molhabilidade do substrato aumentando o embricamento micromecânico, além de promover uma limpeza do substrato, removendo potenciais impurezas presentes (MOON et al., 2016; ÖZCAN; VALLITTU, 2003; PEUTZFELDT; ASMUSSEN, 1988).

Além disso, destaca-se que o mecanismo de adesão promovido pelo jateamento varia com base no tipo de partícula empregada. O uso de partículas de óxido de alumínio resulta em um mecanismo baseado em embricamento micromecânico, pelo aumento da rugosidade superficial (DELLA BONA et al., 2007). Enquanto o uso de partículas de óxido de alumínio revestidas por sílica além de gerar microretenções, leva a um aumento de temperatura localizado, resultando na fusão da sílica e sua fixação na superfície pela colisão das partículas no substrato, tornando-se mais reativo ao agente de união silano que possui dois grupamentos ativos: um organofuncional que permite a união com a matriz resinosa e um grupo hidrolisável que reage com a matriz inorgânica (sílica presente na superfície cerâmica) formando uniões siloxanas (OZCAN; PFEIFFER; NERGIZ, 1998). A literatura também apresenta um novo material de partículas experimentais de óxido de alumínio revestidas com 7% de sílica com o mecanismo de adesão similar ao descrito anteriormente, gerando microretenções e proporcionando a fixação da sílica no substrato cerâmico. Este novo material apresentou resultados similares as partículas de óxido de alumínio revestidas por sílica disponível no mercado odontológico em durabilidade de adesão (CADORE-RODRIGUES et al., 2020a) e comportamento mecânico de uma zircônia de segunda geração (CADORE-RODRIGUES et al., 2019). Portanto, é um material promissor para tratamentos de superfície em cerâmicas de zircônia.

Estudos avaliando jateamento com partículas de óxido de alumínio em zircônias de terceira geração observaram uma redução na resistência flexural devido à dificuldade do mecanismo de transformação de fase (CHEN et al., 2020; KONTONASAKI; GIASIMAKOPOULOS; RIGOS, 2020; SULAIMAN et al., 2017). Assim, as propriedades mecânicas das zircônias de terceira geração são mais influenciadas pela presença de defeitos (KARLSEN; SCHRIWER; ØILO, 2020; KONTONASAKI; GIASIMAKOPOULOS; RIGOS, 2020; SULAIMAN et al., 2017), tornando importante avaliar protocolos de tratamentos de superfície que promovam menos defeitos superficiais nesses materiais para que desempenhem um bom comportamento mecânico.

De acordo com a literatura, métodos alternativos de tratamentos de superfície vêm sendo estudados e podem ser considerados para zircônias de terceira geração. Um dos métodos é a aplicação de uma fina camada de porcelana de baixa fusão (glaze - material rico em sílica) na superfície de cimentação podendo ser seguido de condicionamento com ácido fluorídrico, permitindo retenção micromecânica pela alteração da superfície (aumento da rugosidade) tornando-a reativa ao agente de união silano (uniões siloxanas) (ABOUSHELIB; KLEVERLAAN; FEILZER, 2007; CATTELL et al., 2009; CURA et al., 2012; KITAYAMA et al., 2009). Este protocolo apresentou melhora nos resultados de resistência de união da zircônia a cimentos resinosos (BOTTINO et al., 2014; VANDERLEI; BOTTINO; VALANDRO, 2014), entretanto, o método de aplicação pode prejudicar o comportamento mecânico.

Em termos de técnica de aplicação de glaze, existem duas abordagens: clássica, que exige que o pó seja misturado a um líquido sendo aplicado na superfície cerâmica com um pincel; ou a opção em spray, aplicada pulverizando o material sob a superfície (CARELLI; ANTUNES, 2018). A literatura mostra que a aplicação de glaze pela técnica pó/líquido gera uma camada (~300 µm) com muitos defeitos internos (bolhas de ar) que atuam como concentradores de tensão afetando a sobrevivência das restaurações de zircônia (POZZOBON et al., 2017; ZUCUNI et al., 2017), além disso, a dificuldade de padronização da espessura da camada de glaze pode afetar o assentamento da peça (VANDERLEI; BOTTINO; VALANDRO, 2014). Enquanto a aplicação pela técnica em spray promove uma camada de material mais fina (~12 - 80 µm) e homogênea, reduzindo a população de defeitos e dessa forma, não prejudicando o comportamento mecânico de zircônias de segunda geração (BOTTINO et al., 2014; CHUN et al., 2017; ZUCUNI et al., 2019). Assim, a técnica de aplicação de glaze em spray pode minimizar defeitos superficiais (CADORE-RODRIGUES et al., 2021) podendo ser um método de tratamento de superfície benéfico para zircônias de terceira geração.

Outro método alternativo é a deposição de nanofilmes de sílica por pulverização magnética. Este método é baseado na adesão química, onde o “bombardeio” de partículas altamente energéticas em uma superfície sólida cria radicais livres que podem aumentar as propriedades de adesão entre dois materiais sem comprometer a superfície do substrato (DUARTE et al., 2010). Este método alternativo foi utilizado por Queiroz e colaboradores (2011) para depositar filmes de sílica na superfície da zircônia com o objetivo de facilitar as propriedades de adesão da mesma a cimentos resinosos (DE QUEIROZ et al., 2011). Este protocolo associado a silanização apresenta um aumento na resistência de união, além de não apresentar danos a superfície da zircônia (DRUCK et al., 2015). Como a deposição de sílica não promove alteração superficial do substrato e pouca ou nenhuma transformação de fase em zircônias de segunda geração (estabilizadas com 3% mol de óxido de ítrio) (DRUCK et al., 2015; POZZOBON et al., 2017), esse protocolo também pode ser um tratamento de superfície adequado para zircônias de terceira geração.

Do ponto de vista clínico, o principal fator para a fratura da restauração cerâmica é a fadiga do material por meio do crescimento lento de trincas. Esse fenômeno ocorre a partir da interação entre a cerâmica e o ambiente, na presença de umidade e tensões, no qual a trinca se propaga de um modo estável culminando na diminuição de resistência do material em função do tempo (GONZAGA et al., 2010; KELLY et al., 2017; SCHERRER et al., 2017). Assim, os ensaios de fadiga têm se colocado como uma alternativa para aproximar os testes laboratoriais da realidade clínica a que os materiais restauradores são submetidos, sendo utilizados para comparação de materiais e realização de análises de sobrevivência (WISKOTT; NICHOLLS; BELSER, 1995). Outro ponto importante a ser considerado é o armazenamento em água e a termociclagem que são descritos como prejudiciais para a união silano-cerâmica (HO; MATINLINNA, 2011). O armazenamento em água simula o envelhecimento devido à absorção de água e degradação hidrolítica, enquanto as mudanças de temperatura simulam a expansão das tensões repetitivas de contração-expansão que ocorrem na interface (ÖZCAN; BERNASCONI, 2015; WEGNER et al., 2002). Dessa forma, a combinação de condições de envelhecimento e armazenamento em água são importantes para montar um cenário mais rigoroso para simular condições clínicas de restaurações.

Portanto, de acordo com os pressupostos acima mencionados, a presente tese busca avaliar o impacto da simulação em laboratório do desgaste do CAD/CAM e tratamentos de superfície, associado à condição de envelhecimento, nas características superficiais (topografia e rugosidade) e no comportamento mecânico em fadiga de zircônias de terceira geração com ≥4-5% mol de óxido de ítrio. Desta forma, a presente tese está apresentada sob a forma de três artigos científicos:

ARTIGO 1 - "Surface treatments and its effects on the fatigue behavior of a 5% mol yttria partially stabilized zirconia material". Com o objetivo de avaliar o efeito de diferentes tratamentos de superfície no desempenho à fadiga (resistência à fadiga flexural biaxial) e características superficiais (topografia e rugosidade) de uma cerâmica de zircônia parcialmente estabilizada com 5 mol% de óxido de ítrio.

ARTIGO 2 - "Fatigue performance of fully-stabilized zirconia polycrystals monolithic restorations: The effects of surface treatments at the bonding surface". Com o objetivo de avaliar o efeito de diferentes tratamentos na superfície interna de restaurações simplificadas de uma zircônia estabilizada com 5 mol% de óxido de ítrio adesivamente cimentada no comportamento em fadiga mecânica antes e após envelhecimento.

ARTIGO 3 - "In-lab simulation of CAD/CAM grinding and intaglio surface treatments of 4YSZ monolithic restorations: Effect on its load-bearing capacity under fatigue". Com o objetivo de avaliar o efeito da simulação em laboratório do desgaste do CAD/CAM e tratamentos de superfície interna nas características superficiais (topografia e rugosidade) e comportamento em fadiga de uma zircônia parcialmente estabilizada com 4 mol% de óxido de ítrio cimentada adesivamente a um análogo de dentina.

2. ARTIGO 1 - Surface treatments and its effects on the fatigue behavior of a 5% mol yttria partially stabilized zirconia material

Este artigo está publicado (doi: 10.1016/j.jmbbm.2021.104543) no periódico Journal of the Mechanical Behavior of Biomedical Materials, Elsevier, ISSN: 1751-6161, Fator de impacto = 4.042; Qualis A2. As normas para publicação estão descritas no Anexo A.

Surface treatments and its effects on the fatigue behavior of a 5% mol yttria partially stabilized zirconia material

Ana Carolina Cadore-Rodrigues[a]; Pablo Soares Machado[a]; Jivago Schumacher de Oliveira[b]; Sérgio Luiz Jahn[b]; Lucio Strazzabosco Dorneles[c]; Marília Pivetta Rippe[a]; Gabriel Kalil Rocha Pereira[a]; Luiz Felipe Valandro[a]

[a] Post-Graduate Program in Oral Science, Federal University of Santa Maria, Santa Maria, Rio Grande do Sul State, Brazil.

[b] Post-Graduate Program in Chemical Engineering, Federal University of Santa Maria, Santa Maria, Rio Grande do Sul State, Brazil.

[c] Post-Graduate Program in Physics, Physics Department, Federal University of Santa Maria, Santa Maria, Brazil.

Author's e-mails and contributions:

Ana Carolina Cadore-Rodrigues, anacadorerodrigues@gmail.com - Conceptualization, Methodology, Formal analysis, Investigation, Writing - Original Draft, Writing - Review & Editing

Pablo Soares Machado, P17_SM@hotmail.com - Investigation, Writing - Review & Editing

Jivago Schumacher de Oliveira, jivago.s.o@hotmail.com - Investigation, Writing - Review & Editing

Sérgio Luiz Jahn, sergiojahn@gmail.com - Resources, Writing - Review & Editing

Lucio Strazzabosco Dorneles, lsdorneles@gmail.com - Resources, Writing - Review & Editing

Marília Pivetta Rippe, mariliarippe@mail.ufsm.br - Conceptualization, Methodology, Writing - Review & Editing, Supervision

Gabriel Kalil Rocha Pereira, gabrielkrpereira@hotmail.com - Conceptualization, Methodology, Formal analysis, Writing - Review & Editing, Supervision

Luiz Felipe Valandro, valandrolf@gmail.com - Conceptualization, Methodology, Writing - Review & Editing, Supervision

***Corresponding author at:**

Luiz Felipe Valandro, D.D.S., M.Sci.D., Ph.D., Full Professor,
Federal University of Santa Maria
Faculty of Odontology
Head of Ph.D.-M.Sci.D. Graduate Program in Oral Science
Prosthodontics-Biomaterials Unit
1000 Roraima Av., T Street, Building 26F, Room 2386
UFSM Campus, 97105-900
Rio Grande do Sul State, Santa Maria, Brazil
Phone: +55-55-3220-9276, Fax: +55-55-3220-9272
E-mail: valandrolf@gmail.com (Dr LF Valandro)

Abstract

This study evaluated the effect of distinct surface treatments on the fatigue behavior (biaxial flexural fatigue testing) and surface characteristics (topography and roughness) of a 5% mol yttria partially stabilized zirconia ceramic (5Y-PSZ). Disc-shaped specimens of 5Y-PSZ (IPS e.max ZirCAD MT Multi) were manufactured (ISO 6872–2015) and allocated into six groups (n = 15) considering the following surface treatments: Ctrl – no treatment; GLZ – low-fusing porcelain glaze application; SNF – 5 nm SiO_2 nanofilm; AlOx – aluminum oxide particle air-abrasion; SiC – silica-coated aluminum oxide particles (silica-coating); and 7%Si – 7% silica-coated aluminum oxide particles (silica-coating). The biaxial flexural fatigue tests were performed by the step-stress method (20Hz for 10,000 cycles) with a step increment of 50N starting at 100N and proceeding until failure detection. The samples were tested with the treated surface facing down (tensile stress side). Topography, fractography, roughness, and phase content assessments of treated specimens were performed. GLZ group presented the highest fatigue behavior, while AlOx presented the lowest performance, and was only similar to SiC and 7%Si. Ctrl and SNF presented intermediary fatigue behavior, and were also similar to SiC and 7%Si. GLZ promoted a rougher surface, Ctrl and SNF had the lowest roughness, while the air-abrasion groups presented intermediary roughness. No m-phase content was detected (only *t* and *c* phases were detected). In conclusion, the application of a thin-layer of low-fusing porcelain glaze, the deposition of silica nanofilms and the air-abrasion with silica-coated alumina particles had no detrimental effect on the fatigue behavior of the 5Y-PSZ, while the air-abrasion with alumina particles damaged the fatigue outcomes.

Keywords: Yttrium stabilized zirconia polycrystals; Biaxial flexural fatigue testing; Air-abrasion; Low-fusing glaze; Silica nanofilms; Survival analysis.

Highlights

- Low-fusing porcelain glaze application enhances 5Y-PSZ fatigue performance.
- Silica nanofilm deposition does not affect the mechanical properties of 5Y-PSZ ceramic.
- Alumina particle air-abrasion damages the fatigue behavior of 5Y-PSZ ceramic.

1. Introduction

Monolithic full-contour zirconia restorations have been indicated as an alternative to classic bilayer systems (veneered zirconia) for manufacturing fixed dental prostheses (FDPs) (Konstantinidis et al., 2018), which enable more conservative preparations and avoid the risk of chipping, one of the main reported failures of bilayer-based FDPs with zirconia framework (Sailer et al., 2015). As the demand for esthetics increased in dental practice over time, new generations of zirconia have being proposed with significantly greater translucency for its monolithic use, expanding the range of indications of full-contour zirconia (Tabatabaian, 2018).

The first generation of zirconia is based on tetragonal zirconia partially stabilized by 3mol% yttria (3Y-PSZ) and presents high mechanical properties (strength and toughness), but is very opaque and whitish, being indicated for infrastructure of restorations covered by porcelain only (Stawarczyk et al., 2017; Zhang and Lawn, 2018). The second generation presents a reduction in the number and grain size of the aluminum oxide (Al_2O_3) allowing higher transmittance of light and consequently greater translucency, but it maintained the mechanical properties observed at the first generation (Stawarczyk et al., 2017). The third generation presents an increase in stabilizer content (4-5mol% yttria – 4Y-PSZ/5Y-PSZ) (Stawarczyk et al., 2017; Zhang and Lawn, 2018) leading to a higher amount of cubic phase in their microstructure, which allow superior light transmission through the material structure (Stawarczyk et al., 2017), with optical properties improvements (Zhang and Lawn, 2018).

The increased yttria content in third generation results in reduced damage tolerance for dental zirconia (Chen et al., 2020; Karlsen et al., 2020) and seems to diminish or prevent the toughening mechanism that occurred during tetragonal to monoclinic phase transformation in the former generations (i.e. cubic phase is stable), leading to an inferior mechanical performance in comparison to the 3Y-PSZ zirconia (Kontonasaki et al., 2020; Pereira et al., 2018; Stawarczyk et al., 2017; Sulaiman et al., 2017; Zucuni et al., 2019b). Based on such fact, it is reasonable to assume that 5Y-PSZ may be more influenced by the presence of defects such as the ones triggered by surface treatments in comparison to the former generation zirconia, which is capable of resisting the critical defect/stress by phase transformations and make the crack propagation more difficult (Chen et al., 2020; Karlsen et al., 2020; Kontonasaki et al., 2020; Sulaiman et al., 2017).

The literature has established that the traditional adhesive technique used for glass ceramics (hydrofluoric acid etching + silanization) is not effective for polycrystalline ceramics (Özcan and Vallittu, 2003; Thompson et al., 2011). A well-known surface treatment method for 3Y-PSZ is air-abrasion with aluminum oxide particles, covered or not by silica (Chintapalli et al., 2013; Kosmac et al., 1999; Moon et al., 2016; Özcan and Vallittu, 2003; Thompson et al., 2011), which induce compressive residual stresses from the t-m phase crystallographic transformation, increasing the flexural strength (protective effect) (Aurélio et al., 2016; Chintapalli et al., 2014; Kosmac et al., 1999; Zhang et al., 2004). Nevertheless, studies evaluating air-abrasion with aluminum oxide particles for 5Y-PSZ have observed a reduction in the flexural strength (Kontonasaki et al., 2020; Sulaiman et al., 2017). Therefore, a treatment method introducing less or no surface critical defect should consequently be investigated to prevent its deleterious effects on 5Y-PSZ ceramics.

According to existing literature, some alternative surface treatments are being studied for 3Y-PSZs and could be considered for 5Y-PSZs. One of them is ‘surface glazing’, which is based on applying a thin-layer of low-fusing porcelain glaze and can be followed by hydrofluoric acid etching, promoting increased roughness and making the surface more reactive to the silane agent (Aboushelib et al., 2007; Cattell et al., 2009; Cura et al., 2012; Kitayama et al., 2009). The application of glaze by spray technique promotes a thin layer on the ceramic surface and does not seem to impair the fatigue strength of 3Y-PSZ (Zucuni et al., 2019a). Moreover, this glassy layer promotes a smoother topography of the ceramic surface (Zucuni et al., 2020, 2019a), minimizing surface defects, which could be beneficial as a surface treatment for 5Y-PSZ.

Another explored method is the deposition of silica nanofilms via physical vapor deposition (PVD) using magnetron sputtering, which is a method strictly based on chemical adhesion (Piascik et al., 2009; Queiroz et al., 2011). Silica film deposition seems to be very promising since it promotes stable bond strength between zirconia ceramic and resin cement, even reaching similar levels to those observed with air-abrasion using silica particles (Druck et al., 2015). Previous studies have demonstrated that silica deposition does not damage the surface and generate slight or no t-m phase transformation in 3Y-PSZ, where the deposited silica become inert on the zirconia microstructure (Druck et al., 2015; Pozzobon et al., 2017). Thus, such surface treatment could be suitable for 5Y-PSZ.

Besides, an experimental material composed of aluminum oxide particles coated with 7% of silica was recently developed and proposed for 3Y-PSZ ceramics. The use of this experimental material/surface treatment protocol triggered higher and more stable bonding in comparison to the use of the classic aluminum oxide powders (Cadore-Rodrigues et al., 2020), and also better mechanical performance in such scenarios (Cadore-Rodrigues et al., 2019). Thus, this experimental material containing silica powders can also be considered promising for 5Y-PSZ ceramics, since the air-abrasion of 3Y-PSZ with this experimental powder (45 µm) promoted a topographical pattern less aggressive and with more regular defects compared with the irregular and deeper defects observed when air-abrading with the classical alumina particles (which also presented 45 µm particle size) (Cadore-Rodrigues et al., 2019).

Based on the aforementioned presupposes, those distinct surface treatments could be beneficial to the 5Y-PSZ. Despite that, it lacks studies exploring its influence on the mechanical behavior of 5Y-PSZ. Therefore, this study aimed to evaluate the effect of distinct surface treatments on the fatigue behavior (biaxial flexural fatigue testing) and surface characteristics (topography and roughness) of a 5Y-PSZ ceramic. The study's assumed hypotheses were: (1) particle air-abrasion will damage the fatigue behavior of 5Y-PSZ ceramics; (2) silica nanofilm and application of a thin-layer of porcelain glaze will not damage the fatigue behavior of 5Y-PSZ ceramics.

2. Materials and methods

2.1 Preparation of specimens

Disc-shaped specimens of 5Y-PSZ ceramic (IPS e.max ZirCAD MT Multi, Ivoclar Vivadent, Schaan, Liechtenstein) were produced following the ISO 6872-2015 guidelines for biaxial flexural fatigue testing of ceramic materials (final dimensions: 15 mm Ø and 1.2 ± 0.2 mm in thickness) (Pereira et al., 2018). To do so, 5Y-PSZ blanks (Ø= 98 mm, thickness= 20 mm) were sectioned into smaller blocks (20 mm × 20 mm). Metallic rings with 18 mm diameter were subsequently glued to the parallel surfaces of the blocks, serving as guides for grinding in a polishing machine under water-cooling with silica carbide papers (#600 and #1200-grit) (3M, Sumaré, Brazil) upon obtaining a cylinder (Ø= 18 mm). Next, slices of 1.5 mm thickness were obtained in a cutting machine under water-cooling (ISOMET 1000, Buehler, Lake Bluff, USA). Finally, the obtained 5Y-PSZ discs (N= 90) were polished on both sides with silica carbide papers (#600 and #1200-grit) to remove any surface irregularities introduced during cutting, and then sintered in a furnace (inFire HTC speed, Sirona Dental Systems GmbH, Bensheim, Germany) according to the manufacturer's recommendation, resulting in specimens with final dimensions of 15 mm in diameter and 1.2 mm (± 0.2 mm) in thickness. The specimens were allocated into six testing groups (n = 15) considering the surface treatments as the independent variable.

2.2 Surface treatments

After allocation, the ceramic discs were cleaned in an ultrasonic bath (Vitasonic, Vita Zahnfabrik, Bad Säckingen, Germany) with distilled water for 5 minutes. Next, the ceramic discs (down-side to be subjected to the tensile stresses during the biaxial test) were submitted to the surface treatments as follows:

Control (Ctrl): Ultrasonic bath with distilled water;

Glaze (GLZ): The glaze spray (Glaze Spray VITA Akzent, VITA Zahnfabrik) was applied at a distance of 15 cm between the applicator tip and the ceramic surface. A slight oscillatory movement was performed until the ceramic surface was entirely covered prior to glaze firing (initial temperature: 500 °C for 4 min at a heating rate of 80 °C/min until the final temperature of 950 °C, maintained for 1 min) (Vacumat 6000 MP, VITA Zahnfabrik) (Zucuni et al., 2019a);

Silica nanofilms (SNF): SiO_2 thin film was deposited using the magnetron sputtering PVD process. The discs were exposed to the process for 90 sec to deposit 5 nm – thickness of the nanofilm (Druck et al., 2015);

Particle air-abrasion: The air-abrasion groups were performed for 10 sec at a distance of 10 mm and 2.8 bar of pressure with aluminum oxide particles (*AlOx group*), silica-coated aluminum oxide particles (*SiC group*), or aluminum oxide particles covered by 7% of silica (*7%Si group* – synthesis procedure performed at the Chemical Engineering Laboratory, UFSM, Santa Maria, Brazil) (Cadore-Rodrigues et al., 2020).

2.3 Roughness analysis

The surface roughness of all the specimens were measured prior to the biaxial flexural fatigue testing using a surface roughness tester (n= 15) (Mitutoyo SJ-410, Mitutoyo Corporation, Takatsu-ku, Kawasaki, Japan). The arithmetic mean of three surface roughness measurements was calculated for each specimen according to ISO 4287-1997 (cut-off of 5; λC of 0.8 mm; λS of 2.5 µm) and the Ra and Rz parameters were subsequently obtained. Ra is defined as the arithmetic mean of the absolute values of peaks and valleys measured from a mean plane (in µm), and Rz is the average distance between the five highest peaks and five major valleys of a surface (in µm).

2.4 Biaxial flexural fatigue testing

The specimens (n = 15) were subjected to a biaxial flexural fatigue test on an electric mechanical testing machine (Instron ElectroPuls E3000; Instron Corporation, Norwood, USA) using the step-stress methodology (Kelly et al., 2017; Venturini et al., 2019). Disc-shaped specimens were positioned with the treated surface facing down (tensile side) on three support balls (Ø= 3 mm) under water according to ISO 6872-2015. The specimens were loaded with a flat circular tungsten piston (Ø= 1.6 mm) applied perpendicularly to the center of the discs. An adhesive tape (110 µm) was placed on the occlusal surface of each specimen before testing to reduce contact stress concentration and to prevent contact surface damage (Kelly et al., 2017; Venturini et al., 2019).

Next, cyclical intermittent loads were applied at a frequency of 20 Hz, starting with an initial load of 100N for 5,000 cycles to adjust the sample/piston contact, then followed by steps of 150N, 200N, and so on, with a fixed load increment of 50N for 10,000 cycles at each load step until the occurrence of failure. The specimens were examined in the final execution of each fatigue test step load. If the specimen survived, the load step was increased, and the test proceeded. If fracture occurred, the sample was classified as “failed”, the fatigue test ended for the sample and the collected data was recorded for statistical analysis (FFL – fatigue failure load; CFF – cycles for fatigue failure).

2.5 X-ray diffraction (XRD analysis)

In order to identify the superficial crystalline phase content (monoclinic - *m*, tetragonal - *t*, and/or cubic - *c*) at the intaglio ceramic surface after the surface treatments, two additional specimens of each condition were analyzed by an X-ray Diffractometer (Bruker AXS, D8 Advance, Karlsruhe, Germany) with CuKα radiation (40 kV, 40 mA) in a 2θ angular interval of 27–37° and 72–76°, with a step-size of 0.02° every 2 sec as described in a previously published study (Zucuni et al., 2020).

2.6 Topographic analysis

A descriptive analysis on a scanning electron microscope (SEM) (Vega3, Tescan, Brno, Czech Republic) was performed to determine the topographical pattern of the ceramic surface after the different surface treatments. To do so, one additional treated ceramic specimen of each group was coated with gold-palladium alloy and the images were obtained at 1000× magnification.

2.7 Fractographic analysis

Failed representative samples were evaluated under SEM (Vega3, Tescan) at 1000× magnification to determine the fractographical characteristics. The ceramic specimens were ultrasonically cleaned (1440 DA Odontobras, Ribeirão Preto, Brazil) with isopropyl alcohol for 5 min and coated with gold-palladium alloy prior to evaluation.

2.8 Statistical analysis

The roughness data assumed a non-parametric and homoscedastic distribution according to the Shapiro-Wilk test. Then, the Kruskal Wallis and post-hoc LSD test ($\alpha=0.05$) were performed using IBM SPSS 21 (IBM Analytics, New York, USA).

Statistical analysis for FFL and CFF data were performed using Kaplan Meier and Mantel-Cox (Log-Rank) tests ($\alpha=0.05$; SPSS version 21, IBM Analytics, New York, USA). Additionally, such data was also submitted to Weibull statistical analysis to describe the Weibull modulus using the Super SMITH Weibull 4.0k-32 software program (Wes Fulton, Torrance, USA). The Weibull modulus is used as a distribution measure of the fatigue data, expressing the material’s mechanical structural reliability.

Topographic and fractographic features (SEM data) were descriptively/qualitatively analyzed.

3. Results

The GLZ group promoted the highest surface roughness followed by AlOx, SiC and 7%Si, which were similar to each other statistically (Table 1). The Ctrl and SNF groups were similar in having the lowest statistical roughness values.

The GLZ treatment had the highest fatigue failure load mean (without deleterious effect) (Table 1). The SNF, SiC, and 7%Si treatments presented similar fatigue performance to the Ctrl group (also with no detrimental influence). The air-abrasion with the AlOx treatment induced lower fatigue failure load than the Ctrl group, therefore having a damaging effect. Table 2 demonstrates the survival rates, highlighting the early failure for the air-abrasion groups, mainly the AlOx treatment. The Weibull moduli were not statistically different (similar structural reliability) (Table 1).

The XRD analysis only detected cubic and tetragonal phases, with no *m*-phase content being identified (Figure 1).

Representative SEM micrographs of the treated ceramic surface (Figure 2) show that the air-abrasion treatments (AlOx, SiC and 7% Si) promoted greater surface alteration. The GLZ group promoted a more homogeneous surface, however there were also uncovered regions, which resulted in a rougher surface, as aforementioned. The SNF group was similar to the Ctrl group, corroborating that SNF deposition induces no topographic change.

Fractographic analysis (Figure 3) shows that the fractures originated at the surface/sub-surface defects of the zirconia material from the region subjected to the tensile stress concentration. The blue arrow in the GLZ group points to a probable secondary failure of the specimen. The GLZ group specimens failed in several fragments, making it difficult to find the source of the failure in the fractographic analysis.

4. Discussion

The first hypothesis that particle air-abrasion would damage the fatigue behavior of 5Y-PSZ ceramic was partially accepted, as the alumina air-abrasion (AlOx group) induced lower fatigue behavior than the Ctrl group, while the SiC and 7%Si groups (air-abrasion with particles modified by silica) were similar to the Ctrl group. The second hypothesis was accepted, since the silica nanofilm and the application of a thin-layer of porcelain glaze had no damage effect on the fatigue behavior.

It can be highlighted that although silica or alumina particle air-abrasion is related to better results in terms of adhesion to zirconia (Ozcan and Bernasconi, 2015; Özcan and Vallittu, 2003), the impact of air-abrasion with aluminum oxide (which is a hard and sharp particle) (Zhang et al., 2006) may also lead to significant damage (extensive erosive wear, lateral cracks and deep defects) (Guazzato et al., 2005; Hallmann et al., 2012). In this sense, the surface alterations caused by the air-abrasion promoted defects that was not countered by the zirconia microstructure leading to the crack growth into the material until its catastrophic failure. The higher percentage of c-phase crystals in 5Y-PSZs prevents the toughening mechanism promoting an expected significant reduction of its mechanical properties, as observed herein (Table 1) and shown by previous studies (Chen et al., 2020; Kontonasaki et al., 2020; Pereira et al., 2018; Sulaiman et al., 2017).

The XRD analysis confirmed the presence of cubic and tetragonal phase crystals in the treated 5Y-PSZ surface, with no monoclinic phase grains (Figure 1). In the 3Y-PSZ ceramic, the phase transformation is considered to be triggered by air-abrasion increasing toughness and flexural strength while hindering crack spread (Aurélio et al., 2016; Chen et al., 2020; Denry and Kelly, 2007; Piconi and Maccauro, 1999; Zhang et al., 2004). However, a recent study which evaluated the phase content in an 5Y-PSZ ceramic after air-abrasion with alumina particles and silica-coated alumina particles observed that no m-phase content was present, irrespective of the abrasion treatment type (Chen et al., 2020). This assumption is held by a previous study which evaluated the same 5Y-PSZ used herein and subjected to the different surface treatments (Zucuni et al., 2020). Thus, as 5Y-PSZ presents a higher percentage of cubic phase in its microstructure, surface treatments that induces more aggressive surface defects may impair the mechanical behavior of these ceramics.

The silica-coated aluminum oxide particles are more rounded and softer than the classic un-coated particles (Zhang et al., 2006). Therefore, the potential of introducing defects with silica-coated alumina particles is also softened (Özcan et al., 2013; Souza et al., 2013). Such assumption was proven by a previous study (Cadore-Rodrigues et al., 2019) which assessed the fatigue performance of a bonded 3Y-PSZ ceramic in comparing the same air-abrasion groups (AlOx, SiC and 7% Si) assessed herein. In turn, the groups with particles modified by silica (SiC and 7% Si) presented similar fatigue behavior to the Ctrl group (Table 1). Nevertheless, the defects induced by the alumina air-abrasion group promoted an increased risk of premature failure (lower survival rates) due to the microstructure of 5Y-PSZ ceramic (Table 2).

The SNF group demonstrated similar fatigue behavior and roughness to the Ctrl group (Table 1). SiO_2 nanofilm was deposited on the surface through the processing plasma which consists in a strictly chemical adhesion method (Queiroz et al., 2011). As expected, silica nanofilms with a thickness of 5 nm did not promote any surface alteration (Figure 2) (Druck et al., 2015; Pozzobon et al., 2017), leading to no effect on the mechanical properties of the 5Y-PSZ ceramic, and only being inferior to the GLZ group. The advantages of the silica film deposition by sputtering compared to applying a thin-layer of low-fusing glassy porcelain are that the deposition is rapid and can be performed at low temperatures (potentially avoiding phase transformations on 3Y-PSZs). Furthermore, the thickness (much thinner at a nanoscale) and the chemical composition of the film can also be controlled. However, the disadvantages of silica film deposition for dental laboratory application include requiring special equipment, possibly adding an additional operational cost and specific training for equipment usage.

According to our results (Table 1), the application of low-fusing porcelain glaze promoted higher fatigue performance of the 5Y-PSZ ceramic compared to the other surface treatments and to the Ctrl group. In terms of glaze application technique, there are two approaches: classical, which requires the powder to be mixed with a liquid being applied to the ceramic surface with a brush; or the spray option, applied by spraying the material under the surface (Carelli and Antunes, 2018). The application of glaze by the spray technique promotes a thinner and more homogeneous material layer (~80 µm), reducing the population of defects and thus not impairing the mechanical behavior of 3Y-PSZ ceramics (Chun et al., 2017; Zucuni et al., 2019a). Our results are in agreement with such findings, corroborating similar performance at a 5Y-PSZ. According to Anusavice and Phillips (2003), the glaze application may result in a fill-up mechanism (healing effect), from which the glaze penetrates the existing microcracks and porosities onto the ceramic surface leading to a surface with lesser defects. On the other hand, there is also a risk that the glaze material may accumulate in restrict regions of the material's surface (Chun et al., 2017). In that case, some uncovered areas may be observed, exposing the internal zirconia material (Zucuni et al., 2019a). Figure 2 shows that in our study GLZ promoted a more homogeneous topographic pattern in the 5Y-PSZ ceramic; however, some uncovered areas remained and therefore a rougher surface was also observed.

In contrast to this finding, some studies show that the glaze application on the 3Y-PSZ ceramic could promote a decrease in its biaxial flexure strength (Borba et al., 2011; Pozzobon et al., 2017; White et al., 2005). The literature shows that the application of glaze by the powder/liquid technique generates a thick layer (~300 µm) with many internal defects (air bubbles) that act as stress concentrators affecting the survival of restorations (3Y-PSZ) (Pozzobon et al., 2017; Zucuni et al., 2019a). In addition, these results were related to the fact that glaze is a highly glassy material with very low tensile strength, and as shown in these studies, the properties of a material subjected to the tensile stress during testing may dictate the threshold strength of a structure when the fracture is originated from the defects located within the glaze material, and then propagate toward the 3Y-PSZ ceramic core (Borba et al., 2011; Guazzato et al., 2005; Pozzobon et al., 2017; White et al., 2005). In summary, the energy unleashed during crack propagation originating from a weaker material can become high enough for it to quickly reach the interface at the inner structure, from which it suddenly continues towards the whole structure, even if the other material has higher strength; this means there will be an influence of the weaker material on the lower threshold strength value when the fracture origin is from it. We believe that such negative effects were not observed in our study because we used a spray technique that induced a thinner and homogeneous layer of glaze, as observed by Zucuni et al. (2019a). Thus, the failure origin in our study probably was not located within the glaze material.

A limitation to such statement is that we could not be sure of the fracture origin region at GLZ group because all specimens failed in several fragments, specially at the origin region, which made it difficult to characterize such area during the fractographic analysis.

Finally, it must report that the present study presents inherent limitations. As mentioned, a disadvantage of silica film deposition includes requiring special equipment, possibly adding an additional operational cost and specific training for equipment usage. In regards of glaze application, it is a very sensitive technique, including the operator effect, so standardizing the glaze thickness is necessary and difficult. Considering air-abrasion protocols, differences may be observed when varying the particle size and the parameters used for air-abrasion (pressure, distance, time). Lastly, the samples we only applied axial loads during the fatigue test, without sliding or lateral forces which occur in the clinical environment. The application of multi-axial loads may influence the materials response to the stimuli, altering its mechanical properties and failure pattern. Despite that, the difficulty to provide a complete oral environment simulation is a well-known limitation of *in vitro* studies.

5. Conclusions

- The application of a thin-layer of low-fusing porcelain glaze enhanced the fatigue performance of the 5Y-PSZ ceramic.
- The deposition of silica nanofilms and air-abrasion with silica-coated alumina particles induced similar mechanical properties to non-treatment condition.
- Air-abrasion with alumina particles induced deleterious effects on the fatigue behavior of the 5Y-PSZ ceramic.

ACKNOWLEDGEMENTS

The authors declare no conflicts of interest and emphasize that this study was partly financed by the Brazilian Federal Agency for Coordination of Improvement of Higher Education Personnel (CAPES) (Finance code 001; Doctorate Scholarship of A. C. C-R.). We especially thank Ivoclar Vivadent for donating some materials, and finally we emphasize that those institutions had no role in the study design, data collection or analysis, decision to publish or in preparing the manuscript.

REFERENCES

Aboushelib, M.N., Kleverlaan, C.J., Feilzer, A.J., 2007. Selective infiltration-etching technique for a strong and durable bond of resin cements to zirconia-based materials. J. Prosthet. Dent. 98, 379–388. https://doi.org/10.1016/S0022-3913(07)60123-1

Anusavice, K.J., Phillips, R.W., 2003. Phillip's Science of Dental Materials, eleventh ed. Elsevier, St. Louis.

Aurélio, I.L., Marchionatti, A.M.E., Montagner, A.F., May, L.G., Soares, F.Z.M., 2016. Does air particle abrasion affect the flexural strength and phase transformation of Y-TZP? A systematic review and meta-analysis. Dent. Mater. 32, 827–845. https://doi.org/10.1016/j.dental.2016.03.021

Borba, M., De Araújo, M.D., De Lima, E., Yoshimura, H.N., Cesar, P.F., Griggs, J.A., Della Bona, Á., 2011. Flexural strength and failure modes of layered ceramic structures. Dent. Mater. 27, 1259–1266. https://doi.org/10.1016/j.dental.2011.09.008

Cadore-Rodrigues, A., Prochnow, C., Burgo, T., Oliveira, J., Jahn, S., Foletto, E., Rippe, M., Pereira, G., Valandro, L., 2020. Stable Resin Bonding to Y-TZP Ceramic with Air Abrasion by Alumina Particles Containing 7% Silica 22, 149–159.

Cadore-Rodrigues, A.C., Prochnow, C., Rippe, M.P., Oliveira, J.S. de, Jahn, S.L., Foletto, E.L., Pereira, G.K.R., Valandro, L.F., 2019. Air-abrasion using new silica-alumina powders containing different silica concentrations: Effect on the microstructural characteristics and fatigue behavior of a Y-TZP ceramic. J. Mech. Behav. Biomed. Mater. 98, 11–19. https://doi.org/10.1016/j.jmbbm.2019.05.032

Carelli, M., Antunes, F., 2018. Can low-fusing glass application affect the marginal misfit and bond strength of Y-TZP crowns ? 32, 1–10.

Cattell, M.J., Chadwick, T.C., Knowles, J.C., Clarke, R.L., 2009. The development and testing of glaze materials for application to the fit surface of dental ceramic restorations. Dent. Mater. 25, 431–441. https://doi.org/10.1016/j.dental.2008.09.004

Chen, B., Xie, H., Zhang, H., 2020. Effects of Tribochemical Silica Coating and Alumina-Particle Air Abrasion on 3Y-TZP and 5Y-TZP : Evaluation of Surface Hardness , Roughness , Bonding , and Phase Transformation 22, 373–382. https://doi.org/10.3290/j.jad.a44868

Chintapalli, R.K., Marro, F.G., Jimenez-Pique, E., Anglada, M., 2013. Phase transformation and subsurface damage in 3Y-TZP after sandblasting. Dent. Mater. 29, 566–572. https://doi.org/10.1016/j.dental.2013.03.005

Chintapalli, R.K., Mestra Rodriguez, A., Garcia Marro, F., Anglada, M., 2014. Effect of sandblasting and residual stress on strength of zirconia for restorative dentistry applications. J. Mech. Behav. Biomed. Mater. 29, 126–137. https://doi.org/10.1016/j.jmbbm.2013.09.004

Chun, E.P., Anami, L.C., Bonfante, E.A., Bottino, M.A., 2017. Microstructural analysis and reliability of monolithic zirconia after simulated adjustment protocols. Dent. Mater. 33, 934–943. https://doi.org/10.1016/j.dental.2017.04.024

Cura, C., Isik, G., Saracoglu, A., Özcan, M., 2012. Comparison of alternative adhesive cementation concepts for zirconia ceramic: Glaze layer vs zirconia primer. J. Adhes. Dent. 14, 75–82. https://doi.org/10.3290/j.jad.a21493

Denry, I., Kelly, J.R., 2007. State of the art of zirconia for dental applications 4, 299–307. https://doi.org/10.1016/j.dental.2007.05.007

Druck, C.C., Pozzobon, J.L., Callegari, G.L., Dorneles, L.S., Valandro, L.F., 2015. Adhesion to Y-TZP ceramic: Study of silica nanofilm coating on the surface of Y-TZP. J. Biomed. Mater. Res. - Part B Appl. Biomater. 103, 143–150. https://doi.org/10.1002/jbm.b.33184

Guazzato, M., Quach, L., Albakry, M., Swain, M. V., 2005. Influence of surface and heat treatments on the flexural strength of Y-TZP dental ceramic. J. Dent. 33, 9–18. https://doi.org/10.1016/j.jdent.2004.07.001

Hallmann, L., Ulmer, P., Reusser, E., Hämmerle, C.H.F., 2012. Effect of blasting pressure, abrasive particle size and grade on phase transformation and morphological change of dental zirconia surface. Surf. Coatings Technol. 206, 4293–4302. https://doi.org/10.1016/j.surfcoat.2012.04.043

Karlsen, C.Å., Schriwer, C., Øilo, M., 2020. Damage tolerance of six dental zirconias with different translucencies. Biomater. Investig. Dent. 7, 126–133. https://doi.org/10.1080/26415275.2020.1809420

Kelly, J.R., Cesar, P.F., Scherrer, S.S., Della Bona, A., van Noort, R., Tholey, M., Vichi, A., Lohbauer, U., 2017. ADM guidance-ceramics: Fatigue principles and testing. Dent. Mater. 33, 1192–1204. https://doi.org/10.1016/j.dental.2017.09.006

Kitayama, S., Nikaido, T., Maruoka, R., Zhu, L., Ikeda, M., Watanabe, A., Foxton, R.M., Miura, H., Tagami, J., 2009. Effect of an internal coating technique on tensile bond strengths of resin cements to zirconia ceramics. Dent. Mater. J. 28, 446–453. https://doi.org/10.4012/dmj.28.446

Konstantinidis, I., Trikka, D., Gasparatos, S., Mitsias, M.E., 2018. Clinical outcomes of monolithic zirconia crowns with cad/cam technology. A 1-year follow-up prospective clinical study of 65 patients. Int. J. Environ. Res. Public Health 15. https://doi.org/10.3390/ijerph15112523

Kontonasaki, E., Giasimakopoulos, P., Rigos, A.E., 2020. Strength and aging resistance of monolithic zirconia: an update to current knowledge. Jpn. Dent. Sci. Rev. 56, 1–23. https://doi.org/10.1016/j.jdsr.2019.09.002

Kosmac, T., Oblak, C., Jevnikar, P., Funduku, N., Marion, L., 1999. The effect of surface grinding and sanblasting on flexural strength and reliability of Y-TZP zirconia ceramic. Dent. Mater. 15, 426–433. https://doi.org/10.1016/0038-1101(68)90151-2

Moon, J.E., Kim, S.H., Lee, J.B., Han, J.S., Yeo, I.S., Ha, S.R., 2016. Effects of airborne-particle abrasion protocol choice on the surface characteristics of monolithic zirconia materials and the shear bond strength of resin cement. Ceram. Int. 42, 1552–1562. https://doi.org/10.1016/j.ceramint.2015.09.104

Ozcan, M., Bernasconi, M., 2015. Adhesion to Zirconia Used for Dental Restorations: A Systematic Review and Meta-Analysis. J. Adhes. Dent. 17, 7–26. https://doi.org/10.3290/j.jad.a33525

Özcan, M., John, Vallittu, P., Lassilla, L., 2013. Effect of particle deposition parameters on silica coating of zirconia using a chairside air-abrasion device. J. Adhes. Dent. 15, 211–214. https://doi.org/10.3290/j.jad.a29718

Özcan, M., Vallittu, P.K., 2003. Effect of surface conditioning methods on the bond strength of luting cement to ceramics. Dent. Mater. 19, 725–731. https://doi.org/10.1016/S0109-5641(03)00019-8

Pereira, G.K.R., Guilardi, L.F., Dapieve, K.S., Kleverlaan, C.J., Rippe, M.P., Valandro, L.F., 2018. Mechanical reliability, fatigue strength and survival analysis of new polycrystalline translucent zirconia ceramics for monolithic restorations. J. Mech. Behav. Biomed. Mater. 85, 57–65. https://doi.org/10.1016/j.jmbbm.2018.05.029

Piascik, J.R., Swift, E.J., Thompson, J.Y., Grego, S., Stoner, B.R., 2009. Surface modification for enhanced silanation of zirconia ceramics. Dent. Mater. 25, 1116–1121. https://doi.org/10.1016/j.dental.2009.03.008

Piconi, C., Maccauro, G., 1999. Zirconia as a ceramic biomaterial 20.

Pozzobon, Pereira, G.K.R., Wandscher, V.F., Dorneles, L.S., Valandro, L.F., 2017. Mechanical behavior of yttria-stabilized tetragonal zirconia polycrystalline ceramic after different zirconia surface treatments. Mater. Sci. Eng. C 77, 828–835. https://doi.org/10.1016/j.msec.2017.03.299

Queiroz, J.R.C., Duarte, D.A., De Assunção E Souza, R.O., Fissmer, S.F., Massi, M., Bottino, M.A., 2011. Deposition of SiOx thin films on Y-TZP by reactive magnetron sputtering: Influence of plasma parameters on the adhesion properties between Y-TZP and resin cement for application in dental prosthesis. Mater. Res. 14, 212–216. https://doi.org/10.1590/S1516-14392011005000032

Sailer, I., Makarov, N.A., Thoma, D.S., Zwahlen, M., Pjetursson, B.E., 2015. All-ceramic or metal-ceramic tooth-supported fixed dental prostheses (FDPs)? A systematic review of the survival and complication rates. Part I: Single crowns (SCs). Dent. Mater. 31, 603–623. https://doi.org/10.1016/j.dental.2015.02.011

Souza, R.O.A., Valandro, L.F., Melo, R.M., Machado, J.P.B., Bottino, M.A., Özcan, M., 2013. Air-particle abrasion on zirconia ceramic using different protocols: Effects on biaxial flexural strength after cyclic loading, phase transformation and surface topography. J. Mech. Behav. Biomed. Mater. 26, 155–163. https://doi.org/10.1016/j.jmbbm.2013.04.018

Stawarczyk, B., Keul, C., Eichberger, M., Figge, D., Edelhoff, D., Lümkemann, N., 2017. Three generations of zirconia: From veneered to monolithic. Part I. Quintessence Int. 48, 369–380. https://doi.org/10.3290/j.qi.a38057

Sulaiman, T.A., Abdulmajeed, A.A., Shahramian, K., Lassila, L., 2017. Effect of different treatments on the flexural strength of fully versus partially stabilized monolithic zirconia. J. Prosthet. Dent. 118, 216–220. https://doi.org/10.1016/j.prosdent.2016.10.031

Tabatabaian, F., 2018. Color Aspect of Monolithic Zirconia Restorations : A Review 1–12. https://doi.org/10.1111/jopr.12906

Thompson, J.Y., Stoner, B.R., Piascik, J.R., Smith, R., 2011. Adhesion/cementation to zirconia and other non-silicate ceramics: where are we now? Dent. Mater. 27, 71–82. https://doi.org/10.1016/j.dental.2010.10.022

Venturini, A.B., Prochnow, C., Pereira, G.K.R., Segala, R.D., Kleverlaan, C.J., Valandro, L.F., 2019. Fatigue performance of adhesively cemented glass-, hybrid- and resin-ceramic materials for CAD/CAM monolithic restorations. Dent. Mater. 35, 534–542. https://doi.org/10.1016/j.dental.2019.01.013

White, S.N., Miklus, V.G., McLaren, E.A., Lang, L.A., Caputo, A.A., 2005. Flexural strength of a layered zirconia and porcelain dental all-ceramic system. J. Prosthet. Dent. 94, 125–131. https://doi.org/10.1016/j.prosdent.2005.05.007

Zhang, Y., Lawn, B.R., 2018. Novel Zirconia Materials in Dentistry. J. Dent. Res. 97, 140–147. https://doi.org/10.1177/0022034517737483

Zhang, Y., Lawn, B.R., Malament, K.A., Van Thompson, P., Rekow, E.D., 2006. Damage accumulation and fatigue life of particle-abraded ceramics. Int. J. Prosthodont. 19, 442–8.

Zhang, Y., Lawn, B.R., Rekow, E.D., Thompson, V.P., 2004. Effect of sandblasting on the long-term performance of dental ceramics. J. Biomed. Mater. Res. - Part B Appl. Biomater. 71, 381–386. https://doi.org/10.1002/jbm.b.30097

Zucuni, C.P., Pereira, G.K.R., Dapieve, K.S., Rippe, M.P., Bottino, M.C., Valandro, L.F., 2019a. Low-fusing porcelain glaze application does not damage the fatigue strength of Y-TZP. J. Mech. Behav. Biomed. Mater. 99, 198–205. https://doi.org/10.1016/j.jmbbm.2019.07.022

Zucuni, C.P., Pereira, G.K.R., Valandro, L.F., 2020. Grinding, polishing and glazing of the occlusal surface do not affect the load-bearing capacity under fatigue and survival rates of bonded monolithic fully-stabilized zirconia simplified restorations. J. Mech. Behav. Biomed. Mater. 103, 103528. https://doi.org/10.1016/j.jmbbm.2019.103528

Zucuni, C.P., Venturini, A.B., Prochnow, C., Rocha Pereira, G.K., Valandro, L.F., 2019b. Load-bearing capacity under fatigue and survival rates of adhesively cemented yttrium-stabilized zirconia polycrystal monolithic simplified restorations. J. Mech. Behav. Biomed. Mater. 90, 673–680. https://doi.org/10.1016/j.jmbbm.2018.11.009

TABLES

Table 1. Results: Survival analysis by means of Kaplan-Meier and Mantel-Cox (Log-Rank) tests (mean and respective 95% confidence intervals for FFL – fatigue failure load and CF – number of cycles to failure) and Weibull analysis (Weibull modulus and respective 95% confidence intervals), for fatigue data; and roughness analysis by means of Kruskal Wallis and post-hoc LSD test (Ra and Rz parameters – mean and standard deviation).

Groups	Fatigue Failure Load	Weibull Modulus for FFL	Cycles to Failure	Weibull Modulus for CF	Ra	Rz
Ctrl	480 (433,34 – 526,65)^{BC}	6,3 (4,0 - 9,2)^{A}	81,000 (71668,53 – 90331,46)^{BC}	5,3 (3,4 - 7,8)^{A}	0.20 (0.05)^{C}	1.86 (0.73)^{C}
GLZ	586,66 (531,34 – 641,99)^{A}	5,6 (3,7 - 7,8)^{A}	102,333 (91267,92 – 113398,74)^{A}	4,9 (3,3 - 6,9)^{A}	0.85 (0.31)^{A}	4.93 (1.67)^{A}
SNF	476,66 (437,38 – 515,94)^{C}	7,7 (4,9 - 11,2)^{A}	80,333 (72477,79 – 88188,87)^{C}	6,5 (4,1 - 9,4)^{A}	0.20 (0.05)^{C}	1.76 (0.55)^{C}
AlOx	343,33 (291,06 – 395,60)^{D}	4,0 (2,5 - 5,9)^{A}	53,666 (43213,33 – 64120)^{D}	3,0 (1,9 - 4,5)^{A}	0.32 (0.04)^{B}	2.57 (0.75)^{B}
SiC	423,33 (355,12 – 491,54)^{BCD}	3,6 (2,3 - 5,2)^{A}	69,666 (56024,66 – 83308,66)^{BCD}	2,9 (1,9 - 4,3)^{A}	0.28 (0.04)^{B}	2.46 (0.75)^{B}
7% Si	386,66 (328,12 – 445,20)^{BCD}	3,7 (2,4 - 5,2)^{A}	62,333 (50625,30 – 74041,36)^{BCD}	3,0 (1,9 - 4,2)^{A}	0.32 (0.04)^{B}	2.61 (0.77)^{B}
- Different capital letters indicate statistical differences for each condition.						

Table 2. Survival probabilities of the study groups for different loading steps and number of cycles executed (probability to exceed the respective strength without failure and respective standard error value).

Groups	Load to failure / Number of cycles until failure															
	100/ 5 × 10^3	**150/ 10 × 10^3**	**200/ 15 × 10^3**	**250/ 20 × 10^3**	**300/ 25 × 10^3**	**350/ 30 × 10^3**	**400/ 35 × 10^3**	**450/ 40 × 10^3**	**500/ 45 × 10^3**	**550/ 50 × 10^3**	**600/ 55 × 10^3**	**650/ 60 × 10^3**	**700/ 65 × 10^3**	**750/ 70 × 10^3**	**800/ 75 × 10^3**	**850/ 80 × 10^3**
Ctrl	1.00	1.00	1.00	1.00	1.00	0.80 (0.10)	0.66 (0.12)	0.60 (0.12)	0.33 (0.12)	0.20 (0.10)	0.00 (0.00)	-	-	-	-	-
GLZ	1.00	1.00	1.00	1.00	1.00	1.00	0.93 (0.06)	0.86 (0.08)	0.66 (0.12)	0.60 (0.12)	0.40 (0.12)	0.06 (0.06)	…	…	…	0.00 (0.00)
SNF	1.00	1.00	1.00	1.00	1.00	0.80 (0.10)	…	0.60 (0.12)	0.26 (0.11)	0.06 (0.06)	0.00 (0.00)	-	-	-	-	-
AlOx	1.00	1.00	0.80 (0.10)	0.66 (0.12)	0.60 (0.12)	0.46 (0.12)	0.26 (0.11)	0.06 (0.06)	0.00 (0.00)	-	-	-	-	-	-	-
SiC	1.00	1.00	1.00	0.86 (0.08)	0.60 (0.12)	…	0.53 (0.12)	0.40 (0.12)	0.20 (0.10)	…	0.06 (0.06)	0.00 (0.00)	-	-	-	-
7% Si	1.00	1.00	0.93 (0.06)	0.80 (0.10)	0.66 (0.12)	0.60 (0.12)	0.40 (0.12)	0.13 (0.08)	0.06 (0.06)	…	…	0.00 (0.00)	-	-	-	-
- The symbol "-" indicates absence of specimen being tested on the considered step. - The symbol "…" indicates absence of specimen fracturing in the respective step for each condition.																

FIGURES

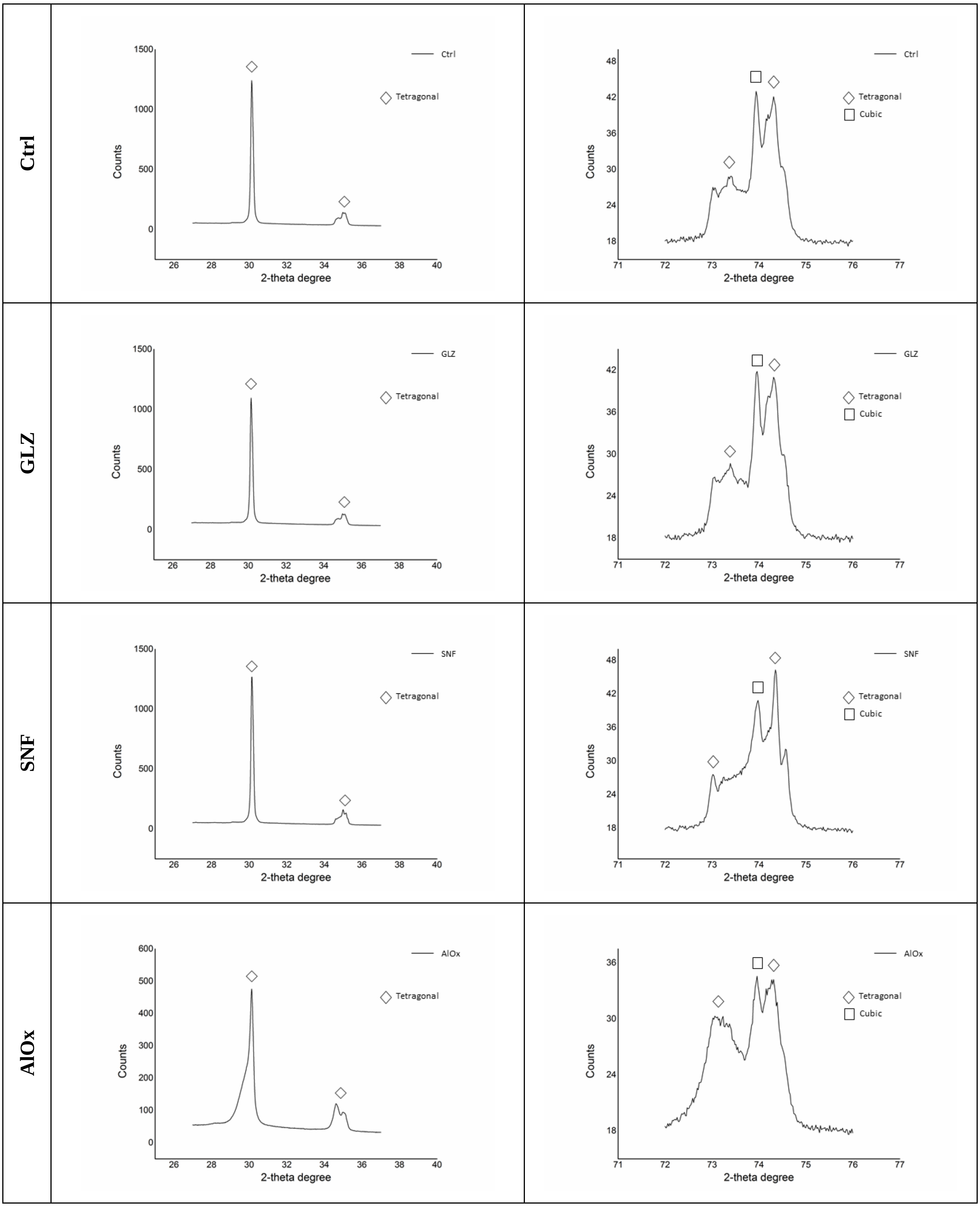

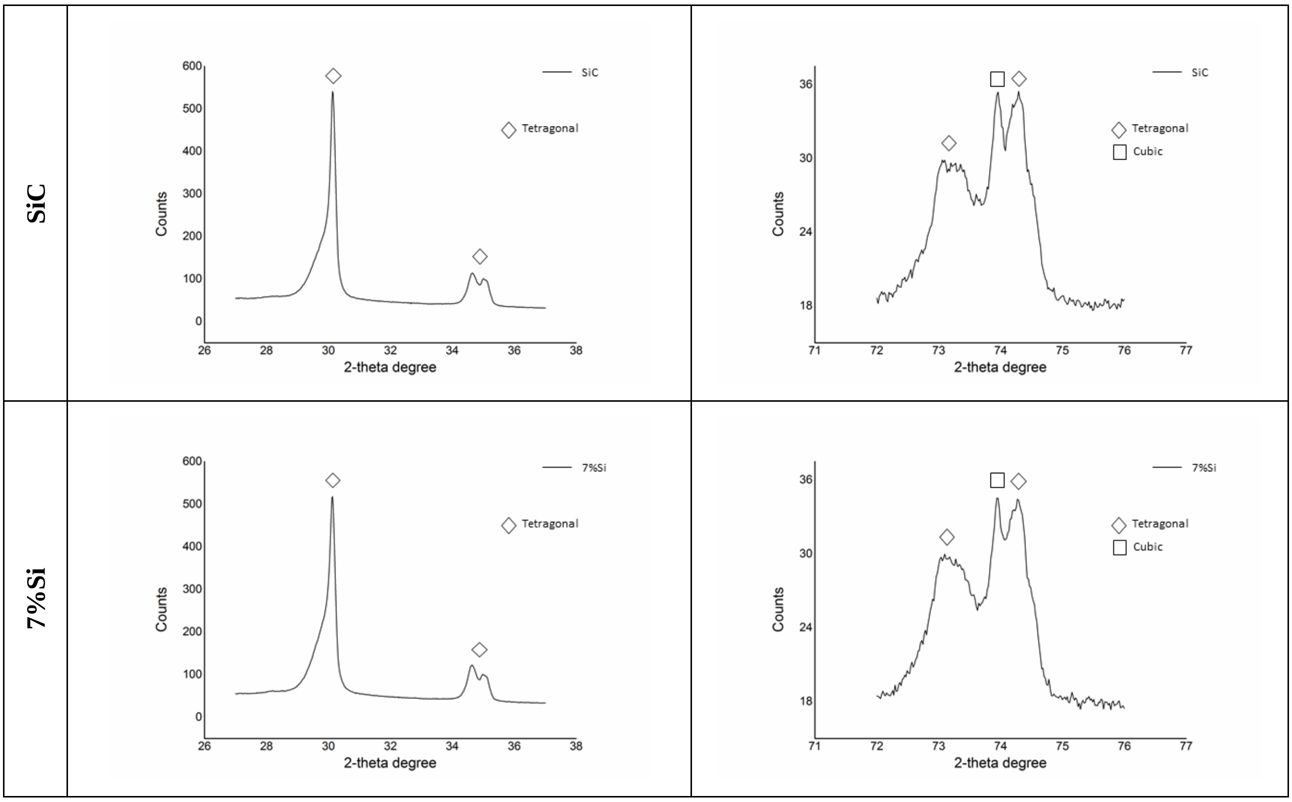

Figure 1. XRD graphs of each evaluated condition depicting the peaks related to each specific crystallographic phase (left graph: 2θ angular interval of 27–37°; right graph: 2θ angular interval of 72–76°), where tetragonal and cubic phase crystals could be observed.

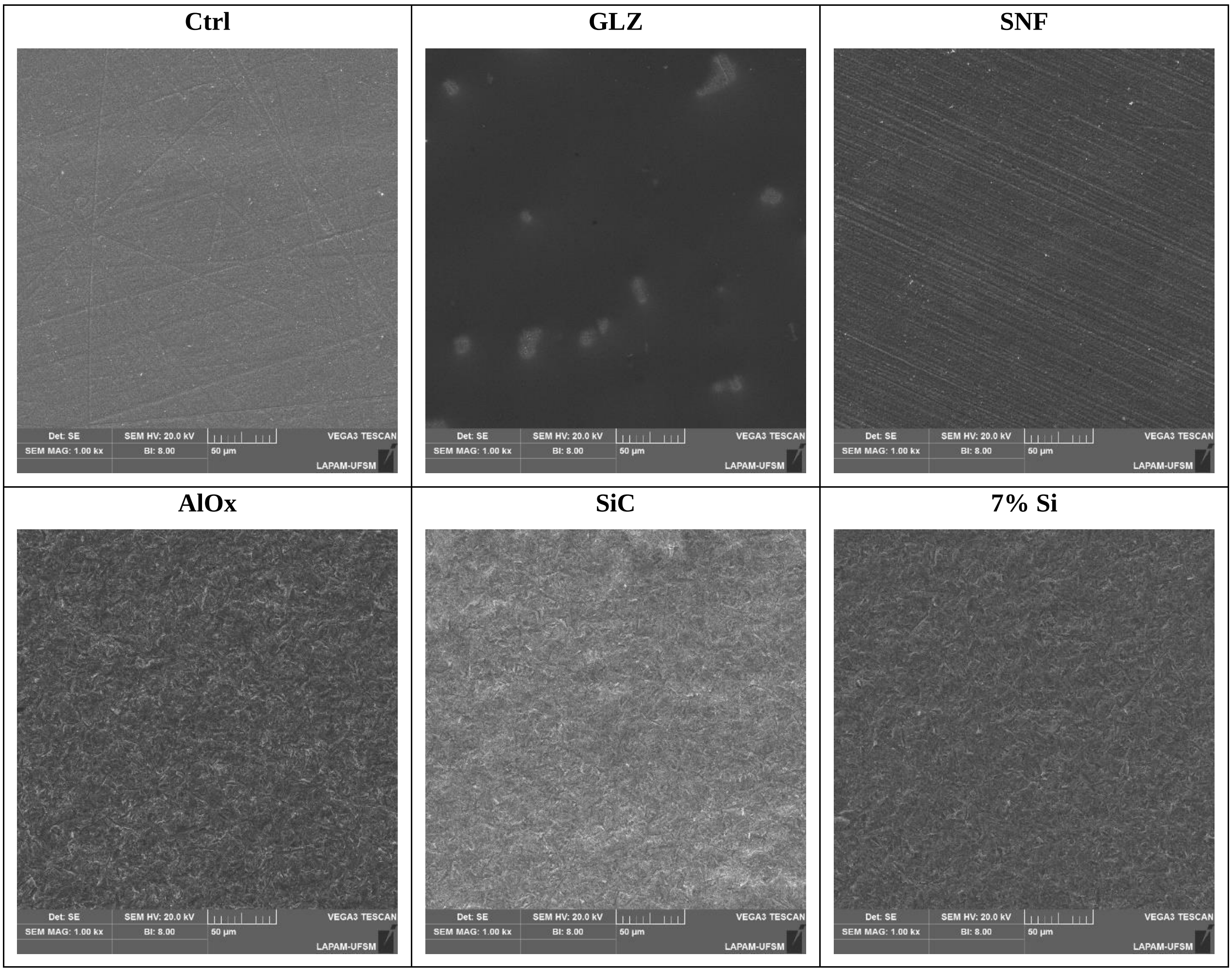

Figure 2. Representative SEM micrographs of the ceramic after each surface treatment at 1000× magnification. It notes that the air-abrasion protocols promoted a more prominent surface alteration compared with the Ctrl group and SNF that do not present alteration. The GLZ promoted a more homogeneous surface, but with remaining uncovered regions.

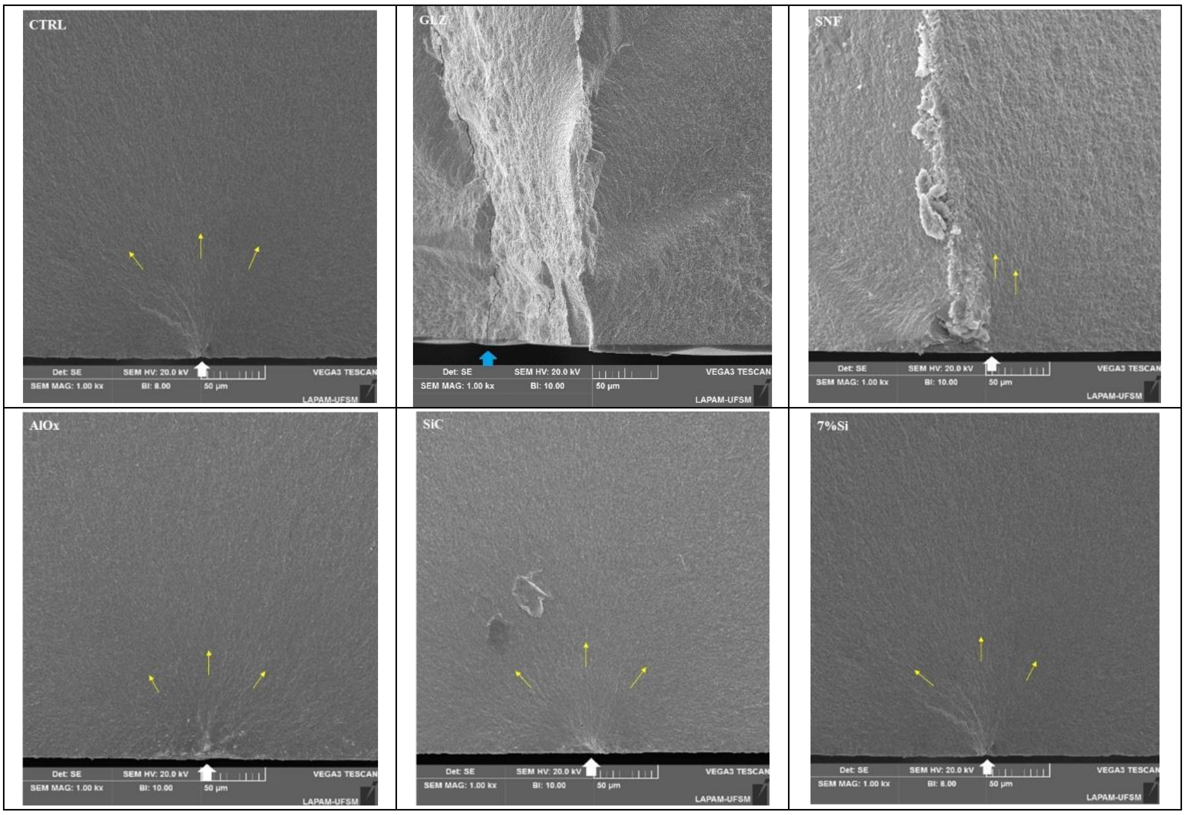

Figure 3. Representative SEM micrographics of fractured surfaces (fractographical examination) at 1000× magnification. It can be noted that the fractures originated from surface/sub-surface defects (indicated by the white arrows) at the center of ceramic surface, which was in the tensile side. The yellow arrows indicate the hackle lines, characteristics of fracture marks. The blue arrow in the GLZ group points to a probable secondary failure of the specimen. The GLZ group specimens failed in several fragments, making it difficult to find the source of the failure in the fractographic analysis.

3. ARTIGO 2 - Fatigue performance of fully-stabilized zirconia polycrystals monolithic restorations: The effects of surface treatments at the bonding surface

Este artigo está publicado (doi: 10.1016/j.jmbbm.2020.103962) no periódico Journal of the Mechanical Behavior of Biomedical Materials, Elsevier, ISSN: 1751-6161, Fator de impacto = 4.042; Qualis A2. As normas para publicação estão descritas no Anexo A.

Fatigue performance of fully-stabilized zirconia polycrystals monolithic restorations: The effects of surface treatments at the bonding surface

Ana Carolina Cadore-Rodrigues[a]; Pablo Soares Machado[a]; Jivago Schumacher de Oliveira[b]; Sérgio Luiz Jahn[b]; Gustavo Luiz Callegari[c]; Lucio Strazzabosco Dorneles[c]; Thiago Augusto de Lima Burgo[c]; Gabriel Kalil Rocha Pereira[a]; Luiz Felipe Valandro[a]

[a]Post-Graduate Program in Oral Science, Federal University of Santa Maria, Santa Maria, Rio Grande do Sul State, Brazil.
[b]Post-Graduate Program in Chemical Engineering, Federal University of Santa Maria, Santa Maria, Rio Grande do Sul State, Brazil.
[c]Post-Graduate Program in Physics, Physics Department, Federal University of Santa Maria, Santa Maria, Brazil.

Author e-mail addresses and contributions:
Ana Carolina Cadore-Rodrigues (anacadorerodrigues@gmail.com) – Conceptualization, Methodology, Formal analysis, Investigation, Writing - Original Draft, Writing - Review & Editing
Pablo Soares Machado (P17_SM@hotmail.com) – Investigation, Writing - Review & Editing
Jivago Schumacher de Oliveira (jivago.s.o@hotmail.com) – Investigation, Writing - Review & Editing
Sérgio Luiz Jahn (sergiojahn@gmail.com) – Resources, Writing - Review & Editing
Gustavo Luiz Callegari (glcallegari@gmail.com) – Investigation, Writing - Review & Editing
Lucio Strazzabosco Dorneles (lsdorneles@gmail.com) – Resources, Writing - Review & Editing
Thiago Augusto de Lima Burgo (burgounicamp@gmail.com) – Investigation, Writing - Review & Editing
Gabriel Kalil Rocha Pereira (gabrielkrpereira@hotmail.com) – Conceptualization, Methodology, Formal analysis, Writing - Review & Editing, Supervision
Luiz Felipe Valandro (valandrolf@gmail.com) – Conceptualization, Methodology, Writing - Review & Editing, Supervision

***Corresponding author at:**
Luiz Felipe Valandro, D.D.S., M.Sci.D., Ph.D., Full Professor,
Federal University of Santa Maria
Faculty of Odontology
Head of Ph.D.-M.Sci.D. Graduate Program in Oral Science
Prosthodontics-Biomaterials Unit
1000 Roraima Av., T Street, Building 26F, Room 2386
UFSM Campus, 97105-900
Rio Grande do Sul State, Santa Maria, Brazil
Phone: +55-55-3220-9276, Fax: +55-55-3220-9272
E-mail: valandrolf@gmail.com (Dr LF Valandro)

Short title: Surface treatment of FSZ monolithic restorations on fatigue behavior

Abstract

This study evaluated the distinct conditioning effect of the intaglio surface of bonded fully-stabilized zirconia (FSZ) simplified restorations on the mechanical fatigue behavior of the set prior to and after aging. Ceramic disc shaped specimens (Ø= 10 mm and 1 mm thick) were randomly allocated into 14 groups considering: “surface treatments” (Ctrl: no-treatment; PM: universal primer; GLZ: low-fusing porcelain glaze; SNF: 5 nm SiO_2 nanofilm deposition; AlOx: air-abrasion with aluminum oxide; SiC: air-abrasion with silica-coated aluminum oxide; 7%Si: air-abrasion with 7% silica-coated aluminum oxide); and “aging” (baseline: 24 hours at 37°C in water; or aged: 90 days at 37°C in water + 12,000 thermal cycles). The discs were treated, luted with resin cement onto the dentin analog, subjected to aging or not, and then tested under a step-stress fatigue test at 20 Hz, 10,000 cycles/step, step-size of 100N starting at 200N, and proceeding until failure detection. Fractographic, topographic, surface roughness, contact angle, and atomic force microscopy analyzes were performed. The surface treatments at baseline led to statistically similar fatigue failure loads (953N–1313N), except for GLZ (1313N), which was significantly higher than 7%Si (953N). Meanwhile, Ctrl had 40% pre-test failures (debonding) after aging, and therefore the worst fatigue performance (notable decrease in fatigue results), while all the other groups presented superior and statistically similar fatigue behavior (973–1271N). In fact, when considering baseline Vs aging conditions, stable fatigue results could only be noted when using surface treatments. In conclusion, internal surface treatments of FSZ ceramic restorations are mandatory for fatigue behavior stability after aging the restorative set, while non-treatment induced unstable results.

Keywords: Yttrium stabilized zirconia polycrystals; Fatigue phenomena; Surface treatments to enhance adhesion; Surface characteristics; Survival analysis.

Highlights

- Conditioning the intaglio surface of FSZ is mandatory for fatigue behavior stability.

- The non-treatment condition showed to be detrimental after aging (unstable results);

- No surface treatment proved to enhance FSZ fatigue performance after aging.

1. Introduction

Yttria stabilized zirconia (YSZ) is currently being used to manufacture full-contour monolithic fixed dental prostheses (FDPs) (Stawarczyk et al., 2017). The main reason is based on the fact that the use of monolithic restorations (without a porcelain covering material layer) avoids the risk of chipping, as this is one of the main reported failures of bilayer-based FDPs with a zirconia framework (Sailer et al., 2015). A new class of YSZ material has more recently been proposed for such use, named fully-stabilized zirconia (FSZ), categorized as a third generation zirconia (Stawarczyk et al., 2017). In comparison to the prior generations (partially-stabilized zirconia - PSZ), the third generation emerged by increasing the percentage of yttrium oxide stabilizer resulting in a fully stabilized material, in which up to 53vol% of cubic phase crystals are found in its microstructure (Stawarczyk et al., 2017). Such a change also enabled satisfactory translucency (Stawarczyk et al., 2017; Zhang et al., 2016). However, as previously explored, the ability to transformation toughening mechanisms (t-m phase transformation) was lost, and in doing so, the ability of the material to respond to existing defects and hinder crack propagation (Pereira et al., 2018; Stawarczyk et al., 2017).

In addition, FSZs still present a polycrystalline structure (Stawarczyk et al., 2017), and therefore they are non-etchable (not susceptible to the action of hydrofluoric acid etching, which is the classic treatment to enhance adhesion to vitreous ceramics), which hinders the micromechanical bonding, as it requires additional and alternative surface treatments (Özcan and Vallittu, 2003; Thompson et al., 2011). In this sense, it is noted that different methods of surface treatments for adhesion enhancement between PSZ and resin cements and the consequent improvements on the fatigue behavior of the restorative set have been already evaluated; however, to the best of the authors' knowledge, there are no studies which have investigated such a theme for FSZ ceramics.

The gold standard method of surface treatments for PSZ materials is air-abrasion with aluminum oxide particles covered (or not) by silica (Melo et al., 2015; Mosele and Borba, 2014; Özcan and Bernasconi, 2015; Thompson et al., 2011; Tzanakakis et al., 2016). This protocol creates a rough surface providing mechanical retention for the cements and making the ceramic surface more chemically reactive to silane agents, increasing the adhesive potential of such surface to resin cements (Mosele and Borba, 2014; Ozcan and Bernasconi, 2015). Prior studies (Amaral et al., 2016; Özcan et al., 2013; Scherrer et al., 2011; Souza et al., 2013) have shown that the defects introduced by such treatment were not detrimental to the fatigue performance of PSZ materials because they are usually counteracted by the transformation toughening mechanism, which is corroborated by a systematic review with meta-analysis (Aurélio et al., 2016). However, when considering FSZ ceramics (with no toughening mechanism as aforementioned), recent studies show a reduction in mechanical strength after air-abrasion (Kontonasaki et al., 2020; Sulaiman et al., 2017). Thus, this scenario raises the questions: "How should we proceed to treat the surface of FSZ ceramics without predisposing it to premature failure?” or even “Which is the best surface treatment to induce great fatigue behavior, preventing early failure?”.

An alternative surface treatment method which was studied for PSZs was the application of a thin layer of porcelain glaze which makes the external zirconia surface rich in silica (Pozzobon et al., 2017b; Valentino et al., 2012; A Vanderlei et al., 2014). This method also optimized the interaction between the adhesive and substrate, and enhanced siloxane chemical bonds between the deposited silica (the silane component), and posteriorly to the resin cements (Cattell et al., 2009; Cura et al., 2012; Kitayama et al., 2009; Valentino et al., 2012). Despite this, its inferior performance compared to air-abrasion was attributed to the inferior micromechanical retention generated as air-abrasion unleashed greater surface topographical alterations (Zucuni et al., 2019) and a probable incompatibility (weak adhesion) between the glaze and zirconia surface (Pozzobon et al., 2017a). Therefore, it is hypothesized that such inferior potential to promote topographic alteration in FSZ may be beneficial because this minor induced damage can soften or prevent the negative effects on the mechanical performance of such a ceramic which is not able to respond through transformation toughening.

Another alternative surface treatment for PSZs is silica deposition on ceramic surface through the physical vapor deposition (PVD) using magnetron sputtering (De Queiroz et al., 2011; Piascik et al., 2009). This treatment is also a method based on chemical adhesion, in which SiO_2 nanofilms associated with silanization showed an increase in bond strength, as well as not causing damage to the zirconia surface (De Queiroz et al., 2011; Druck et al., 2015). The same statements presented in glaze application can also be considered for PSZ materials, as this treatment triggered lesser surface alteration, and it also unleashed lower micromechanical retention, and were therefore inferior to air-abrasion. However, a third generation could present the opposite effect, being positive based on less defect introduction.

Lastly, a new silica-coated aluminum oxide particle powder was also developed for PSZ and appears as a potential alternative for FSZ (Cadore-Rodrigues et al., 2019). In these studies it was demonstrated that this new material promoted better mechanical performance (Cadore-Rodrigues et al., 2019) along with higher and more stable bonding (Cadore-Rodrigues et al., 2020) in comparison to the classic aluminum oxide powders, since they also provided a more regular and shallower topographical defect pattern, and which could be promising for FSZ.

Thus, based on the aforementioned information, this study aimed to evaluate the distinct conditioning effect of the intaglio surface of bonded FSZ ceramic simplified restorations on the mechanical fatigue behavior of the set prior to and after aging. Based on the scarce data of FSZ performance, we assumed the null hypotheses that the FSZ simplified zirconia restorations would present similar fatigue behavior, regardless of the surface treatments and aging conditions.

2. Materials and methods

Simplified geometry was used for testing in the present study to mimic the behavior of adhesively luted monolithic restorations of a posterior tooth (Chen et al., 2014). In this sense, ceramic discs were made simulating monolithic restorations and epoxy resin discs (dentin analog material) the tooth to be restored, where both substrates had its surface treated and then luted with a resin cement. The description of the materials used in this study are presented in Table 1.

2.1 Sample Preparations

2.1.1 Ceramic discs

FSZ blocks (IPS e.Max ZirCAD MT Multi, Ivoclar Vivadent, Schaan, Liechtenstein) were shaped into cylinders with #600 and #1200 grit silicon carbide paper (3M, Sumare, Brazil) under refrigeration. Next, two hundred and ten ceramic discs were obtained using a precision cutting machine with a diamond blade (ISOMET 1000, Buehler, IL, USA). The discs were polished with #600 to #1200 grit silicon carbide paper (3M, Sumare, Brazil) to remove surface irregularities inherent to cutting, and the specimens were subsequently sintered (1550 °C for 2 h) in a specific furnace (Zyrcomat 6000 MS, Vita Zahnfabrik, Bad Säckingen, Germany), presenting 10 mm diameter and 1 mm thickness in the final dimensions. Finally, the specimens were randomly allocated into 14 groups (n=15), taking into account the factors ‘surface treatments’ and ‘aging conditions’ (Table 2).

2.1.2 Epoxy resin discs

Epoxy resin plates with 2 mm thickness (Epoxy Plate 150 Plate 150 × 350 x 2.0 mm; Carbotec GmbH & Co. KG, Königs Wusterhausen, Germany) were used to make two hundred and ten discs of dentin analog material using a cylindrical trephine drill (internal diameter of 10 mm - Diamant Boart, Brussels, Belgium), under constant water irrigation and then randomly allocated into pairs with the ceramic discs, i.e. into the 14 groups.

2.2 Surface Treatments

The ceramic discs were first cleaned in distilled water in ultrasonic bath (Vitasonic, Vita Zahnfabrik, Bad Säckingen, Germany) for 5 minutes. Afterward, the intaglio surfaces of the simplified FSZ restorations were subjected to the surface treatments as described in Table 2, and the primer (Monobond Plus, Ivoclar Vivadent) was applied according to the manufacturer’s recommendations (except for the control group, which did not receive primer application).

For the bonding surface conditioning of the epoxy resin discs, 10% hydrofluoric acid (Condac Porcelain, FGM, Joinville, Brazil) was applied for 1 min, followed by air-water spray for 30 sec and ultrasonic bath (Vitasonic, Vita Zahnfabrik) with distilled water for 5 min. Next, a mixture of primers A and B (ratio 1:1; Multilink Automix, Ivoclar Vivadent) was scrubbed onto the treated surfaces for 30 sec and air-dried until a thin layer was obtained.

2.3 Cementation procedure

For the cementation procedure, the dual-cured resin cement pastes (Multilink Automix, Ivoclar Vivadent) were mixed and applied onto the ceramic surface. The discs were then placed over the epoxy resin discs under a constant load of 2.5N for 5 min. The cement excesses were removed with a microbrush and light-cured (intensity of the light curing: 1200 mW/cm^2; Radii-cal LED curing light, SDI, Bayswater, Australia) for 20 sec in the four directions of the bonded area (0°, 90°, 180° and 270°), and at the occlusal surface.

2.4 Aging conditions

Two storage conditions were considered: the specimens for the baseline groups (not aged) were stored in distilled water for 24 h at 37°C prior to testing; however, the specimens for the aging condition were stored in distilled water at 37°C for 90 days and then subjected to additional thermal-cycling (12,000 cycles, 5-55°C, 30 sec dwell time, 2 sec transfer time from one bath to the other; Nova Etica, Varzea Grande Paulista, Brazil) prior to testing.

2.5 Fatigue tests (Step-stress approach)

The cemented assemblies (n=15) were submitted to a fatigue test on an electrical mechanical testing machine (Instron ElectroPuls E3000; Instron Corporation, Norwood, USA) using the step-stress methodology (Kelly et al., 2017; Venturini et al., 2019). A cylindrical metal ring was used to control specimen positioning, ensuring that the load application occurred in the center of the specimens, always at the exact same position. The specimens were loaded by a hemispherical stainless-steel piston with 40 mm in diameter positioned in the center of the occlusal ceramic surface stabilized in a flat steel base under water (Figure 1). An adhesive tape (110µm) was fixed on the occlusal side of each specimen before testing to improve contact with the piston and to prevent contact surface damage (i.e. Hertzian cone cracks) (Prochnow et al., 2018b).

Next, cyclic intermittent loads were applied at a frequency of 20Hz, starting with an initial load of 200N for 5,000 cycles to adjust the sample/piston contact, followed by steps of 400N, 500N, and so on, with a fixed load increment of 100N for 10,000 cycles at each load step until the occurrence of failure. At the final execution of each step load of the fatigue test, the specimens were examined under oblique light transmission to visually inspect for radial cracks. If they were not detected, the load level was increased and the test proceeded. However, if radial cracks were detected, the sample was classified as “failed”, the fatigue test ended for the sample and the collected data was recorded for statistical analysis (FFL – fatigue failure load and CFF – cycles for fatigue failure).

The failed specimens were inspected after testing for fractographic analysis. To do so, the ceramic fragments which presented a radial crack and were still attached to the epoxy resin substrate were carefully detached with a scalpel and submitted to further Scanning Electron Microscopy analysis (SEM - VEGA3, Tescan, Brun, Czech Republic) (Acceleration Voltage: 20 KV; Emission Current: 86 pA; Detector: SE - Secundary Electron; Beam Intensity: 8; Work Distance: 15 mm) at 250× and 1,000× magnifications to determine the origin of failure, among other fractographic features.

2.6 Roughness analysis

Additional specimens were produced (n=15) and submitted to the surface treatments (Table 2). A micrometric analysis was performed with a profilometer (Mitutoyo SJ-410, Mitutoyo, São Paulo, Brazil) where three measurements for each specimen were executed considering Ra and Rz parameters of ISO 4287:1997 (cut-off of 5; λC of 0.8 mm; λS of 2.5 µm). Ra is defined as the arithmetical mean of the absolute values of peaks and valleys measured from a mean plane (in µm), and Rz is the average distance between the five highest peaks and five major valleys of a surface (in µm).

2.7 Scanning electron microscopy (SEM)

Analyses by SEM (VEGA3, Tescan) were also performed to determine the topographical pattern of the ceramic surfaces after the different surface treatments. To do so, one additional treated ceramic specimen of each group was coated with gold-palladium alloy, and images in second electron mode (SE) (Acceleration Voltage: 1 kV; Working distance: 5.0 mm; Detector: SE – Secundary electron) were obtained at 5000× and 30000× magnifications.

The Energy Dispersive Spectroscopy (EDS) mode (VEGA3, Tescan, Brun, Czech Republic) was then used to determine the elemental chemical composition of ceramic surfaces and to confirm (or discard) the presence of silica at the treated surfaces.

2.8 Atomic Force Microscopy (AFM) measurements

One additional specimen of each condition was produced for AFM measurements. Specimens were imaged in tapping or non-contact mode, and 3D topography maps were recorded on a Park NX10 microscope (Park Systems, Suwon, Korea) equipped with SmartScan software version 1.0.RTM11a. Fractal dimension (FD) is a measure which enables estimating the surface topographical complexity, and was obtained at five different regions of each specimens and calculated using the box-counting (BC) method with Park XEI software version 4.3.4 Build 22.RTM1. The BC approach is one of the most used techniques to estimate the FD of an image for its simplicity and automaticity, and is based on the linear interpolation of the pixels in the AFM topography image. In the BC method, the image is imagined to be enclosed in a cubic area. The BC algorithms find an optimized way to subdivide the cubes into smaller pieces to reach the image resolution and thus the collective volume of the cubes increases as their size decreases. The FD is formally calculated as $D = \lim_{\varepsilon \to 0} \frac{log\ N(\varepsilon)}{log\ (\varepsilon)}$, where N(ε) is the minimum number of n-dimensional cubes of side ε to properly cover the image. Thus, the FD for AFM topography images is a non-integer number between 2 and 3 (Schestatsky et al., 2019).

2.9 Contact angle measurement

Additional specimens were also produced for contact angle analysis (n=5) to evaluate the surface wettability according to the surface treatments (Table 2). The contact angle was measured by the sessile drop technique using a goniometer (Drop Shape analysis, model DSA 30S, Krüss GmbH, Hamburg, Germany), which was connected to a computer with a dedicated software program (DSA3, V1 .0.3-08, Kruss GmbH, Hamburg, Germany). One drop (11 μl) of distilled water at room temperature (± 24ºC) was placed at the center of each treated ceramic surfaces using a syringe. After 5 sec, 5 contact angle measurements were taken to produce a mean contact angle value for each tested sample.

2.10 Statistical analysis

After aging conditions, the Ctrl presented 40% of debonding (pre-test failures) and no value was assigned to them. Statistical analysis for FFL and CFF were performed using Kaplan Meier and Mantel-Cox (Log-Rank) tests (α=0.05; SPSS version 21, IBM Analytics, New York, USA). The FFL and CFF data were also submitted to Weibull statistical analysis to describe the Weibull modulus (shape m - mechanical reliability of the material) using the maximum likelihood estimation method at the Super SMITH Weibull 4.0k-32 software program (Wes Fulton, Torrance, USA). Fractographic features and SEM analysis were descriptively/qualitatively analyzed. As FD assumed a parametric and homoscedastic distribution, One-Way ANOVA and Tukey's post-hoc test (α=0.05) were used (SPSS 21, IBM Analytics). According Shapiro-Wilk test, the contact angle and roughness data assumed a non-parametric but homoscedastic distribution, and therefore the Kruskal Wallis and LSD post-hoc tests (α=0.05) were employed (SPSS 21, IBM Analytics).

3. Results

The surface treatments led to statistically similar fatigue performance (FFL, CFF, survival rates) when considering the baseline condition, except for the GLZ group which was statistically superior to 7%Si (Table 3). When analyzing the aged groups, the Ctrl group presented 40% pre-test failure and therefore had the worst fatigue performance, showing unstable results (baseline > aging). All the other groups had no statistically significant difference compared to each other, as all of them promoted stable fatigue values (baseline = aging, i.e. stability through aging). Table 4 demonstrates the survival rates, highlighting the early failure (lower survival rates) for the aged Ctrl group. SEM analysis of fractured specimens (Figure 3) showed that all failures were radial cracks starting from the intaglio surface of the FSZ restorations. Cracks due to contact damage between the piston and the ceramic surface were not found. According Weibull analysis, all groups presented similar Weibull modulus, except for the Ctrl group in aging condition that presented the lowest values (Table 3, Figure 4).

Regarding roughness data (Table 5) and topography alterations (Figure 2), the GLZ group presented the highest surface roughness (despite the most homogeneous surface at SEM and the lowest FD at AFM), while the Ctrl and SNF groups presented the lowest values (where SEM images clearly shows the crystallographic grains of zirconia, and FD was similar to GLZ). The air-abrasion with AlOx, 7% Si and SiC promoted similar surface roughness, as the SiC was also similar to the SNF group. SEM images clearly corroborate AlOx, 7% Si and SiC as promoting surface deformation and introducing a more heterogeneous surface pattern, which was also the highest FD in the AFM analysis.

EDS analysis of the powders confirmed the presence of silica in GLZ, SiC and 7% Si groups (Table 5), where the GLZ group presented a greater amount of silica deposited than the other groups (which showed similar content to each other). Finally, the contact angle values showed that the SiC and 7% Si groups presented the lowest contact angle values, followed by the AlOx and GLZ groups (Table 5). The SNF and Ctrl groups presented the two highest contact angle values.

4. Discussion

The assumed null hypothesis that the FSZ zirconia restorations would present similar fatigue behavior regardless of the surface treatments and aging conditions, was rejected, as distinct fatigue results were shown for the assessed surface treatments. This was mainly notable in the decrease in fatigue performance of the Ctrl group after aging, and was different from the other groups.

According to the findings of this study, different surface treatments of FSZ restorations evaluated in a short period of time (baseline) do not show a beneficial statistical influence on the fatigue performance of the set when compared to the control group (without treatment) (Table 3).

However, air-abrasion with 7%Si led to a statistically lower fatigue performance in comparison to the application of a glaze material. In fact, when considering the absence of beneficial influence of surface treatments in comparison to non-treatment at baseline (non-aged) condition, it could reinforce the classic indication of manufacturers in terms of cementing YSZ restorations by using conventional strategies (non-adhesive) (Stawarczyk et al., 2017b). Such a statement is also justified by the polycrystalline microstructure of YSZ and its inherent superior mechanical performance in comparison to glass-ceramics, for example (Stawarczyk et al., 2017b). Nevertheless, the literature has shown that resin-zirconia interface is unstable under long-time storage (Druck et al., 2015; May et al., 2010; Ozcan and Bernasconi, 2015; Passos et al., 2010; A Vanderlei et al., 2014; Wegner et al., 2002) due to the bond hydrolyzation and degradation processes trigged during aging, meaning that long-term aging is necessary to achieve reliable results when evaluating zirconia substrate bonded to resin materials. Thus, the current findings at baseline condition should be viewed with caution.

From this point of view, we observed that the absence of surface treatment (or the hypothesized use of a non-adhesive cementation protocol) when aging occurs (temperature changes and storage inducing dimensional expansion/contraction, residual stresses, and luting agent hydrolysis) can strongly influence the mechanical fatigue performance of the set (FSZ restorations luted onto dentin analog), which confirms that surface treatments of the intaglio surface of FSZ restorations and adhesive cementation (using resin cement) is mandatory for stable fatigue behavior. Existing *in vivo* observations also confirm this assumption, as the use of conventional cement for zirconia ceramic cementation was related to an increased rate of retention loss (Rinke et al., 2013). Moreover, *in vitro* studies have demonstrated significantly lower fatigue resistance when YSZ restorations are cemented with non-adhesive approaches (Anami et al., 2016; Campos et al., 2016; Fraga et al., 2018; Guilardi et al., 2019).

It is also important and undeniable that all surface treatments explored herein were not able to promote differences in mechanical fatigue performance of adhesively luted FSZ restorations. They inherently showed potential to generate different topographical features, superficial roughness, fractal dimension, contact angle measurements, as observed in the present data and also corroborated in existing literature (Bottino et al., 2014; Druck et al., 2015; Pozzobon et al., 2017a; Vanderlei et al., 2014). In fact, they even showed the potential to induce different bond strengths by *in vitro* studies (Pozzobon et al., 2017b; Vanderlei et al., 2014). Nevertheless, such differences were not able to alter the mechanical fatigue performances when the restorative set was aged. Thus, from the fatigue behavior improvement viewpoint, we understand that all of the assessed surface treatment have some potential for high zirconia/resin bond strength and induce high fatigue performance of FSZ restorations, as observed when glass ceramics are subjected to acid etching and silanization (de Kok et al., 2017; Prochnow et al., 2018a). Other studies strengthen this claim, demonstrating that zirconia surface treatments promote a beneficial effect for fatigue improvements compared to a non-treated condition, or the use of a non-adhesive strategy (Campos et al., 2016; Fraga et al., 2018; Guilardi et al., 2019).

It is known that aging by thermocycling affects the adhesive joint by the fact that the materials (ceramic/cement/substrate) present different lineal thermal expansion coefficients (LTEC) (they contract and expand differently) (Andreatta Filho et al., 2005). Water storage and thermal cycling might alter the properties of resin materials due to their different LTEC, leading to stresses at the adhesive interface which accelerate their structural weakness, in turn promoting bond flaws (Andreatta Filho et al., 2005; Wegner et al., 2002), which consequently might induce material fatigue resistance reduction. Thus, as already mentioned, the aging performed herein induced a reduction in the fatigue outcome of the control group (without treatment) (Table 4 and 5), probably due to the weak adhesion between the resin and FSZ substrate, inducing high susceptibility for interface degradation, uneven stress distribution in the set, and consequently greater probability of failure. This is supported by the high failure percentage before the test (40%) observed in the control group, and that the specimens which fractured during testing were usually associated with ceramic fragment detachment (debonding), which was not observed on the surface treated groups. In summary, the poor adhesion damaged the fatigue performance of this group, therefore confirming that the FSZ treatments are mandatory for improved fatigue outcomes.

Successful adhesion among ceramic, cement and substrate requires a bonding mechanism which associates micro-mechanical interlocking and chemical bonding (Blatz et al., 2018). Surface treatments that promotes surface alterations can increase the roughness, leading to micro retentions that can enhance the adhesion with the substrates (Özcan and Vallittu, 2003). Whereas, for chemical bonding, a surface with a chemical composition rich in silica increases the possibility of siloxane bonds with the silane coupling agent that promotes lower contact angle and consequently increases the wettability of the substrate (Özcan and Bernasconi, 2015). Proper adhesion can better distribute stress during loading, increasing the material's resistance (Attia et al., 2006; Chen et al., 2014). Thus, adhesive cementation significantly increases the restorative material's fracture loads (de Kok et al., 2017). Nevertheless, a higher contact angle and micro retentions not filled by resin cement can promote air bubbles and reminiscent defects that may act as critical defects leading to stress concentration, crack propagation, and consequently causing premature failure of the assembly (Prochnow et al., 2018b; Venturini et al., 2018).

In this sense, the capacity of the resin cement to completely fill the introduced superficial defects is an important predictor of the restoration performance (Thompson et al., 1998). Cements with low viscosity are more prone to penetrate the ceramic irregularities than cement with high viscosity (Kelly et al., 1996); a complete filling of the irregularities is necessary to better distribute stress through the assembly during loading, increasing the material's resistance (de Kok et al., 2017; Guilardi et al., 2020). Accordingly, although the surface treatments promote different topography and roughness, the resin cement used may have been able to infiltrate the created defects, thus providing better stress distribution and promoting similar fatigue performance. Therefore, it may be pertinent to explore the performance of cements which contain different viscosities.

According to the chemical elemental analysis, the application of low-fusing glaze (GLZ group) promoted the higher percentage of silica in the ceramic surface compared to the other surface treatments (Table 5). Even with the higher percentage, all surface treatments were able to remain stable after aging (Table 3). The analysis of Energy Dispersive Spectroscopy (EDS) is an analytical technique used for elementary analysis or chemical characterization of a sample. EDS is a local analysis which presents limited depth, being limited to the external surface of the analysis. As Glaze is applied covering the ceramic surface, the thickness of the glaze surpasses the depth of the EDS analysis. Thus, a low percentage of Zr is observed in this group. The low content observed can be related to a place where the glaze layer was thinner or absent.

The PM group surprisingly presented adequate fatigue performance which was similar to the other groups (Table 4 and 5) after aging. According to the literature, mechanical and chemical surface treatments have been proposed for bonding to zirconia in order to modify its surface properties and enhance bond strength (Özcan and Vallittu, 2003; Thompson et al., 2011). The mechanical interlocking generated by the roughness present on the zirconia surface associated with the chemical interaction generated by the primer were probably already sufficient to optimize some degree of adhesion, thereby being responsible for maintaining the fatigue performance. However, in our opinion this finding for PM groups should be confirmed by future studies.

Finally, the step-stress methodology optimizes the time of testing, employs varying stress amplitudes in the same specimen and may be used to estimate longer lifetimes (Kelly et al., 2017). Despite all the previously explored strengths in the study, it is important to highlight that it also presents some inherent limitations such as: the application of only axial loads during the fatigue test (without sliding and lateral forces), the absence of a complete oral environment simulation such as pH/temperature changes, and the use of a simplified restorative set to mimic posterior restorations (disc-shaped specimens without occlusal anatomy).

5. Conclusions

- Intaglio surface conditionings of FSZ restorations promoted stable fatigue behavior after aging of the restorative set, while non-treatment induced unstable results.
- Internal surface treatments of FSZ ceramic restorations are mandatory in terms of fatigue outcomes.

ACKNOWLEDGEMENTS

The authors declare no conflict of interests and emphasize that this study was partly financed by the Brazilian Federal Agency for Coordination of Improvement of Higher Education Personnel (*CAPES*) (Finance code 001; Doctorate Scholarship of A. C. C-R). We especially thank Ivoclar Vivadent for donating some materials, and finally we emphasize that those institutions had no role in the study design, data collection or analysis, decision to publish or in preparing the manuscript.

REFERENCES

Amaral, M., Cesar, P.F., Bottino, M.A., Lohbauer, U., Valandro, L.F., 2016. Fatigue behavior of Y-TZP ceramic after surface treatments. J. Mech. Behav. Biomed. Mater. 57, 149–156. https://doi.org/10.1016/j.jmbbm.2015.11.042

Anami, L.C., Lima, J.M.C., Valandro, L.F., Kleverlaan, C.J., Feilzer, A.J., Bottino, M.A., 2016. Fatigue resistance of Y-TZP/porcelain crowns is not influenced by the conditioning of the intaglio surface. Oper. Dent. 41, E1–E12. https://doi.org/10.2341/14-166-L

Andreatta Filho, O.D., Araújo, M.A.J. de, Bottino, M.A., Nishioka, R.S., Menezes, M.M., 2005. Study of thermocycling effect on the bond strength between an aluminous ceramic and a resin cement. J. Appl. Oral Sci. 13, 53–57. https://doi.org/10.1590/s1678-77572005000100011

Attia, A., Abdelaziz, K.M., Freitag, S., Kern, M., 2006. Fracture load of composite resin and feldspathic all-ceramic CAD/CAM crowns. J. Prosthet. Dent. 95, 117–123. https://doi.org/10.1016/j.prosdent.2005.11.014

Aurélio, I.L., Marchionatti, A.M.E., Montagner, A.F., May, L.G., Soares, F.Z.M., 2016. Does air particle abrasion affect the flexural strength and phase transformation of Y-TZP? A systematic review and meta-analysis. Dent. Mater. 32, 827–845. https://doi.org/10.1016/j.dental.2016.03.021

Blatz, M.B., Vonderheide, M., Conejo, J., 2018. The Effect of Resin Bonding on Long-Term Success of High-Strength Ceramics. J. Dent. Res. 97, 132–139. https://doi.org/10.1177/0022034517729134

Bottino, M.A., Bergoli, C.D., Lima, E.G., Marocho, S.M.S., Souza, R.O.A., Valandro, L.F., 2014. Bonding of Y-TZP to dentin: Effects of Y-TZP surface conditioning, resin cement type, and aging. Oper. Dent. 39, 291–300. https://doi.org/10.2341/12-235-L

Cadore-Rodrigues, A.C., Prochnow, C., Rippe, M.P., Oliveira, J.S. de, Jahn, S.L., Foletto, E.L., Pereira, G.K.R., Valandro, L.F., 2019. Air-abrasion using new silica-alumina powders containing different silica concentrations: Effect on the microstructural characteristics and fatigue behavior of a Y-TZP ceramic. J. Mech. Behav. Biomed. Mater. 98, 11–19. https://doi.org/10.1016/j.jmbbm.2019.05.032

Cadore-Rodrigues, A.C., Prochnow, C., Burgo, T.A.L., Oliveira, J.S. de, Jahn, S.L., Foletto, E.L., Rippe, M.P., Pereira, G.K.R., Valandro, L.F., 2020. Stable Resin Bonding to Y-TZP Ceramic With Air Abrasion by Alumina Particles Containing 7% Silica. J Adhes Dent. 22(2), 149-159. https://doi.org/10.3290/j.jad.a44151

Campos, Sa, V., Cj, F., 2016. Adhesive Cementation Promotes Higher Fatigue Resistance to Zirconia Crowns. https://doi.org/10.2341/16-002-L

Cattell, M.J., Chadwick, T.C., Knowles, J.C., Clarke, R.L., 2009. The development and testing of glaze materials for application to the fit surface of dental ceramic restorations. Dent. Mater. 25, 431–441. https://doi.org/10.1016/j.dental.2008.09.004

Chen, C., Trindade, F.Z., De Jager, N., Kleverlaan, C.J., Feilzer, A.J., 2014. The fracture resistance of a CAD/CAM Resin Nano Ceramic (RNC) and a CAD ceramic at different thicknesses. Dent. Mater. 30, 954–962. https://doi.org/10.1016/j.dental.2014.05.018

Cura, C., Isik, G., Saracoglu, A., Özcan, M., 2012. Comparison of alternative adhesive cementation concepts for zirconia ceramic: Glaze layer vs zirconia primer. J. Adhes. Dent. 14, 75–82. https://doi.org/10.3290/j.jad.a21493

de Kok, P., Pereira, G.K.R., Fraga, S., de Jager, N., Venturini, A.B., Kleverlaan, C.J., 2017. The effect of internal roughness and bonding on the fracture resistance and structural reliability of lithium disilicate ceramic. Dent. Mater. 33, 1416–1425. https://doi.org/10.1016/j.dental.2017.09.018

De Queiroz, J.R.C., Duarte, D.A., De Assunção E Souza, R.O., Fissmer, S.F., Massi, M., Bottino, M.A., 2011. Deposition of SiOx thin films on Y-TZP by reactive magnetron sputtering: Influence of plasma parameters on the adhesion properties between Y-TZP and resin cement for application in dental prosthesis. Mater. Res. 14, 212–216.

https://doi.org/10.1590/S1516-14392011005000032

Druck, C.C., Pozzobon, J.L., Callegari, G.L., Dorneles, L.S., Valandro, L.F., 2015. Adhesion to Y-TZP ceramic: Study of silica nanofilm coating on the surface of Y-TZP. J. Biomed. Mater. Res. - Part B Appl. Biomater. 103, 143–150. https://doi.org/10.1002/jbm.b.33184

Fraga, S., Jager, D., Campos, F., Valandro, F., 2018. Does Luting Strategy Affect the Fatigue Behavior of 20, 307–316. https://doi.org/10.3290/j.jad.a40988

Guilardi, L., Kalil, G., Pereira, R., Carlos, J., Johannes, C., Felipe, L., Pivetta, M., 2019. Journal of the Mechanical Behavior of Biomedical Materials E ff ect of zirconia surface treatment , resin cement and aging on the load- bearing capacity under fatigue of thin simpli fi ed full-contour Y-TZP restorations. J. Mech. Behav. Biomed. Mater. 97, 21–29. https://doi.org/10.1016/j.jmbbm.2019.04.050

Guilardi, L.F., Pereira, G., Vallau, A.S., Silva, I.A., Giordani, J.C., Valandro, L.F., Rippe, M.P., 2020. Fatigue Failure Load of a Bonded Simplified Monolithic Feldspathic Ceramic: Influence of Hydrofluoric Acid Etching and Thermocycling. Oper. Dent. 45, E21–E31. https://doi.org/10.2341/19-069-L

Kelly, J.R., Cesar, P.F., Scherrer, S.S., Della Bona, A., van Noort, R., Tholey, M., Vichi, A., Lohbauer, U., 2017. ADM guidance-ceramics: Fatigue principles and testing. Dent. Mater. 33, 1192–1204. https://doi.org/10.1016/j.dental.2017.09.006

Kelly, J.R., Nishimura, I., Campbell, S.D., 1996. Ceramics in dentistry: Historical roots and current perspectives. J. Prosthet. Dent. 75, 18–32. https://doi.org/10.1016/S0022-3913(96)90413-8

Kitayama, S., Nikaido, T., Maruoka, R., Zhu, L., Ikeda, M., Watanabe, A., Foxton, R.M., Miura, H., Tagami, J., 2009. Effect of an internal coating technique on tensile bond strengths of resin cements to zirconia ceramics. Dent. Mater. J. 28, 446–453. https://doi.org/10.4012/dmj.28.446

Kontonasaki, E., Giasimakopoulos, P., Rigos, A.E., 2020. Strength and aging resistance of monolithic zirconia: an update to current knowledge. Jpn. Dent. Sci. Rev. 56, 1–23. https://doi.org/10.1016/j.jdsr.2019.09.002

May, L.G., Passos, S.P., Capelli, D.B., Özcan, M., Bottino, M.A., Valandro, L.F., 2010. Effect of silica coating combined to a MDP-based primer on the resin bond to Y-TZP ceramic. J. Biomed. Mater. Res. - Part B Appl. Biomater. 95, 69–74. https://doi.org/10.1002/jbm.b.31684

Melo, R.M., Souza, R.O.A., Dursun, E., Monteiro, E.B.C., Valandro, L.F., Bottino, M.A., 2015. Surface treatments of zirconia to enhance bonding durability. Oper. Dent. 40, 636–643. https://doi.org/10.2341/14-144-L

Mosele, J.C., Borba, M., 2014. Efeito do jateamento de partículas na resistência de união e comportamento mecânico de cerâmicas à base de zircônia -Revisão (Effect of particle sandblasting on the bond strength and mechanical behavior of zirconia-based ceramics -Review). Cerâmica 60, 179–186. https://doi.org/10.1590/S0366-69132014000200003

Ozcan, M., Bernasconi, M., 2015. Adhesion to Zirconia Used for Dental Restorations: A Systematic Review and Meta-Analysis. J. Adhes. Dent. 17, 7–26. https://doi.org/10.3290/j.jad.a33525

Özcan, M., Melo, R.M., Souza, R.O.A., Machado, J.P.B., Felipe Valandro, L., Botttino, M.A., 2013. Effect of air-particle abrasion protocols on the biaxial flexural strength, surface characteristics and phase transformation of zirconia after cyclic loading. J. Mech. Behav. Biomed. Mater. 20, 19–28. https://doi.org/10.1016/j.jmbbm.2013.01.005

Özcan, M., Vallittu, P.K., 2003. Effect of surface conditioning methods on the bond strength of luting cement to ceramics. Dent. Mater. 19, 725–731. https://doi.org/10.1016/S0109-5641(03)00019-8

Passos, S.P., May, L.G., Barca, D.C., Özcan, M., Bottino, M.A., Valandro, L.F., 2010. Adhesive quality of self-adhesive and conventional adhesive resin cement to Y-TZP ceramic before and after aging conditions. Oper. Dent. 35, 689–696. https://doi.org/10.2341/10-157-L

Pereira, G.K.R., Guilardi, L.F., Dapieve, K.S., Kleverlaan, C.J., Rippe, M.P., Valandro, L.F., 2018. Mechanical reliability, fatigue strength and survival analysis of new polycrystalline translucent zirconia ceramics for monolithic restorations. J. Mech. Behav. Biomed. Mater. 85, 57–65. https://doi.org/10.1016/j.jmbbm.2018.05.029

Piascik, J.R., Swift, E.J., Thompson, J.Y., Grego, S., Stoner, B.R., 2009. Surface modification for enhanced silanation of zirconia ceramics. Dent. Mater. 25, 1116–1121. https://doi.org/10.1016/j.dental.2009.03.008

Pozzobon, Pereira, G.K.R., Wandscher, V.F., Dorneles, L.S., Valandro, L.F., 2017a. Mechanical behavior of yttria-stabilized tetragonal zirconia polycrystalline ceramic after different zirconia surface treatments. Mater. Sci. Eng. C 77, 828–835. https://doi.org/10.1016/j.msec.2017.03.299

Pozzobon, Wandscher, V.F., Rippe, M.P., Valandro, L.F., 2017b. Influence of zirconia surface treatments on resin cement bonding and phase transformation. J. Adhes. Sci. Technol. 31, 1671–1682. https://doi.org/10.1080/01694243.2016.1268413

Prochnow, C., Venturini, A.B., Grasel, R., Gundel, A., Bottino, M.C., Valandro, L.F., 2018a. Adhesion to a lithium disilicate glass ceramic etched with hydrofluoric acid at distinct concentrations. Braz. Dent. J. 29, 492–499. https://doi.org/10.1590/0103-6440201802080

Prochnow, C., Venturini, A.B., Guilardi, L.F., Pereira, G.K.R., Burgo, T.A.L., Bottino, M.C., Kleverlaan, C.J., Valandro, L.F., 2018b. Hydrofluoric acid concentrations: Effect on the cyclic load-to-failure of machined lithium disilicate restorations. Dent. Mater. 34, e255–e263. https://doi.org/10.1016/j.dental.2018.06.028

Rinke, S., Gersdorff, N., Lange, K., Roediger, M., 2013. Prospective Evaluation of Zirconia Posterior Fixed Partial Dentures: 7-Year Clinical Results. Int. J. Prosthodont. 26, 164–171. https://doi.org/10.11607/ijp.3229

Sailer, I., Makarov, N.A., Thoma, D.S., Zwahlen, M., Pjetursson, B.E., 2015. All-ceramic or metal-ceramic tooth-supported fixed dental prostheses (FDPs)? A systematic review of the survival and complication rates. Part I: Single crowns (SCs). Dent. Mater. 31, 603–623. https://doi.org/10.1016/j.dental.2015.02.011

Scherrer, S.S., Cattani-Lorente, M., Vittecoq, E., De Mestral, F., Griggs, J.A., Wiskott, H.W.A., 2011. Fatigue behavior in water of Y-TZP zirconia ceramics after abrasion with 30 μm silica-coated alumina particles. Dent. Mater. 27, 28–42. https://doi.org/10.1016/j.dental.2010.10.003

Schestatsky, R., Zucuni, C.P., Venturini, A.B., de Lima Burgo, T.A., Bacchi, A., Valandro, L.F., Rocha Pereira, G.K., 2019. CAD-CAM milled versus pressed lithium-disilicate monolithic crowns adhesively cemented after distinct surface treatments: Fatigue performance and ceramic surface characteristics. J. Mech. Behav. Biomed. Mater. 94, 144–154. https://doi.org/10.1016/j.jmbbm.2019.03.005

Souza, R.O.A., Valandro, L.F., Melo, R.M., Machado, J.P.B., Bottino, M.A., Özcan, M., 2013. Air-particle abrasion on zirconia ceramic using different protocols: Effects on biaxial flexural strength after cyclic loading, phase transformation and surface topography. J. Mech. Behav. Biomed. Mater. 26, 155–163. https://doi.org/10.1016/j.jmbbm.2013.04.018

Stawarczyk, B., Keul, C., Eichberger, M., Figge, D., Edelhoff, D., Lümkemann, N., 2017. Three generations of zirconia: From veneered to monolithic. Part I. Quintessence Int. 48, 369–380. https://doi.org/10.3290/j.qi.a38057

Sulaiman, T.A., Abdulmajeed, A.A., Shahramian, K., Lassila, L., 2017. Effect of different treatments on the flexural strength of fully versus partially stabilized monolithic zirconia. J. Prosthet. Dent. 118, 216–220. https://doi.org/10.1016/j.prosdent.2016.10.031

Thompson, J.Y., Rapp b, M.M., Parker c, A.J., 1998. Microscopic and energy dispersive x-ray analysis of surface adaptation of dental cements to dental ceramic surfaces. J. Prosthet. Dent. 79, 378–383. https://doi.org/10.1016/S0022-3913(98)70148-9

Thompson, J.Y., Stoner, B.R., Piascik, J.R., Smith, R., 2011. Adhesion/cementation to zirconia and other non-silicate ceramics: where are we now? Dent. Mater. 27, 71–82. https://doi.org/10.1016/j.dental.2010.10.022

Tzanakakis, E.G.C., Tzoutzas, I.G., Koidis, P.T., 2016. Is there a potential for durable adhesion to zirconia restorations? A systematic review. J. Prosthet. Dent. 115, 9–19. https://doi.org/10.1016/j.prosdent.2015.09.008

Valentino, T.A., Borges, G.A., Borges, L.H., Platt, J.A., Correr-Sobrinho, L., 2012. Influence of glazed zirconia on dual-cure luting agent bond strength. Oper. Dent. 37, 181–187. https://doi.org/10.2341/10-220-L

Vanderlei, A, Bottino, M., Valandro, L., 2014. Evaluation of Resin Bond Strength to Yttria-stabilized Tetragonal Zirconia and Framework Marginal Fit: Comparison of Different Surface Conditionings. Oper. Dent. 39, 50–63. https://doi.org/10.2341/12-269-L

Venturini, A.B., Prochnow, C., May, L.G., Kleverlaan, C.J., Valandro, L.F., 2018. Fatigue failure load of feldspathic ceramic crowns after hydrofluoric acid etching at different concentrations. J. Prosthet. Dent. 119, 278–285. https://doi.org/10.1016/j.prosdent.2017.03.021

Venturini, A.B., Prochnow, C., Pereira, G.K.R., Segala, R.D., Kleverlaan, C.J., Valandro, L.F., 2019. Fatigue performance of adhesively cemented glass-, hybrid- and resin-ceramic materials for CAD/CAM monolithic restorations. Dent. Mater. 35, 534–542. https://doi.org/10.1016/j.dental.2019.01.013

Wegner, S.M., Dent, M., Gerdes, W., Kern, M., Dent, M., 2002. Effect of Different Artificial Aging Conditions on Ceramic- Composite Bond Strength. Int. J. Prosthodont. 15.

Zhang, F., Inokoshi, M., Batuk, M., Hadermann, J., Naert, I., Van Meerbeek, B., Vleugels, J., 2016. Strength, toughness and aging stability of highly-translucent Y-TZP ceramics for dental restorations. Dent. Mater. 32, e327–e337. https://doi.org/10.1016/j.dental.2016.09.025

Zucuni, C.P., Pereira, G.K.R., Dapieve, K.S., Rippe, M.P., Bottino, M.C., Valandro, L.F., 2019. Low-fusing porcelain glaze application does not damage the fatigue strength of Y-TZP. J. Mech. Behav. Biomed. Mater. 99, 198–205. https://doi.org/10.1016/j.jmbbm.2019.07.022

TABLES

Table 1. List of materials used: commercial names, manufacturers and composition based on the manufacturer's information.

Commercial names (Manufacturer)	**Composition**
IPS e.Max ZirCAD MT Multi (Ivoclar Vivadent)	86.0 ≤ 93.5% ZrO_2; 6.5 ≤ 8.0% Y_2O_3; ≤ 5.0% HfO_2; ≤ 1.0% Al_2O_3
Epoxy Resin (Carbotec GmbH)	Fiberglass filament, epoxy resin
10% hydrofluoric acid (FGM Produtos Odontológicos)	10% concentration hydrofluoric acid
VITA Akzent Plus (VITA Zahnfabrik)	Amorphous glassy substance (silica based material)
Aluminum oxide (Polidental)	Aluminum oxide particles (45 µm)
Cojet Sand (3M ESPE)	Aluminum oxide particles (30 µm), amorphous silica
Experimental material	7% Silica coated aluminum oxide particles (45 µm)
Monobond Plus (Ivoclar Vivadent)	Alcohol solution of silane methacrylate, phosphoric acid methacrylate and sulphide methacrylate.
Multilink Primer A (Ivoclar Vivadent)	Water and initiators
Multilink Primer B (Ivoclar Vivadent)	Phosphonic acid acrylate, hydroxyethyl methacrylate, methacrylate mod. polyacrylic acid stabilizer
Multilink Automix (Ivoclar Vivadent)	Dimethacrylates, HEMA, Barium Glass, Ba-Al-Fluoro-Silicate Glass, Ytterbium Trifluoride, Highly Dispersed Silica, Catalysts and Stabilizers, Pigments

Table 2. Experimental Design.

Groups	**Surface Treatment**	**Aging Condition***	**N**
Ctrl	Ultrasonic bath with distilled water;	Baseline	15
		Aging	15
PM	Primer Monobond Plus – applied actively for 15 sec and allowed to react for 60 sec;	Baseline	15
		Aging	15
GLZ	Glaze Spray VITA Akzent Plus – applied at a distance of 15 cm until a uniform layer was obtained and submitted to firing (initial temperature: 500 °C for 4 min at a heating rate of 80 °C/min until the final temperature of 950 °C, maintained for 1 min)	Baseline	15
		Aging	15
SNF	Silica nanofilms – SiO_2 thin films were deposited using the magnetron sputtering PVD process. The discs were exposure for 90 sec to deposit 5 nm of nanofilm thicknesses;	Baseline	15
		Aging	15
AlOx	Aluminum oxide particles – air-abrasion for 10 sec at 10 mm of distance and pressure of 2.8 bar;	Baseline	15
		Aging	15
SiC	Silica-coated aluminum oxide particles - air-abrasion for 10 sec at 10 mm of distance and pressure of 2.8 bar;	Baseline	15
		Aging	15
7% Si	7% Silica-coated aluminum oxide particles - air-abrasion for 10 sec at 10 mm of distance and pressure of 2.8 bar;	Baseline	15
		Aging	15

*Baseline: 24 hours at 37° C in water;
Aging: 90 days at 37° C in water + 12,000 thermal cycles;

Table 3. Results (Mean, 95% confidence intervals and Weibull modulus) for fatigue failure load (FFL) and number of cycles until failure (CFF).

Groups	Baseline				Aging			
	FFL (N)		CFF		FFL (N)		CFF	
	Mean (95% CI)	Weibull modulus	Mean (95% CI)	Weibull modulus	Mean (95% CI)	Weibull modulus	Mean (95% CI)	Weibull modulus
Ctrl	1040 (886 - 1193)^{ABa}	4.30 (2.70 - 6.35)^{Aa}	79,000 (63,602 - 94,397)^{ABa}	3.05 (1.89 - 4.54)^{Aa}	466 (267 - 665)^{Bb}*	1.76 (1.01 - 2.73)^{Ba}	25,000 (7,107 - 42,892)^{Bb} *	1.04 (0.59 - 1.62)^{Ba}
PM	1206 (1050 - 1362)^{ABa}	4.69 (3.00 - 6.79)^{Aa}	88,766 (69,981 - 107,551)^{ABa}	2.65 (1.66 - 3.91)^{Aa}	1207 (1064 - 1350)^{Aa}	5.37 (3.36 - 7.98)^{Aa}	95,714 (81,410 - 110,017)^{Aa}	4.23 (2.64 - 6.30)^{Aa}
GLZ	1313 (1099 - 1527)^{Aa}	3.76 (2.38 - 5.51)^{Aa}	106,333 (84,959 - 127,707)^{Aa}	2.92 (1.84 - 4.31)^{Aa}	1146 (895 - 1398)^{Aa}	2.62 (1.68 - 3.82)^{Aba}	89,666 (64,517 - 114,815)^{Aa}	1.93 (1.22 - 2.84)^{ABa}
SNF	1186 (1057 - 1316)^{ABa}	5.25 (3.42 - 7.45)^{Aa}	93,666 (80,712 - 106,620)^{ABa}	4.18 (2.71 - 5.95)^{Aa}	1271 (1062 - 1480)^{Aa}	3.75 (2.36 - 5.52)^{Aba}	102,142 (81,247 - 123,038)^{Aa}	2.98 (1.87 - 4.40)^{Aa}
AlOx	1040 (907 -1172)^{ABa}	5.12 (3.21 - 7.58)^{Aa}	79,000 (65,775 - 92,224)^{ABa}	3.76 (2.35 - 5.60)^{Aa}	1180 (1037 - 1322)^{Aa}	5.02 (3.21 - 7.31)^{Aa}	93,000 (78,788 - 107,211)^{Aa}	3.93 (2.51 - 5.74)^{Aa}
SiC	1006 (830 - 1182)^{ABa}	3.26 (2.12 - 4.66)^{Aa}	75,666 (58,087 - 93,246)^{ABa}	2.45 (1.58 - 3.52)^{Aa}	973 (811 - 1135)^{Aa}	3.37 (2.20 - 4.78)^{Aba}	72,333 (56,163 - 88,503)^{Aa}	2.53 (1.65 - 3.61)^{Aa}
7% Si	953 (820 - 1085)^{Ba}	4.43 (2.81 - 6.49)^{Aa}	70,333 (57,099 - 83,566)^{Ba}	3.19 (2.01 - 4.70)^{Aa}	1000 (873 - 1126)^{Aa}	4.85 (3.09 - 7.07)^{Aa}	75,000 (62,312 - 87,687)^{Aa}	3.58 (2.27 - 5.25)^{Aa}

*40% Pre-test failure which were discarded from statistical analysis.
- Different capital letters (columns) indicate statistical differences for each outcome on each condition (baseline and aged).
- Different lower case letters (rows) indicate statistical differences comparing baseline and aged condition for each outcome.

Table 4. Survival probabilities for different load steps and number of cycles parameters.

Groups	Aging	Load to failure / Number of cycles until failure																	
		200/ 5 x 10^3	400/ 15 x 10^3	500/ 25 x 10^3	600/ 35 x 10^3	700/ 45 x 10^3	800/ 55 x 10^3	900/ 65 x 10^3	1000/ 75 x 10^3	1100/ 85 x 10^3	1200/ 95 x 10^3	1300/ 105 x 10^3	1400/ 115 x 10^3	1500/ 125 x 10^3	1600/ 135 x 10^3	1700/ 145 x 10^3	1800/ 155 x 10^3	1900/ 165 x 10^3	2000/ 175 x 10^3
Ctrl	**Without**	1	0.93 (0.06)	0.93 (0.06)	0.86 (0.08)	0.80 (0.10)	0.73 (0.11)	0.66 (0.12)	0.60 (0.12)	0.46 (0.12)	0.26 (0.11)	0.06 (0.06)	0.06 (0.06)	0 (0)	-	-	-	-	-
	With	0.66 (0.15)	0.33 (0.15)	0.22 (0.13)	…	…	0.11 (0.10)	…	…	0 (0)	-	-	-	-	-	-	-	-	-
PM	**Without**	1	1	1	0.93 (0.06)	0.93 (0.06)	0.86 (0.08)	0.86 (0.08)	0.66 (0.12)	0.53 (0.12)	0.40 (0.12)	0.40 (0.12)	0.26 (0.11)	0.13 (0.08)	0.06 (0.06)	0 (0)	-	-	-
	With	1	1	1	1	1	0.92 (0.06)	0.78 (0.11)	0.57 (0.13)	0.50 (0.13)	…	…	0.21 (0.11)	0.07 (0.06)	0 (0)	-	-	-	-
GLZ	**Without**	1	1	0.93 (0.06)	0.93 (0.06)	0.86 (0.08)	0.86 (0.08)	0.73 (0.11)	0.73 (0.11)	0.66 (0.12)	0.60 (0.12)	0.60 (0.12)	0.46 (0.12)	0.26 (0.11)	0.20 (0.10)	0.13 (0.08)	0.06 (0.06)	0.06 (0.06)	0 (0)
	With	1	0.93 (0.06)	0.86 (0.08)	0.80 (0.10)	0.73 (0.11)	0.66 (0.12)	0.60 (0.12)	0.53 (0.12)	0.53 (0.12)	0.46 (0.12)	0.40 (0.12)	0.26 (0.11)	0.20 (0.10)	0.13 (0.08)	…	…	0.06 (0.06)	0 (0)
SNF	**Without**	1	1	1	1	1	0.93 (0.06)	0.73 (0.11)	0.66 (0.12)	0.53 (0.12)	0.53 (0.12)	0.20 (0.10)	0.13 (0.08)	0.06 (0.06)	0.06 (0.06)	0 (0)	-	-	-
	With	1	1	1	1	0.92 (0.06)	0.78 (0.11)	0.71 (0.12)	0.64 (0.12)	0.57 (0.13)	0.50 (0.13)	0.50 (0.13)	0.35 (0.12)	0.28 (0.12)	0.21 (0.11)	0.14 (0.09)	0.07 (0.06)	0 (0)	-
AlOx	**Without**	1	1	1	0.86 (0.08)	0.80 (0.10)	0.73 (0.11)	0.66 (0.12)	0.60 (0.12)	0.46 (0.12)	0.20 (0.10)	0.06 (0.06)	0 (0)	-	-	-	-	-	-
	With	1	1	1	1	0.93 (0.06)	0.86 (0.08)	0.80 (0.10)	0.60 (0.12)	0.53 (0.12)	0.40 (0.12)	0.33 (0.12)	0.26 (0.11)	0.06 (0.06)	0 (0)	-	-	-	-
SiC	**Without**	1	1	1	0.80 (0.10)	0.73 (0.11)	0.53 (0.12)	0.53 (0.12)	0.40 (0.12)	0.40 (0.12)	0.26 (0.11)	0.13 (0.08)	0.13 (0.08)	0.06 (0.06)	0.06 (0.06)	0 (0)	-	-	-
	With	1	1	1	0.86 (0.08)	0.80 (0.10)	0.40 (0.12)	…	…	0.33 (0.12)	0.20 (0.10)	0.13 (0.08)	0.13 (0.08)	0.06 (0.06)	-	-	-	-	-
7% Si	**Without**	1	1	1	0.73 (0.11)	0.73 (0.11)	0.66 (0.12)	0.60 (0.12)	0.40 (0.12)	0.20 (0.10)	0.20 (0.10)	0 (0)	-	-	-	-	-	-	-
	With	1	1	1	0.93 (0.06)	0.73 (0.11)	0.66 (0.12)	0.60 (0.12)	0.53 (0.12)	0.33 (0.12)	0.13 (0.08)	0.06 (0.06)	0 (0)	-	-	-	-	-	-

- The symbol "-" indicates absence of specimen being tested on the considered step.
- The symbol "…" indicates absence of specimen fracturing in the respective step for each condition.

Table 5. Results of contact angle measurements (mean and standard deviation), fractal dimension (mean and standard deviation), roughness (mean and standard deviation - Ra and Rz parameters) and chemical composition (percentage by weight) of the ceramic surface after each surface treatment.

Groups	**Contact angle**	**Fractal Dimension**	**Roughness**		**Chemical composition**			
			Ra	**Rz**	**Zr**	**O**	**Al**	**Si**
Ctrl	86.9 (6.02)^{D}	Ctrl: 2.28 (0.04)^{AB}	0.21 (0.05)^{D}	2.02 (0.95)^{C}	64.56	35.44	-	-
PM		PM: 2.14 (0.01)^{CD}						
GLZ	24.24 (4.76)^{B}	2.07 (0.05)^{D}	0.88 (0.35)^{A}	5.29 (1.89)^{A}	1.08	52.48	2.16	20.95
SNF	65.70 (2.29)^{C}	2.22 (0.01)^{BC}	0.23 (0.07)^{CD}	2.02 (0.77)^{C}	55.70	31.48	-	-
AlOx	26.58 (12.52)^{B}	2.24 (0.04)^{B}	0.33 (0.05)^{B}	2.73 (0.71)^{B}	57.48	40.63	1.88	-
SiC	7.50 (2.97)^{A}	2.34 (0.02)^{A}	0.28 (0.04)^{BC}	2.44 (0.66)^{BC}	51.77	43.31	1.63	1.17
7% Si	10.49 (2.49)^{A}	2.28 (0.04)^{AB}	0.32 (0.04)^{B}	2.74 (0.88)^{B}	52.15	41.70	1.36	0.70

FIGURES

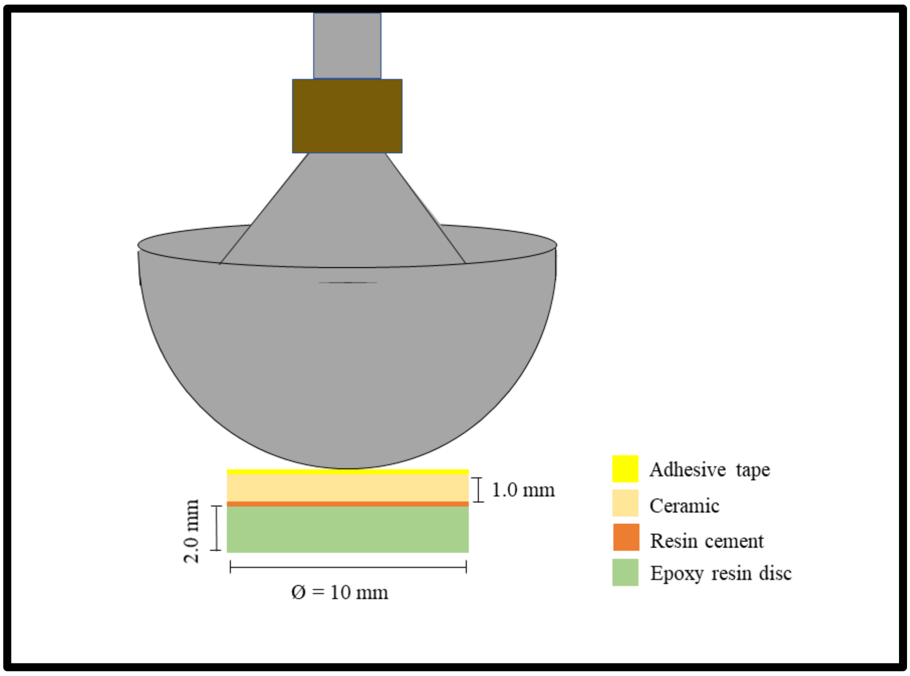

Figure 1. Illustrative image of the fatigue test assembly using a hemispheric stainless-steel piston (Ø = 40 mm) in the center of the specimens' occlusal surface, submerged in distilled water.

Ctrl / PM	GLZ	SNF
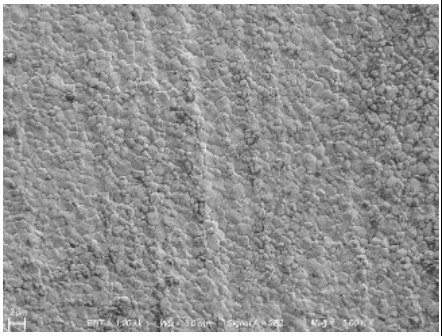	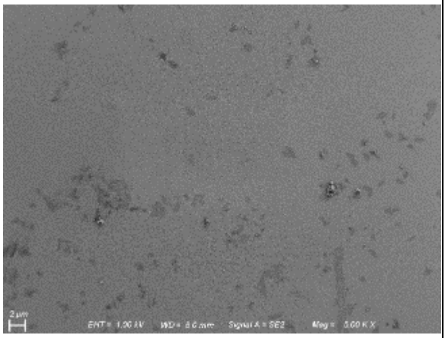	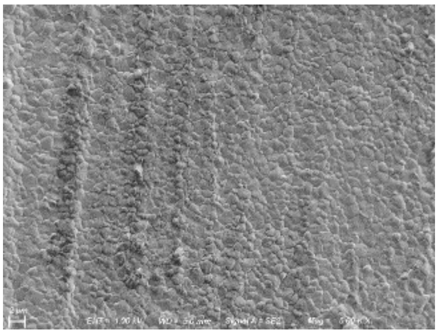
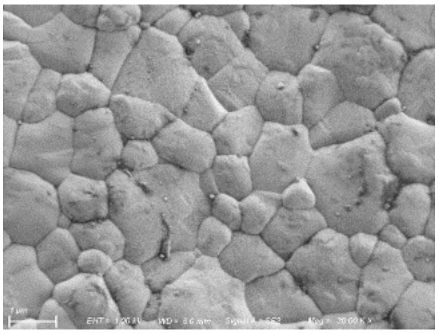	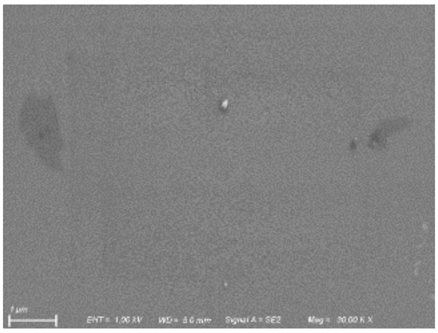	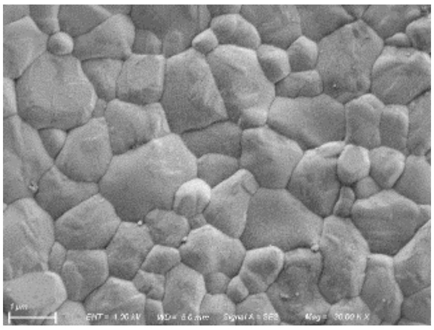
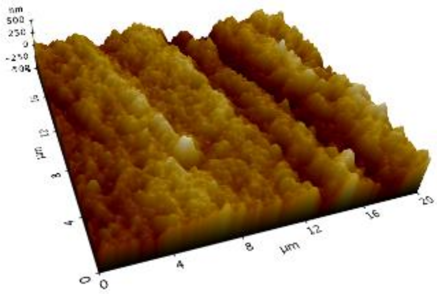 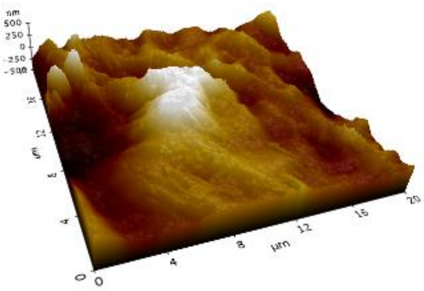	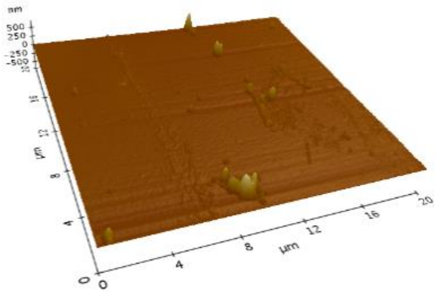	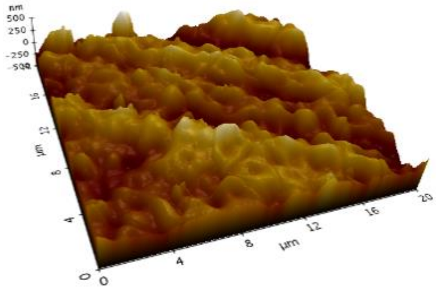
AlOx	**SiC**	**7% Si**
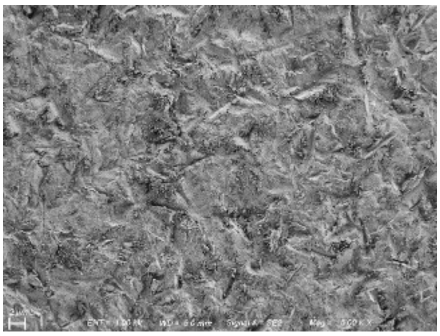	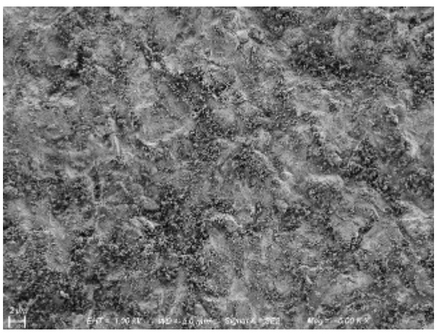	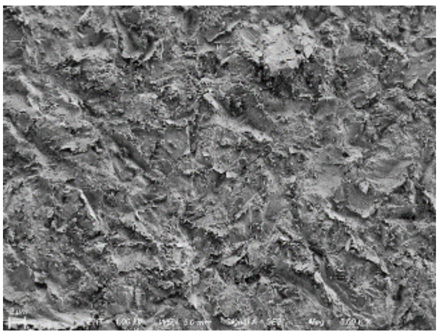

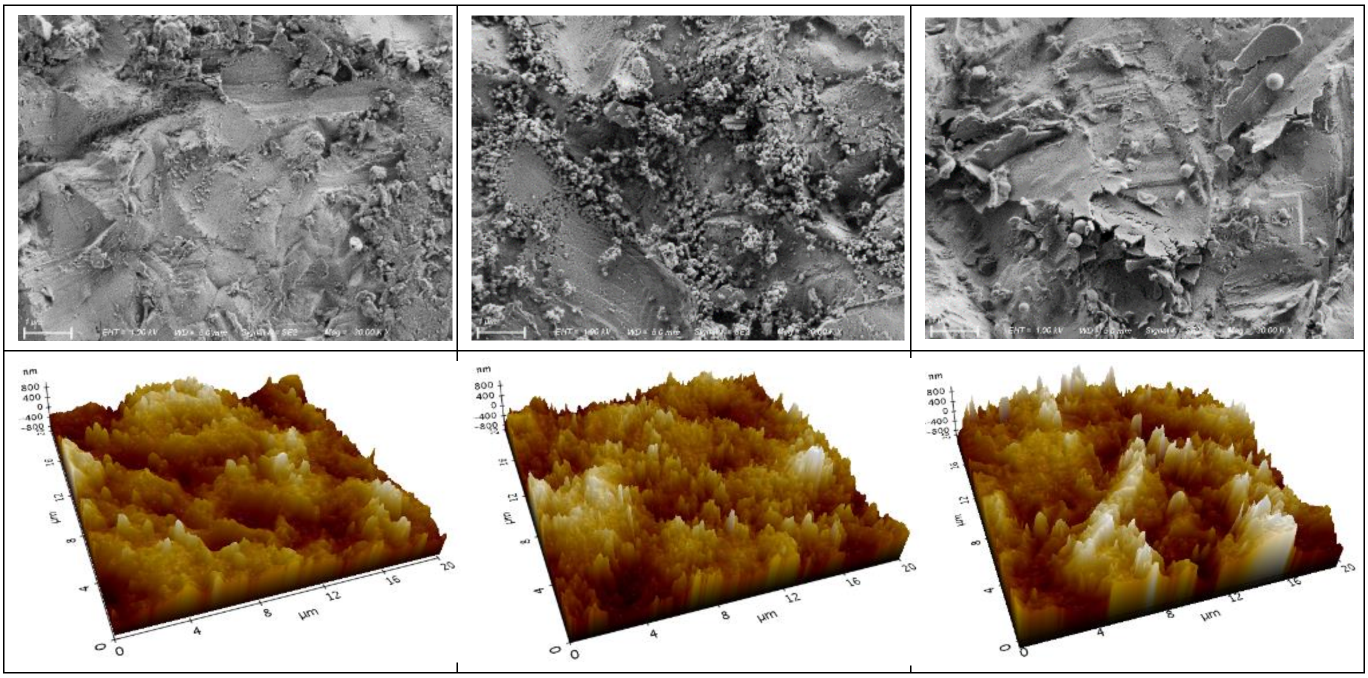

Figure 2. SEM micrographs of the ceramic surfaces after each surface treatment at 5000× (top) and 30000× (bottom) magnifications and 3D patterns by Atomic Force Microscopy analysis. It is noted that the deposition of silica nanofilms did not alter the ceramic surface, presenting topography similar to the Ctrl group. The air-abrasion groups promoted higher superficial alterations due to the impact of the particle's powders compared to the homogeneous surface promoted by GLZ group.

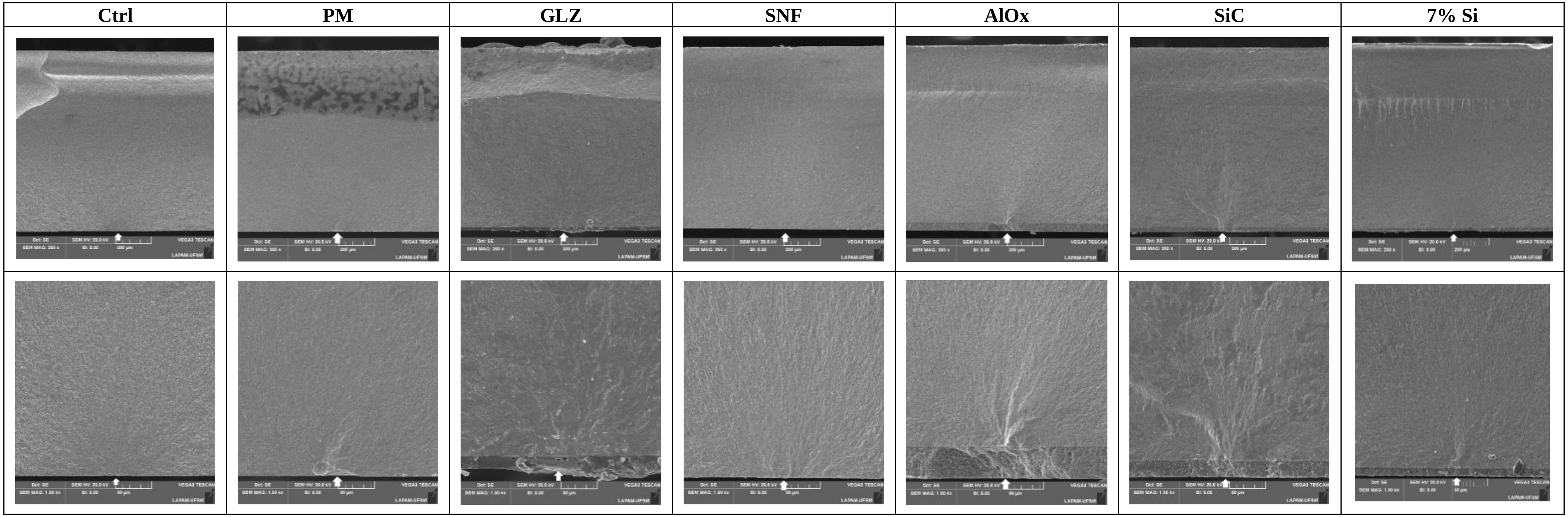

Figure 3. Representative SEM micrographs of fractured surfaces (fractographical examination) at 250× (top) and 1,000× (bottom) magnifications. The white arrows indicate the crack origin where tensile stress was concentrated. It can be noted that all fractures originated from surface/sub-surface defects at the center of ceramic surface, which was in contact with the resin cement and propagated into the ceramics' opposite side, where the load was applied.

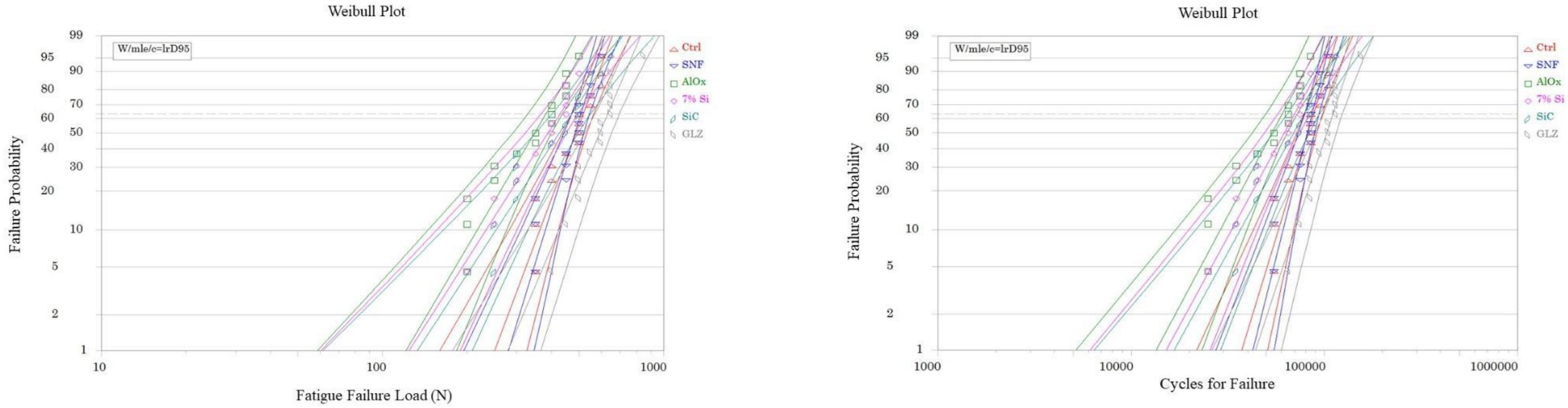

Figure 4. Weibull plot for fatigue failure load (N) (left image) and number of cycles for failure (right image).

4. ARTIGO 3 - In-lab simulation of CAD/CAM grinding and intaglio surface treatments of 4YSZ monolithic restorations: Effect on its load-bearing capacity under fatigue

Este artigo está publicado (doi: 10.1016/j.jmbbm.2022.105417) no periódico Journal of the Mechanical Behavior of Biomedical Materials, Elsevier, ISSN: 1751-6161, Fator de impacto = 4.042; Qualis A2. As normas para publicação estão descritas no Anexo A.

In-lab simulation of CAD/CAM grinding and intaglio surface treatments of 4YSZ monolithic restorations: Effect on its load-bearing capacity under fatigue

Ana Carolina Cadore-Rodrigues[a], Renan Vaz Machry[a], Kiara Serafini Dapieve[a], Arie Werner[b], Gabriel Kalil Rocha Pereira[a], Luiz Felipe Valandro[a]*, Cornelis Johannes Kleverlaan[b]

[a] MSciD-PhD Post-Graduate Program in Oral Science, Faculty of Odontology, Federal University of Santa Maria, Santa Maria, Rio Grande do Sul, Brazil
[b] Department of Dental Materials Science, Academic Centre for Dentistry Amsterdam (ACTA), Universiteit van Amsterdam and Vrije Universiteit, Amsterdam, Noord-Holland, The Netherlands

Authors' addresses and contributions:
Ana Carolina Cadore-Rodrigues (anacadorerodrigues@gmail.com) - Study conception and design, experimental part, acquisition of data or analysis, interpretation of data, article writing – original draft, and review
Renan Vaz Machry (renanmachry@gmail.com) - Study conception and design, experimental part, acquisition of data or analysis, interpretation of data, article writing, and review
Kiara Serafini Dapieve (kiara_s_d@hotmail.com) - Study conception and design, experimental part, acquisition of data or analysis, interpretation of data, article writing, and review
Arie Werner (a.werner@acta.nl) - Acquisition of data or analysis**,** article writing, and review
Gabriel Kalil Rocha Pereira (gabrielkrpereira@hotmail.com) - Interpretation of data, article writing, and review
Luiz Felipe Valandro* (valandrolf@gmail.com) - Interpretation of data, article writing and review
Cornelis Johannes Kleverlaan (c.kleverlaan@acta.nl) - Study conception and design, experimental part, acquisition of data or analysis, interpretation of data, article writing, and review

***Corresponding author at:**
Luiz Felipe Valandro, D.D.S., M.Sci.D., Ph.D., Full Professor,
Federal University of Santa Maria
Faculty of Odontology
Ph.D.-M.Sci.D. Graduate Program in Oral Science
Prosthodontics-Biomaterials Unit
1000 Roraima Av., T Street, Building 26F, Room 2386
UFSM Campus, 97105-900
Rio Grande do Sul State, Santa Maria, Brazil
Phone: +55-55-3220-9276, Fax: +55-55-3220-9272
E-mail: valandrolf@gmail.com (Dr LF Valandro)

Running title: CAD/CAM grinding and surface treatments of 4YSZ

Abstract

Objectives: To evaluate the effect of in-lab simulation of CAD/CAM grinding and intaglio surface treatments on the surface characteristics (topography and roughness) and fatigue behavior of adhesively luted 4YSZ simplified restorations. *Methods:* Ceramic discs (Ø= 10 mm, thickness= 1 mm) were randomly allocated into 6 groups considering: “In-lab simulation of CAD/CAM grinding” (ground or polished) and “intaglio surface treatments”: Ctrl (without surface treatment), AlOx (aluminum oxide air abrasion) or GLZ (glaze spray application). The surface roughness of all samples was measured, the treated discs received a ceramic primer, were luted with resin cement onto a dentin analogue material (woven glass-reinforced epoxy resin), and tested under a cyclic fatigue test (step-stress approach, n= 15; 1.4Hz, 10,000 cycles/step, step-size of 100N starting at 200N until failure). A complementary analysis was performed to corroborate the findings in the fatigue test that the glaze fill defects increase the mechanical properties of the ceramic. To do so, bars (n= 10; 1.0 × 1.0 × 12 mm; considering the groups: N-ID: non-indented; ID: indented; ID-GLZ: indented plus glaze spray application) were indented in a vickers hardness tester to produce a crack pattern, treated with glaze or not, and then submitted to flexural strength tests (FS). Fractographic and topographic analysis were performed. *Results:* In-lab simulation of CAD/CAM grinding decreased the fatigue failure load of the 4YSZ ceramic when comparing polished and ground groups, regardless of surface treatment. GLZ induced better fatigue performance compared to the air abrasion, regardless of the grinding condition (ground or polished surface). The results of the flexural strength test corroborated the findings in the fatigue test, as the ID-GLZ group presented superior FS than the ID group, however, both had inferior FS than N-ID. There is an inverse association between roughness and fatigue failure load, as the higher the surface roughness, the lower the fatigue failure load. Failures in the fatigue and flexural strength tests started from the face subjected to tensile stress. *Conclusion:* In-lab simulation of CAD/CAM grinding had a detrimental effect on the fatigue behavior of 4YSZ and glaze spray induced better 4YSZ performance compared to the air abrasion. The intaglio surface treatments differently influenced the 4YSZ fatigue performance, however, only glaze spray can reverse the damage caused by the grinding.

Keywords: Computer-aided manufacturing, Flexural strength, Resin bonding, Survival rates, Yttrium stabilized zirconia

HIGHLIGHTS

- The higher the 4YSZ surface roughness, the lower the fatigue behavior of the assembly;
- CAD/CAM grinding simulation produces a deleterious effect on the fatigue behavior of 4YSZ;
- Glaze spray induces better 4YSZ fatigue performance compared to air abrasion;

- Aluminum oxide air abrasion damaged 4YSZ performance.

1. Introduction

Computer-aided design and manufacturing systems (*Computer-Aided Design/Computer-Aided Machining* – CAD/CAM) allow fabrication of restorations in a shorter period of time, with less technical sensibility and higher precision and efficiency (Blatz and Conejo, 2019). Among the restorative materials available for these systems, zirconia-based dental materials have earned popularity due to their mechanical properties and excellent biocompatibility (Piconi and Maccauro, 1999; Stawarczyk et al., 2017). Soft machining (using pre-sintered blocks) is the most used process to manufacture yttrium stabilized zirconia ceramic restorations (YSZ) because fully sintered blocks (used in hard machining) are hard to mill, decreasing the longevity of diamond burs, are time-consuming, and introduce more surface defects (Miyazaki and Hotta, 2011; Zarone et al., 2011). The literature states that CAD/CAM machining (hard and soft) results in radial and lateral cracks, and defects or flaws on the ceramic surface and subsurface (Marshall and Evans, 1983; Rekow and Thompson, 2005; Sindel et al., 1998; Zhang et al., 1994) which significantly reduce the strength of YSZ ceramic (Fraga et al., 2017; Wang et al., 2008).

Several steps from obtaining the material to its cementation in the oral environment introduce defects in the ceramic which are prone to slow crack growth mechanisms unleashing the failure of the material when subjected to intermittent cyclic loads (Kelly et al., 2017; Scherrer et al., 2017). In addition to the material manufacturing process, treatments of the intaglio surface of the restoration are also an important step, as they interact with the existing surface defects and are essential to promote stable adhesion (Malysa et al., 2021; Özcan and Bernasconi, 2015; Özcan and Vallittu, 2003). According to the literature, the resin cement can change the filling potential of defects resulting from machining and surface conditioning, and consequently promotes a strengthening mechanism of the material through better distribution stress during loading, thereby increasing the material's resistance (Addison et al., 2010; de Kok et al., 2017; Spazzin et al., 2016).

As YSZ presents polycrystalline content with absence of the glassy phase, air abrasion with aluminum oxide particles covered or not by silica is the gold standard surface treatment due to the micromechanical interlocking and chemical reaction to silane coupling agent and posteriorly interaction with a resin cement (Mosele and Borba, 2014; Özcan and Bernasconi, 2015; Özcan and Vallittu, 2003). In turn, technology and ceramics evolved over the years and new generations of yttrium stabilized zirconia (YSZ) emerged to improve the optical characteristics for its use as monolithic restorations. In this sense, translucent zirconia was developed with a higher percentage of yttrium oxide (≥ 4-5% mol) (Konstantinidis et al., 2018; Stawarczyk et al., 2017; Zhang and Lawn, 2018), which resulted in a more cubic phase in its microstructure, however, it reduced the t-to-m transformation toughening mechanism (Cadore-Rodrigues et al., 2021; Chen et al., 2020; Karlsen et al., 2020; Pereira et al., 2018; Sulaiman et al., 2017). Thus, studies have found that particle air abrasion introduces surface defects that are not contained by YSZ with more yttria content – and consequently, it does not hinder the crack to spread into the material (Cadore-Rodrigues et al., 2021; Chen et al., 2020; Sulaiman et al., 2017).

Due to this concern, glaze spray application has been evaluated as an alternative surface treatment for promoting an intaglio surface rich in silica resulting in a stable bond (Valentino et al., 2012; Vanderlei et al., 2014) and for its healing effect (Anusavice and Phillips, 2003). The glaze application results in a fill-up mechanism, penetrating microcracks and porosities, which leads to a smoother surface with less defects increasing the energy required for crack propagation and consequently increasing the material's resistance (Cadore-Rodrigues et al., 2021; Chun et al., 2017; Zucuni et al., 2019).

Taking into account the aforementioned assumptions, CAD/CAM machining and intaglio surface treatments can influence the 4 mol% yttria-stabilized zirconia (4YSZ) mechanical performance. Therefore, the aim of the present study was to evaluate the effect of in-lab simulation of CAD/CAM grinding and intaglio surface treatments on the surface characteristics (topography and roughness) and fatigue behavior of adhesively luted 4YSZ simplified restorations. The hypotheses of this study were: (1) CAD/CAM grinding will decrease the fatigue behavior of 4YSZ ceramic compared to a polished surface; (2) the glaze spray surface treatment will promote better fatigue performance compared to air abrasion.

2. Materials and methods

The general description (manufacturers, batch number and composition) of the materials used in the present study are presented in Table 1.

2.1 Study design

A test set-up was used to simulate the fatigue behavior of adhesively luted monolithic restorations of a posterior tooth (Chen et al., 2014). Thus, ceramic discs were made simulating 4YSZ monolithic restorations and woven glass-reinforced epoxy resin discs (dentin analogue material) simulating the tooth to be restored, both prepared to present diameter of 10 mm to mimic the average dimension of molars (Chen et al., 2014). For the fatigue testing, 6 groups (n= 15) were designed considering two factors: "In-lab simulation of CAD/CAM grinding" (ground: submitted to the in-lab simulation of CAD/CAM grinding; or polished surface) and "surface treatments" (control – no treatment, air-abrasion with aluminum oxide particles (50 µm), and glaze spray application; Figure 1).

2.2 Preparation of ceramic discs for fatigue testing

For the ceramic discs, 4YSZ blanks (IPS e.max ZirCAD MT, Ivoclar, Schaan, Liechtenstein) were manually sectioned into smaller blocks (20 mm × 20 mm). Metallic rings with 12 mm diameter were subsequently glued to the parallel surfaces of the blocks, serving as guides for grinding in a polishing machine with silicon carbide papers (#400, #600 and #1200-grit, CarbiMet SiC Abrasive Paper, Buehler, Lake Bluff, USA) under refrigeration (Ø= 12 mm). Next, 90 ceramic discs with 1.4 mm of thickness were obtained using a precision cutting machine with a diamond blade (ISOMET 1000, Buehler). Then, the ceramic discs were allocated according to the factor "in-lab simulation of CAD/CAM grinding" (polished or ground - submitted to the in-lab simulation of CAD/CAM grinding).

2.2.1 Polished

Next, 45 discs were manually polished with silicon carbide papers (#600 and #1200-grit, CarbiMet SiC Abrasive Paper, Buehler) until reaching 1.25 mm of thickness to remove surface irregularities inherent to cutting and sintered in a furnace (Programat P100, Ivoclar) according to the manufacturer's recommendation, resulting in specimens with final dimensions of 10 mm in diameter and 1 mm in thickness (Digital caliper, Absolute 500-196-20, Mitutoyo, Takatsu-ku, Japan). Then, the discs were randomly allocated into three testing groups (n= 15) considering the surface treatments (Figure 1).

2.2.2 In-lab simulation of CAD/CAM grinding

A total of 45 discs were subjected to an in-lab simulation of CAD/CAM grinding according to a previous study (Pilecco et al., 2021). To do so, the specimen was first polished with silicon carbide papers (#600 and #1200-grit, CarbiMet SiC Abrasive Paper, Buehler) and the bonding surface was subsequently marked with a permanent marking pen (Edding 3000, Edding International GmbH, Ahrensburg, Germany) to guarantee that the entire surface was ground. An electric motor handpiece up to 30,000 rpm (W&H Dentalwerk, Bürmoos, Austria) was used for grinding by a single trained operator (RVM). A mandrel was fabricated to adapt the Cylinder Pointed Bur of the CAD/CAM system (12S cylinder pointed bur, CEREC inLab, Sirona Dental, Charlotte, USA) in the handpiece. Grinding was performed in one direction under gentle pressure until the pen marks were eliminated. The burs of the system were replaced for each group.

After grinding, the thickness of the specimens was verified (Digital caliper, Absolute 500-196-20, Mitutoyo, Japan) and the opposite side (occlusal side) of each disc was polished with silicon carbide papers (#600 to #1200 grit, CarbiMet SiC Abrasive Paper, Buehler) until 1.25 mm of thickness and then sintered in a specific furnace (Programat P100, Ivoclar), presenting 10 mm diameter and 1 mm thickness in the final dimensions.

2.3 Preparation of dentin analogue discs

Woven glass-reinforced epoxy resin plates with 2 mm of thickness (Epoxydplatte 150 × 350 × 2.0 mm; Carbotec GmbH & Co. KG, Konigs Wusterhausen, Germany) were used to perform 90 discs of dentin analogue material using a cylindrical diamond drill (internal diameter = 10 mm; Diamant Boart, Brussels, Belgium) coupled to a bench drill (SBE 1010 Plus, Metabo; Nürtingen, Germany) under refrigeration, and then randomly allocated into pairs with the ceramic discs.

2.4 Surface treatments

All the ceramic discs were cleaned in ultrasonic bath with distillate water for 5 min. Afterward, the intaglio surfaces of the simplified 4YSZ restorations were subjected to the surface treatments according to Figure 1. It is important to highlight that the specimens treated with glaze spray were measured (Absolute 500-196-20, Mitutoyo) before and after the surface treatment to assess whether the application of glaze would promote an increase in thickness. The thickness variability was approximately 0.01 mm (10 µm).

2.5 Luting procedure

Before the luting procedure, the treated surface of all ceramic discs received a ceramic primer (Monobond N, Ivoclar) applied actively for 15 s and allowed to react for 60 s. Then, 9% hydrofluoric acid (Porcelain etch, Ultradent, South Jordan, USA) was applied for 1 min for the bonding surface conditioning of the dentin analogue discs, followed by air-water spray for 30 s and ultrasonic bath with distilled water for 5 min. Next, a mixture of primers A and B (ratio 1:1; Multilink N, Ivoclar) was scrubbed onto the treated surfaces for 30 s and air-dried until a thin layer was obtained.

The dual-cured resin cement pastes (Multilink N, Ivoclar) were mixed and applied onto the ceramic surface. The discs were then placed over the dentin analogue discs and bonded under a constant load of 1.5 N. The cement excesses were removed with a micro brush and light-cured (Bluephase N, Ivoclar) for 20 s in the four directions of the bonded area (0°, 90°, 180°, and 270°), and at the occlusal surface. All the luted specimens were stored in distilled water (24 h up to 7 days; 37 °C) until the fatigue testing.

2.6 Fatigue tests

The luted assemblies (n= 15) were submitted to a fatigue test in an adapted fatigue tester (Fatigue Tester, ACTA, Amsterdam, The Netherlands) using a cyclic fatigue methodology (step-stress approach) (Kelly et al., 2017). The specimens were positioned in a steel ring with an inner diameter of 6.5 mm (Chen et al., 2014) and cyclic loads were applied in the center of the assemblies by a stainless-steel sphere of 40 mm diameter under distilled water at a frequency of 1.4 Hz (Fraga et al., 2017).

The intermittent cyclic loads were applied starting with an initial load of 200 N followed by steps of 300 N, 400 N, 500 N, and so on, with a fixed load increment of 100 N for 10,000 cycles at each load step until the occurrence of failure. At the end of each step, the specimens were examined under oblique light transmission to visually inspect for radial cracks. If they were not detected, the load level was increased and the test proceeded. However, if radial cracks were detected, the sample was classified as “failed”, the fatigue test ended for the sample and the collected data was recorded for statistical analysis (fatigue failure load - FFL and cycles for failure - CFF).

2.7 Surface roughness analysis

A micrometric analysis was performed in all the specimens (n= 15) with a contact profilometer (Mitutoyo SJ 400 Profilometer, Mitutoyo Corporation, Kawasaki, Japan) to verify the surface roughness of the groups, in which four measurements for each specimen were executed considering Ra and Rz parameters of ISO 4287:1997 (cut-off of 5; λC of 0.8 mm; λS of 2.5 µm). Ra is defined as the arithmetical mean of the absolute values of peaks and valleys measured from a mean plane (in µm), and Rz is the average distance between the five highest peaks and five major valleys of a surface (in µm).

2.8 Complementary analysis

A complementary analysis using a flexural strength test was performed to evaluate the ability of glaze to fill the surface defects and increase the fatigue performance of ceramic. To do so, the specimens were indented in a Vickers hardness tester (HM-124, Mitutoyo) to produce an acceptable crack pattern, as previous study (Aurélio et al., 2017), to be covered or not by glaze spray application and posteriorly tested. In this sense, 3 groups (n= 10) were designed using 4YSZ bars (IPS e.max ZirCAD MT, Ivoclar), considering: N-ID group (non-indented), ID group (indented without glaze spray application), and ID-GLZ group (indented with glaze spray application). Next, 30 4YSZ bars were cut (Isomet 1000, Buehler) and manually polished with silicon carbide papers (#600 and #1200-grit, CarbiMet SiC Abrasive Paper, Buehler) under refrigeration presenting a final dimension of 1.0 × 1.0 × 12 mm after sintering (Programat P100, Ivoclar). Then, they were randomly allocated in the three aforementioned groups.

The bars from the ID and ID-GLZ groups were indented in the center of one of the sides using a hardness testing machine (HM-124, Mitutoyo) with a Vickers diamond indenter under a load of

19.6 N and a dwell time of 20 s (Ludovichetti et al., 2018; Osiewicz et al., 2022). The bars were subsequently cleaned in an ultrasonic bath with distilled water for 5 min and the bars from ID-GLZ group were submitted to the glaze spray application (Figure 1). Next, the bars (n= 10) were positioned with the indented side facing down on a ball-in-hole device and tested in a universal testing machine (crosshead speed of 1 mm/min; Instron 6022; Instron, Norwood, USA). The ball-in-hole device consists of a metallic base with a perforation (10.1 mm in diameter) through which the sample bar was positioned internally stabilized by two support bases separated by 10 mm. A stainless-steel ball (10 mm in diameter) positioned through the hole ensures punctual contact with the center of the sample.

The flexural strength for each group was calculated in MPa using the formula: $FS = \frac{3PL}{2bh^2}$, in which “P” is the load in Newton, “L” is the test span in millimeters (mm), “b” is the specimen width in mm, and “h” is the specimen thickness in mm (ISO: 6872, 2015).

2.9 Scanning electron microscopy (SEM)

The failed specimens (discs and bars) were inspected after testing for fractographic analysis to determine the origin of failure, among other fractographic features. Representative samples of all conditions were ultrasonically cleaned (distilled water, 5 min), air-dried, gold-sputtered (Edwards S150B, BOC Edwards, Burgess Hill, United Kingdom), and analyzed under Scanning Electron Microscopy (SEM, Evo LS15, Carl Zeiss, Gottingen, Germany) at 400× magnification for the discs and at 600× magnification for the bars.

In addition, SEM analysis was performed in the discs to determine the topographical pattern of the ceramic surfaces of each group. To do so, one additional ceramic specimen of each group was produced, gold-sputtered (Edwards S150B, BOC Edwards), and analyzed by SEM (Evo LS15, Carl Zeiss).

2.10 Data analysis

According to the Shapiro-Wilk test, the surface roughness data assumed a non-parametric but homoscedastic distribution, and therefore the Kruskal Wallis and LSD post-hoc tests (α= 0.05) were employed (SPSS version 21, IBM Analytics).

Statistical analysis for FFL and CFF data was performed using non-parametric analysis of Kaplan Meier and Mantel-Cox (Log-Rank) tests (α=0.05; SPSS version 21, IBM Analytics, New York, USA). The power calculation was performed considering all groups through the FFL data using the G*Power 3.1 program (Heinrich-Heine-Universität Düsseldorf, Düsseldorf, Germany) through the mean differences. The FFL and CFF data were also submitted to Weibull analysis using the Super

SMITH Weibull 4.0k-32 software (Wes Fulton, Torrance, USA) under the maximum-likelihood method to obtain the Weibull modulus, which is a way to statistically access the mechanical reliability of a condition/parameter.

Unadjusted linear regression analysis (SPSS version 21, IBM Analytics) was used to investigate the association between FFL and surface roughness (Ra parameter). The results are presented as coefficient (β), 95% confidence intervals (95% CI) and coefficient of determination (R^2).

The statistical analysis for the flexural strength data was performed using the Kruskal Wallis and LSD post-hoc tests (α=0.05), as the data assumed a non-parametric but homoscedastic distribution. A power calculation was also performed considering all groups using the G*Power 3.1 program (Heinrich-Heine-Universität Düsseldorf) through the mean differences.

Fractographic features and SEM analysis were descriptively/qualitatively analyzed.

3. Results

3.1 Surface roughness and fatigue test

The CAD/CAM AlOx presented the highest surface roughness values (Ra and Rz parameters), while the lowest values were promoted by Ctrl and Pol AlOx groups (Table 2).

In terms of fatigue behavior, power calculation for FFL data indicated a power of 100%. The Pol GLZ group obtained the highest results, followed by CAD/CAM GLZ, being that both were statistically similar to the Ctrl group. The CAD/CAM AlOx had the worst mechanical behavior (Tables 2 and 3).

There is an inverse association between FFL and roughness (i.e. the higher the surface roughness, the lower the fatigue failure load) (Figure 2 and Table 4). The linear regression showed that an increase of one unit in the Ra and Rz parameters decreased the FFL to 49.49 N (-70.79; -28.20) and 8.67 N (-12.46; -4.88), being statistically significant (Table 4). However, the Ra and Rz parameters presented lower coefficient of determination (0.195; 0.191).

The Weibull modulus was similar between all groups (Table 2).

Regarding polished groups, the air abrasion (Pol AlOx group) promoted topographical changes (Figure 3) compared with the Ctrl group due to the impact of the aluminum oxide particles; however, this surface alteration was homogenous on the ceramic surface. The Pol GLZ promoted a homogeneous topography, but there were uncovered regions. The CAD/CAM group presented a topographical alteration with pronounced grooves from the grinding bur. It is possible to observe that the air abrasion after grinding (CAD/CAM AlOx group) modified the defect pattern. On the other hand, the glaze spray application after grinding (CAD/CAM GLZ group) covered some surface defects promoted by the bur; nevertheless, some uncovered regions still remain.

Representative SEM micrographs of the fracture surfaces showed that the fractures originated at the intaglio surface of the zirconia material from the region subjected to the tensile stress concentration (Figure 4).

3.2 Complementary analysis (Flexural strength)

Regarding the flexural strength results, the power calculation indicated a power of 100%. The N-ID group presented the highest values followed by the ID-GLZ group. The ID group presented the lowest flexural strength (Table 5).

The micrographs of the failed bars (Figure 5) showed that all groups also failed at the region of concentrated tensile stresses. It is possible to observe that the ID and ID-GLZ groups failed near the center of the bar, probably at the same place as the indentation. Furthermore, there was a bubble in the ID-GLZ group from applying the glaze near the failure, which may have corroborated the increase in the stress concentration at the site.

4. Discussion

The findings of this study suggest that 4YSZ fatigue behavior is deleteriously influenced by the in-lab simulation of CAD/CAM grinding, and the application of glaze spray induces better 4YSZ mechanical performance compared to air abrasion. Thus, the first and the second hypothesis were accepted, as all ground groups had worse fatigue behavior than their polished counterpart groups, and the glaze spray promoted the highest fatigue performance in both conditions (Pol GLZ and CAD/CAM GLZ groups).

The fracture strength of the ceramic is strongly influenced by the presence of defects, especially those located in the region of tensile stress concentration (Kelly, 1995; Kelly et al., 1990). Procedures such as milling process (Addison et al., 2012; Fraga et al., 2017; Guilardi et al., 2020; Sindel et al., 1998), intaglio surface treatments (Cadore-Rodrigues et al., 2021; Prochnow et al., 2018), and internal adjustments (Rodrigues et al., 2018; Zucuni et al., 2020) can be considered predictors of the mechanical behavior of restorations, as they are performed at the bonded surface of the ceramic which concentrates the higher tensile stresses responsible for initiating and nucleating the crack and its subsequent growth and propagation along the material (Kelly et al., 2017; Scherrer et al., 2017). It is clearly observed in the SEM images that the in-lab simulation of CAD/CAM grinding generated a large surface alteration at the bonding surface with pronounced grooves (Figure 3), which resulted in deleterious behavior of the 4YSZ ceramic when comparing polished and ground groups with the same surface treatment (Table 2). The CAD/CAM milling creates surface alterations that are capable of producing defects on the surface and subsurface of ceramics which can act as stress concentration sources leading to crack propagation (Denry, 2013; Fraga et al., 2017; Guilardi et al., 2020; Quinn et al., 2005; Sindel et al., 1998; Wang et al., 2008). It is important to highlight that the topographic pattern produced by the CAD/CAM group in this study differs from the pattern observed in previous studies which considered specimens machined by the CAD/CAM system (Fraga et al., 2017; Guilardi et al., 2020). Despite this topographic difference, the condition performed in this study using a CAD/CAM bur allowed for evaluating a more complex surface with subsequent interaction with surface treatments.

Considering the ceramic tested in our study (4 mol% yttria-stabilized zirconia – 4YSZ), these defects might be more difficult to contain compared with a 3 mol% yttria-stabilized zirconia since these translucent materials have smaller amounts of tetragonal phase, leading to a reduced possibility of t-to-m transformation and therefore less transformation toughening (Pereira et al., 2018; Stawarczyk et al., 2017). Thus, the mechanical properties of 4YSZ may be more influenced by the presence of defects introduced during manufacturing or processing (Sulaiman et al., 2017). In turn, protocols are needed to minimize these defects in order to promote better mechanical behavior of the material. However, studies normally consider the effect of the surface treatments on a polished surface, which does not represent the real condition in dental practice. The deleterious effect of the milling process has been reported (Fraga et al., 2017; Guilardi et al., 2020; Wang et al., 2008) and the surface treatment applied after milling might minimize or intensify the damage in the 4YSZ restoration.

Finding a surface treatment for dental zirconia allying stable adhesion without damage to its mechanical behavior has been widely studied in the literature (Cadore-Rodrigues et al., 2020b, 2021; De Queiroz et al., 2011; Druck et al., 2015; Pozzobon et al., 2017b, 2017a; Vanderlei et al., 2014), mainly considering 4YSZ ceramics (Cadore-Rodrigues et al., 2021, 2020a). Air-abrasion with aluminum oxide particles covered (or not) by silica is considered as the gold-standard method to treat the surface of YSZ ceramic due to the micromechanical retention promoted by the impact of the particles onto the surface and chemical interaction with silane (Özcan and Bernasconi, 2015; Thompson et al., 2011; Tzanakakis et al., 2016). The impact of the particles against the zirconia substrate promoted a homogeneous topographic alteration on a polished surface (Pol AlOx; Figure 3), increasing the roughness values (Table 2). Previous studies have pointed that AlOx particles promote irregular defects, as the particles are hard and sharp (Zhang et al., 2006), being capable of acting as sources of failure due to the higher stress concentration (Cadore-Rodrigues et al., 2021, 2019), which explain the worse fatigue behavior of the Pol AlOx group compared to the other polished groups (Table 2).

On the other hand, glaze spray as surface treatment promoted the highest fatigue performance in both polished and ground conditions (Pol GLZ and CAD/CAM GLZ groups; Table 2). The glaze is able to promote a more homogeneous surface, covering the defects still existing on the polished surface of 4YSZ (Pol GLZ group), as well as the defects produced by the grinding (CAD/CAM GLZ; Figure 3). Even so, some regions still remained uncovered (in both conditions; Figure 3) because the material may accumulate in restricted areas, thereby exposing the zirconia material and increasing the surface roughness (Cadore-Rodrigues et al., 2020a, 2021; Chun et al., 2017; Machry et al., 2021a; Zucuni et al., 2019). In fact, these uncovered regions were responsible for the highest roughness values in the polished surface condition group (Pol GLZ group), and the roughness in the CAD/CAM GLZ group (Table 2) due to the fact that the glaze was not capable of covering all pronounced grooves (Figure 3).

The better performance of 4YSZ after glazing on the intaglio surface is supported by previous studies (Cadore-Rodrigues et al., 2021; Chun et al., 2017). Glaze infiltration onto surface defects might produce a healing effect (Anusavice and Phillips, 2003) by filling existing microcracks (Chun et al., 2017; Zucuni et al., 2019), which can contribute to containing the crack propagation along the material. Nevertheless, the literature also states that the glaze over the material can behave as a bilayer system and decrease its mechanical performance due to its very low tensile strength (Borba et al., 2011; Guazzato et al., 2005; White et al., 2005). However, we measured all the specimens before and after the glaze application and the thickness variation was approximately 0.01 mm (10 µm), which does not correspond to a bilayer system. This thickness is in accordance with a previous study that applied the same low-fusing porcelain glaze as surface treatment and obtained a mean thickness value of 12 µm (Bottino et al., 2014).

As mentioned above, in addition to intaglio surface treatments promoting a more reactive surface for adhesion, they could minimize surface defects such as those caused by the in-lab simulation of CAD/CAM grinding bur, as observed in the CAD/CAM GLZ group. However, the air abrasion after grinding (CAD/CAM AlOx group) promoted the worst fatigue behavior of the 4YSZ ceramic (Table 2). The impact of the air abrasion particles at the substrate is characterized by extensive erosive wear (Chintapalli et al., 2013; Guazzato et al., 2005). According to the SEM images (Figure 3), the impact of the particles from the air abrasion modified the topographic pattern of defects generated by grinding; although some grooves were mitigated, it seems to have generated a more difficult surface for adhesion, possibly due to superficial erosion of the particles, leading to the highest surface roughness (Table 2).

It is important to mention that the complexity of the topographic pattern is a factor that can influence the ceramic strengthening mechanism. The resin cement's ability to fill surface irregularities (complexity topography) promotes a "resin-ceramic hybrid layer" (homogeneous interface), increasing the energy required for the fracture to spread (Addison et al., 2010; Dapieve et al., 2022; de Kok et al., 2017; Prochnow et al., 2018; Spazzin et al., 2017, 2016). In this case, air abrasion produced a surface with more heterogeneous in the polished condition (Pol AlOx group) and even more complex when applied after grinding (CAD/CAM AlOx), which probably made it difficult for the resin cement to fill irregularities, in turn resulting in tensile stress concentration around these defects and consequently the worst behavior (Table 2).

We report herein the inverse association between roughness and fatigue failure load (Figure 2). According to the linear regression analysis, the increase of one unit in the Ra and Rz parameters decreased the FFL by 49.49 N and 8.67 N, respectively (Table 4), which also contributes to understanding the fatigue behavior of the bonded 4YSZ ceramic considering the conditions evaluated in this study (Table 2). Although significant, the variation of roughness value explained 19% of the FFL variation. Therefore, it can be considered that several other factors may be correlated with the mechanical behavior of the set, such as internal adjustments (grinding with diamond burs) of the restorations (de Kok et al., 2017), resin cement viscosity (Dapieve et al., 2022), adhesion between different substrates (Machry et al., 2021b), and others.

The infiltration ability of glaze spray is remarkable. Thus, we performed a flexural strength test parallel to the fatigue test to analyze the mechanical behavior of indented bars with or without glaze application, and also comparing to bars without indentation (non-indented group). The flexural strength increased after the glaze application over the indentation (Table 5). The glaze possibly filled the crack indentation containing the stress concentration; however, as aforementioned, it presents a very low tensile strength, which probably resulted in a lower flexural strength compared to the non-indented group (N-ID > ID-GLZ > ID). Another observation is regarding the fractographic image of the ID-GLZ group (Figure 5), with it is possible to observe a bubble near the origin of the bar failure. The glaze spray technique inherently promotes bubbles, even promoting fewer ones than the powder and liquid technique (Zucuni et al., 2019), which probably led to the increase in stress concentration at the failure zone.

Finally, studies present zirconia roughness values after CAD/CAM milling of approximately 1.8 µm for Ra and 11.4 µm for Rz (Fraga et al., 2017; Zucuni et al., 2017). Although we used the same bur of a CAD/CAM system and the operator was trained for grinding, the roughness (3.58 µm for Ra and 14.67 µm for Rz parameters) was higher than mentioned in previous studies. In addition, the grinding was performed only in one direction, differently from what occurs in the CAD/CAM system. Even with these limitations, we consider that our results contribute to understand the 4YSZ fatigue behavior under the test conditions explored herein, being important to consider the final ceramic processing topography when exploring its performance *in vitro*. Furthermore, the ceramic processing topography altered the response to surface treatments and consequently the mechanical properties of a restorative set.

5. Conclusions

- The in-lab simulation of CAD/CAM grinding has a detrimental effect on the fatigue behavior of 4YSZ adhesively luted to a dentin analogue material.
- Intaglio surface treatments differently influences the 4YSZ fatigue performance, however, only glaze spray can reverse the damage caused by in-lab simulation of CAD/CAM grinding.
- Glaze spray induces better 4YSZ performance compared to the air abrasion with the aluminum oxide particles.
- The higher the 4YSZ surface roughness the lower the fatigue behavior of the bonded assembly.

REFERENCES

Addison, O., Cao, X., Sunnar, P., Fleming, G.J.P., 2012. Machining variability impacts on the strength of a “chair-side” CAD-CAM ceramic. Dent. Mater. 28, 880–887. https://doi.org/10.1016/j.dental.2012.04.017

Addison, O., Sodhi, A., Fleming, G.J.P., 2010. Seating load parameters impact on dental ceramic reinforcement conferred by cementation with resin-cements. Dent. Mater. 26, 915–921. https://doi.org/10.1016/j.dental.2010.05.006

Anusavice, K.J., Phillips, R.W., 2003. Phillip’s Science of Dental Materials, 11th ed. Elsevier, St Louis.

Aurélio, I.L., Dorneles, L.S., May, L.G., 2017. Extended glaze firing on ceramics for hard machining: Crack healing, residual stresses, optical and microstructural aspects. Dent. Mater. 33, 226–240. https://doi.org/10.1016/j.dental.2016.12.002

Blatz, M.B., Conejo, J., 2019. The Current State of Chairside Digital Dentistry and Materials. Dent. Clin. North Am. 63, 175–197. https://doi.org/10.1016/j.cden.2018.11.002

Borba, M., De Araújo, M.D., De Lima, E., Yoshimura, H.N., Cesar, P.F., Griggs, J.A., Della Bona, Á., 2011. Flexural strength and failure modes of layered ceramic structures. Dent. Mater. 27, 1259–1266. https://doi.org/10.1016/j.dental.2011.09.008

Bottino, M.A., Bergoli, C.D., Lima, E.G., Marocho, S.M.S., Souza, R.O.A., Valandro, L.F., 2014. Bonding of Y-TZP to dentin: Effects of Y-TZP surface conditioning, resin cement type, and aging. Oper. Dent. 39, 291–300. https://doi.org/10.2341/12-235-L

Cadore-Rodrigues, A.C., Machado, P.S., Oliveira, J.S. de, Jahn, S.L., Callegari, G.L., Dorneles, L.S., Burgo, T.A. de L., Rippe, M.P., Pereira, G.K.R., Valandro, L.F., 2020a. Fatigue performance of fully-stabilized zirconia polycrystals monolithic restorations: The effects of surface treatments at the bonding surface. J. Mech. Behav. Biomed. Mater. 110. https://doi.org/10.1016/j.jmbbm.2020.103962

Cadore-Rodrigues, A.C., Machado, P.S., Oliveira, J.S. de, Jahn, S.L., Dorneles, L.S., Rippe, M.P., Pereira, G.K.R., Valandro, L.F., 2021. Surface treatments and its effects on the fatigue behavior of a 5% mol yttria partially stabilized zirconia material. J. Mech. Behav. Biomed. Mater. 120. https://doi.org/10.1016/j.jmbbm.2021.104543

Cadore-Rodrigues, A.C., Prochnow, C., Burgo, T.A.L., Oliveira, J.S., Jahn, S.L., Foletto, E.L., Rippe, M.P., Pereira, G.K.R., Valandro, L.F., 2020b. Stable resin bonding to Y-TZP ceramic with air abrasion by alumina particles containing 7% silica. J. Adhes. Dent. 22, 149–159. https://doi.org/10.3290/j.jad.a44151

Cadore-Rodrigues, A.C., Prochnow, C., Rippe, M.P., Oliveira, J.S. de, Jahn, S.L., Foletto, E.L., Pereira, G.K.R., Valandro, L.F., 2019. Air-abrasion using new silica-alumina powders containing different silica concentrations: Effect on the microstructural characteristics and fatigue behavior of a Y-TZP ceramic. J. Mech. Behav. Biomed. Mater. 98, 11–19. https://doi.org/10.1016/j.jmbbm.2019.05.032

Chen, B., Yan, Y., Xie, H., Meng, H., Zhang, H., Chen, C., 2020. Effects of tribochemical silica coating and alumina-particle air abrasion on 3Y-TZP and 5Y-TZP: Evaluation of surface hardness, roughness, bonding, and phase transformation. J. Adhes. Dent. 22, 373–382. https://doi.org/10.3290/j.jad.a44868

Chen, C., Trindade, F.Z., De Jager, N., Kleverlaan, C.J., Feilzer, A.J., 2014. The fracture resistance of a CAD/CAM Resin Nano Ceramic (RNC) and a CAD ceramic at different thicknesses. Dent. Mater. 30, 954–962. https://doi.org/10.1016/j.dental.2014.05.018

Chintapalli, R.K., Marro, F.G., Jimenez-Pique, E., Anglada, M., 2013. Phase transformation and subsurface damage in 3Y-TZP after sandblasting. Dent. Mater. 29, 566–572. https://doi.org/10.1016/j.dental.2013.03.005

Chun, E.P., Anami, L.C., Bonfante, E.A., Bottino, M.A., 2017. Microstructural analysis and reliability of monolithic zirconia after simulated adjustment protocols. Dent. Mater. 33, 934–943. https://doi.org/10.1016/j.dental.2017.04.024

Dapieve, K.S., Pereira, G.K.R., Venturini, A.B., Daudt, N., Valcanaia, A., Bottino, M.C., Valandro, L.F., 2022. Do resin cement viscosity and ceramic surface etching influence the fatigue performance of bonded lithium disilicate glass-ceramic crowns? Dent. Mater. 38, e59–e67. https://doi.org/10.1016/j.dental.2021.12.015

de Kok, P., Pereira, G.K.R., Fraga, S., de Jager, N., Venturini, A.B., Kleverlaan, C.J., 2017. The effect of internal roughness and bonding on the fracture resistance and structural reliability of lithium disilicate ceramic. Dent. Mater. 33, 1416–1425. https://doi.org/10.1016/j.dental.2017.09.018

De Queiroz, J.R.C., Duarte, D.A., De Assunção E Souza, R.O., Fissmer, S.F., Massi, M., Bottino, M.A., 2011. Deposition of SiOx thin films on Y-TZP by reactive magnetron sputtering: Influence of plasma parameters on the adhesion properties between Y-TZP and resin cement for application in dental prosthesis. Mater. Res. 14, 212–216. https://doi.org/10.1590/S1516-14392011005000032

Denry, I., 2013. How and when does fabrication damage adversely affect the clinical performance of ceramic restorations? Dent. Mater. 29, 85–96. https://doi.org/10.1016/j.dental.2012.07.001

Druck, C.C., Pozzobon, J.L., Callegari, G.L., Dorneles, L.S., Valandro, L.F., 2015. Adhesion to Y-TZP ceramic: Study of silica nanofilm coating on the surface of Y-TZP. J. Biomed. Mater. Res. - Part B Appl. Biomater. 103, 143–150. https://doi.org/10.1002/jbm.b.33184

Fraga, S., Amaral, M., Bottino, M.A., Valandro, L.F., Kleverlaan, C.J., May, L.G., 2017. Impact of machining on the flexural fatigue strength of glass and polycrystalline CAD/CAM ceramics. Dent. Mater. 33, 1286–1297. https://doi.org/10.1016/j.dental.2017.07.019

Guazzato, M., Quach, L., Albakry, M., Swain, M. V., 2005. Influence of surface and heat treatments on the flexural strength of Y-TZP dental ceramic. J. Dent. 33, 9–18. https://doi.org/10.1016/j.jdent.2004.07.001

Guilardi, L.F., Soares, P., Werner, A., de Jager, N., Pereira, G.K.R., Kleverlaan, C.J., Rippe, M.P., Valandro, L.F., 2020. Fatigue performance of distinct CAD/CAM dental ceramics. J. Mech. Behav. Biomed. Mater. 103, 103540. https://doi.org/10.1016/j.jmbbm.2019.103540

ISO: 6872, 2015. INTERNATIONAL STANDARD ISO Dentistry — Ceramic materials.

Karlsen, C.A., Schriwer, C., Øilo, M., 2020. Damage tolerance of six dental zirconias with different translucencies. Biomaterial Investigations in Dentistry 7 (1), 126–133. doi:10.1080/26415275.2020.1809420.

Kelly, J.R., 1995. Perspectives on strength. Dent. Mater. 11, 103–110. https://doi.org/10.1016/0109-5641(95)80043-3

Kelly, J.R., Cesar, P.F., Scherrer, S.S., Della Bona, A., van Noort, R., Tholey, M., Vichi, A., Lohbauer, U., 2017. ADM guidance-ceramics: Fatigue principles and testing. Dent. Mater. 33, 1192–1204. https://doi.org/10.1016/j.dental.2017.09.006

Kelly, J.R., Giordano, R., Pober, R., Cima, M.J., 1990. Fracture surface analysis of dental ceramics: clinically failed restorations. Int. J. Prosthodont. 3, 430–40.

Konstantinidis, I., Trikka, D., Gasparatos, S., Mitsias, M.E., 2018. Clinical outcomes of monolithic zirconia crowns with cad/cam technology. A 1-year follow-up prospective clinical study of 65 patients. Int. J. Environ. Res. Public Health 15. https://doi.org/10.3390/ijerph15112523

Ludovichetti, F.S., Trindade, F.Z., Werner, A., Kleverlaan, C.J., Fonseca, R.G., 2018. Wear resistance and abrasiveness of CAD-CAM monolithic materials. J. Prosthet. Dent. 120, 318.e1-318.e8. https://doi.org/10.1016/j.prosdent.2018.05.011

Machry, R.V., Cadore-Rodrigues, A.C., Borges, A.L.S., Pereira, G.K.R., Kleverlaan, C.J., Venturini, A.B., Valandro, L.F., 2021a. Fatigue resistance of simplified CAD–CAM restorations: Foundation material and ceramic thickness effects on the fatigue behavior of partially- and fully-stabilized zirconia. Dent. Mater. 37, 568–577. https://doi.org/10.1016/j.dental.2021.01.001

Machry, R.V., Cadore-Rodrigues, A.C., Packaeser, M.G., Lorenzett, E., Burgo, T.A. de L., Pereira, G.K.R., Valandro, L.F., 2021b. Influence of surface treatment of resin composite substrate on the load-bearing capacity under fatigue of lithium disilicate monolithic simplified restorations. J. Mech. Behav. Biomed. Mater. 124, 104792. https://doi.org/10.1016/j.jmbbm.2021.104792

Malysa, A., Wezgowiec, J., Orzeszek, S., Florjanski, W., Zietek, M., Wieckiewicz, M., 2021. Effect of different surface treatment methods on bond strength of dental ceramics to dental hard tissues: A systematic review. Molecules 26. https://doi.org/10.3390/molecules26051223

Marshall, D.B., Evans, A.G., 1983. The nature of machining damage in brittle materials. … R. … 385, 461–475.

Miyazaki, T., Hotta, Y., 2011. CAD/CAM systems available for the fabrication of crown and bridge restorations. Aust. Dent. J. 56, 97–106. https://doi.org/10.1111/j.1834-7819.2010.01300.x

Mosele, J.C., Borba, M., 2014. Efeito do jateamento de partículas na resistência de união e comportamento mecânico de cerâmicas à base de zircônia -Revisão (Effect of particle sandblasting on the bond strength and mechanical behavior of zirconia-based ceramics -Review). Cerâmica 60, 179–186. https://doi.org/10.1590/S0366-69132014000200003

Osiewicz, M.A., Werner, A., Roeters, F.J.M., Kleverlaan, C.J., 2022. Wear of bulk-fill resin composites. Dent. Mater. 38, 549–553. https://doi.org/10.1016/j.dental.2021.12.138

Özcan, M., Bernasconi, M., 2015. Adhesion to Zirconia Used for Dental Restorations: A Systematic Review and Meta-Analysis. J. Adhes. Dent. 17, 7–26. https://doi.org/10.3290/j.jad.a33525

Özcan, M., Vallittu, P.K., 2003. Effect of surface conditioning methods on the bond strength of luting cement to ceramics. Dent. Mater. 19, 725–731. https://doi.org/10.1016/S0109-5641(03)00019-8

Pereira, G.K.R., Guilardi, L.F., Dapieve, K.S., Kleverlaan, C.J., Rippe, M.P., Valandro, L.F., 2018. Mechanical reliability, fatigue strength and survival analysis of new polycrystalline translucent zirconia ceramics for monolithic restorations. J. Mech. Behav. Biomed. Mater. 85, 57–65. https://doi.org/10.1016/j.jmbbm.2018.05.029

Piconi, C., Maccauro, G., 1999. Zirconia as a ceramic biomaterial. Biomaterials 20, 1–25. https://doi.org/10.1016/S0142-9612(98)00010-6

Pilecco, R.O., Dalla-Nora, F., Guilardi, L.F., Pereira, G.K.R., de Andrade, G.S., de Melo, R.M., Valandro, L.F., Rippe, M.P., 2021. In-lab simulation of CAD/CAM milling of lithium disilicate glass-ceramic specimens: Effect on the fatigue behavior of the bonded ceramic. J. Mech. Behav. Biomed. Mater. 121, 104604.

https://doi.org/10.1016/j.jmbbm.2021.104604

Pozzobon, J.L., Pereira, G.K.R., Wandscher, V.F., Dorneles, L.S., Valandro, L.F., 2017a. Mechanical behavior of yttria-stabilized tetragonal zirconia polycrystalline ceramic after different zirconia surface treatments. Mater. Sci. Eng. C 77, 828–835. https://doi.org/10.1016/j.msec.2017.03.299

Pozzobon, J.L., Wandscher, V.F., Rippe, M.P., Valandro, L.F., 2017b. Influence of zirconia surface treatments on resin cement bonding and phase transformation. J. Adhes. Sci. Technol. 31, 1671–1682. https://doi.org/10.1080/01694243.2016.1268413

Prochnow, C., Venturini, A.B., Guilardi, L.F., Pereira, G.K.R., Burgo, T.A.L., Bottino, M.C., Kleverlaan, C.J., Valandro, L.F., 2018. Hydrofluoric acid concentrations: Effect on the cyclic load to failure of machined lithium disilicate restorations. Dent. Mater. 34, e255–e263. https://doi.org/10.1016/j.dental.2018.06.028

Quinn, G.D., Ives, L.K., Jahanmir, S., 2005. On the nature of machining cracks in ground ceramics: Part I: SRBSN strengths and fractographic analysis. Mach. Sci. Technol. 9, 169–210. https://doi.org/10.1081/MST-200059038

Rekow, D., Thompson, V.P., 2005. Near-surface damage - A persistent problem in crowns obtained by computer-aided design and manufacturing. Proc. Inst. Mech. Eng. Part H J. Eng. Med. 219, 233–243. https://doi.org/10.1243/095441105X9363

Rodrigues, C.D.S., Guilardi, L.F., Follak, A.C., Prochnow, C., May, L.G., Valandro, L.F., 2018. Internal adjustments decrease the fatigue failure load of bonded simplified lithium disilicate restorations. Dent. Mater. 34, e225–e235. https://doi.org/10.1016/j.dental.2018.05.015

Scherrer, S.S., Lohbauer, U., Della Bona, A., Vichi, A., Tholey, M.J., Kelly, J.R., van Noort, R., Cesar, P.F., 2017. ADM guidance—Ceramics: guidance to the use of fractography in failure analysis of brittle materials. Dent. Mater. 33, 599–620. https://doi.org/10.1016/j.dental.2017.03.004

Sindel, J., Petschelt, A., Grellner, F., Dierken, C., Greil, P., 1998. Evaluation of subsurface damage in CAD / CAM machined dental ceramics. J Mater Sci Mater Med 9, 291–295.

Spazzin, A.O., Bacchi, A., Alessandretti, R., Santos, M.B., Basso, G.R., Griggs, J., Moraes, R.R., 2017. Ceramic strengthening by tuning the elastic moduli of resin-based luting agents. Dent. Mater. 33, 358–366. https://doi.org/10.1016/j.dental.2017.01.002

Spazzin, A.O., Guarda, G.B., Oliveira-Ogliari, A., Leal, F.B., Correr-Sobrinho, L., Moraes, R.R., 2016. Strengthening of porcelain provided by resin cements and flowable composites. Oper. Dent. 41, 179–188. https://doi.org/10.2341/15-025-L

Stawarczyk, B., Keul, C., Eichberger, M., Figge, D., Edelhoff, D., Lümkemann, N., 2017. Three generations of zirconia: From veneered to monolithic. Part I. Quintessence Int. 48, 369–380. https://doi.org/10.3290/j.qi.a38057

Sulaiman, T.A., Abdulmajeed, A.A., Shahramian, K., Lassila, L., 2017. Effect of different treatments on the flexural strength of fully versus partially stabilized monolithic zirconia. J. Prosthet. Dent. 118, 216–220. https://doi.org/10.1016/j.prosdent.2016.10.031

Thompson, J.Y., Stoner, B.R., Piascik, J.R., Smith, R., 2011. Adhesion/cementation to zirconia and other non-silicate ceramics: where are we now? Dent. Mater. 27, 71–82. https://doi.org/10.1016/j.dental.2010.10.022

Tzanakakis, E.G.C., Tzoutzas, I.G., Koidis, P.T., 2016. Is there a potential for durable adhesion to zirconia restorations? A systematic review. J. Prosthet. Dent. 115, 9–19. https://doi.org/10.1016/j.prosdent.2015.09.008

Valentino, T.A., Borges, G.A., Borges, L.H., Platt, J.A., Correr-Sobrinho, L., 2012. Influence of glazed zirconia on dual-cure luting agent bond strength. Oper. Dent. 37, 181–187. https://doi.org/10.2341/10-220-L

Vanderlei, A., Bottino, M., Valandro, L., 2014. Evaluation of Resin Bond Strength to Yttria-stabilized Tetragonal Zirconia and Framework Marginal Fit: Comparison of Different Surface Conditionings. Oper. Dent. 39, 50–63. https://doi.org/10.2341/12-269-L

Wang, H., Aboushelib, M.N., Feilzer, A.J., 2008. Strength influencing variables on CAD/CAM zirconia frameworks. Dent. Mater. 24, 633–638. https://doi.org/10.1016/j.dental.2007.06.030

White, S.N., Miklus, V.G., McLaren, E.A., Lang, L.A., Caputo, A.A., 2005. Flexural strength of a layered zirconia and porcelain dental all-ceramic system. J. Prosthet. Dent. 94, 125–131. https://doi.org/10.1016/j.prosdent.2005.05.007

Zarone, F., Russo, S., Sorrentino, R., 2011. From porcelain-fused-to-metal to zirconia: Clinical and experimental considerations. Dent. Mater. 27, 83–96. https://doi.org/10.1016/j.dental.2010.10.024

Zhang, G.., Satish, K.., Ko, W.., 1994. The mechanics of material removal mechanisms in the machining of ceramics. Institute for Systems Research.

Zhang, Y., Lawn, B.R., 2018. Novel Zirconia Materials in Dentistry. J. Dent. Res. 97, 140–147. https://doi.org/10.1177/0022034517737483

Zhang, Y., Lawn, B.R., Malament, K.A., Van Thompson, P., Rekow, E.D., 2006. Damage accumulation and fatigue life of particle-abraded ceramics. Int. J. Prosthodont. 19, 442–448.

Zucuni, C.P., Guilardi, L.F., Fraga, S., May, L.G., Pereira, G.K.R., Valandro, L.F., 2017. CAD/CAM machining Vs pre-sintering in-lab fabrication techniques of Y-TZP ceramic specimens: Effects on their mechanical fatigue behavior. J. Mech. Behav. Biomed. Mater. 71, 201–208. https://doi.org/10.1016/j.jmbbm.2017.03.013

Zucuni, C.P., Ilha, B.D., May, M.M., May, L.G., Valandro, L.F., 2020. Grinding the intaglio surface of yttria partially- and fully-stabilized zirconia polycrystals restorations: Effect on their fatigue behavior. J. Mech. Behav. Biomed. Mater. 109, 103800. https://doi.org/10.1016/j.jmbbm.2020.103800

Zucuni, C.P., Pereira, G.K.R., Dapieve, K.S., Rippe, M.P., Bottino, M.C., Valandro, L.F., 2019. Low-fusing porcelain glaze application does not damage the fatigue strength of Y-TZP. J. Mech. Behav. Biomed. Mater. 99, 198–205. https://doi.org/10.1016/j.jmbbm.2019.07.022

TABLES

Table 1. List of materials used in the study: commercial name, manufacturer, batch number and composition based on the manufacturer's information.

Commercial name	**Manufacturer (batch number)**	**Composition**
IPS e.max ZirCAD MT	Ivoclar (Y34224)	86.0 ≤ 93.5% ZrO_2; 6.5 ≤ 8.0% Y_2O_3; ≤ 5.0% HfO_2; ≤ 1.0% Al_2O_3
Epoxydplatte	Carbotec GmbH	Woven glass-reinforced epoxy resin
9% hydrofluoric acid	Ultradent Products (BKSS4)	9% concentration hydrofluoric acid
VITA Akzent Plus	VITA Zahnfabrik (E78440)	Amorphous glassy substance (silica-based material)
Aluminum oxide	Harnisch+Rieth	Aluminum oxide particles (50 µm)
Monobond N	Ivoclar (Y45831)	Alcohol solution of silane methacrylate, phosphoric acid methacrylate and sulphide methacrylate.
Multilink Primer A	Ivoclar (Y37839)	Aqueous solution of initiators
Multilink Primer B	Ivoclar (Y41401)	HEMA, phosphonic acid and acrylic acid monomers
Multilink N	Ivoclar (Y30903)	Dimethacrylates, HEMA, barium glass, Ba–Al-fluoro-silicate glass, ytterbium trifluoride, highly dispersed silica, catalysts and stabilizers, pigments

Table 2. Roughness analysis by means of Kruskal Wallis and post-hoc LSD test (Ra and Rz parameters – mean and standard deviation) according to each group; and survival analysis by means of Kaplan-Meier and Mantel-Cox (Log-Rank) tests (mean and respective 95% confidence intervals for fatigue failure load - FFL and cycles for failure - CFF) and Weibull modulus with respective 95% confidence intervals for fatigue data (FFL and CFF).

Groups	Surface Roughness		Fatigue Failure Load (N)	Cycles to Failure (counts)	Weibull Modulus	
	Ra	Rz			FFL	CFF
Ctrl	0.48 (0.37)^{D}	2.57 (1.58)^{E}	860 (773 – 947)^{AB}	76,000 (67,276 – 84,723)^{AB}	5.85 (3.77 – 8 .47)^{A}	5.18 (3.33 – 7.50)^{A}
Pol AlOx	0.36 (0.17)^{D}	3.24 (1.16)^{E}	580 (552 – 608)^{C}	48,000 (45,163 – 50,837)^{C}	11.41 (7.54 – 15.83)^{A}	9.53 (6.28 – 13.25)^{A}
Pol GLZ	1.00 (0.18)^{C}	6.13 (1.29)^{D}	980 (901 – 1,059)^{A}	88,000 (80,067 – 95,933)^{A}	6.32 (4.20 – 8.80)^{A}	5.72 (3.81 – 7.97)^{A}
CAD/CAM	3.58 (0.73)^{B}	14.67 (1.48)^{C}	600 (549 – 651)^{C}	50,000 (44,939 – 55,061)^{C}	6.77 (4.43 – 9.55)^{A}	5.69 (3.71 – 8.04)^{A}
CAD/CAM AlOx	4.87 (1.05)^{A}	29.87 (4.20)^{A}	486 (449 – 524)^{D}	38,667 (34,905 – 42,428)^{D}	7.40 (4.81 – 10.58)^{A}	5.92 (3.84 – 8.48)^{A}
CAD/CAM GLZ	3.57 (0.40)^{B}	21.99 (3.00)^{B}	753 (693 – 813)^{B}	65,334 (59,325 – 71,341)^{B}	7.78 (4.99 – 11.3)^{A}	6.75 (4.32 – 9.80)^{A}
Different capital letters indicate statistical differences for each condition.						

Table 3. Survival probabilities for different load steps and number of cycles parameters.

Groups	Load to failure / Number of cycles for fatigue failure											
	200N/ $10x10^3$	300N/ $20x10^3$	400N/ $30x10^3$	500N/ $40x10^3$	600N/ $50x10^3$	700N/ $60x10^3$	800N/ $70x10^3$	900N/ $80x10^3$	1000N/ $90x10^3$	1100N/ $100x10^3$	1200N/ $110x10^3$	1300N/ $120x10^3$
Ctrl	1	1	1	1	0.86 (0.08)	0.73 (0.11)	0.46 (0.12)	0.33 (0.12)	0.20 (0.10)	0 (0)	-	-
Pol AlOx	1	1	1	0.73 (0.11)	0.06 (0.06)	0 (0)	-	-	-	-	-	-
Pol GLZ	1	1	1	1	1	1	0.80 (0.10)	0.53 (0.12)	0.20 (0.10)	0.13 (0.08)	…	0 (0)
CAD/CAM	1	1	0.93 (0.06)	0.73 (0.11)	0.26 (0.11)	0.06 (0.06)	0 (0)	-	-	-	-	-
CAD/CAM AlOx	1	1	0.66 (0.12)	0.20 (0.10)	0 (0)	-	-	-	-	-	-	-
CAD/CAM GLZ	1	1	1	0.93 (0.06)	0.86 (0.08)	0.46 (0.12)	0.26 (0.11)	0 (0)	-	-	-	-
The symbol "-" indicates absence of specimen being tested on the considered step. The symbol "…" indicates absence of specimen fracturing in the respective step for each condition.												

Table 4. Association between fatigue failure load and roughness (Ra and Rz parameters) determined by linear regression.

Variable	Fatigue failure load		
	β1 (95% IC)	**p-value**	**R^2**
Ra	-49.49 (-70.79; -28.20)	<0.01	0.195
Rz	-8.67 (-12.46; -4.88)	<0.01	0.191

β1: linear coefficient; IC: confidence interval; R^2: coefficient of determination.

Table 5. Flexural strength (mean and standard deviation in MPa) of the bars by means of Kruskal Wallis and post-hoc LSD test.

Groups	Flexural strength*
N-ID	975.65 (128.05)^{A}
ID	312.19 (40.14)^{C}
ID-GLZ	546.26 (215.39)^{B}
*Different capital letters indicate statistical differences for each condition.	

FIGURES

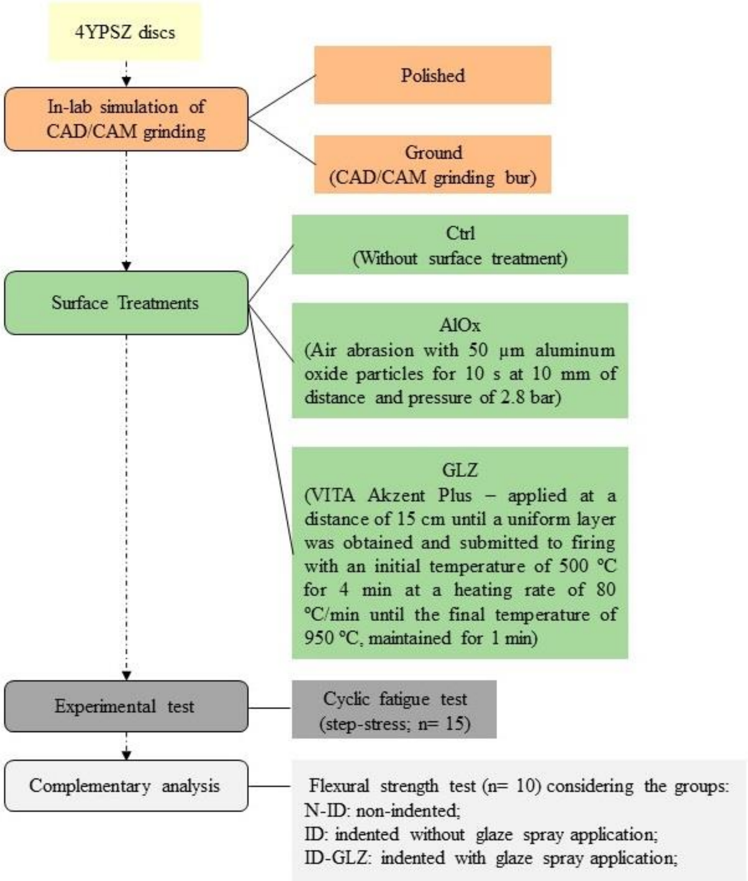

Figure 1. Flow diagram of study design.

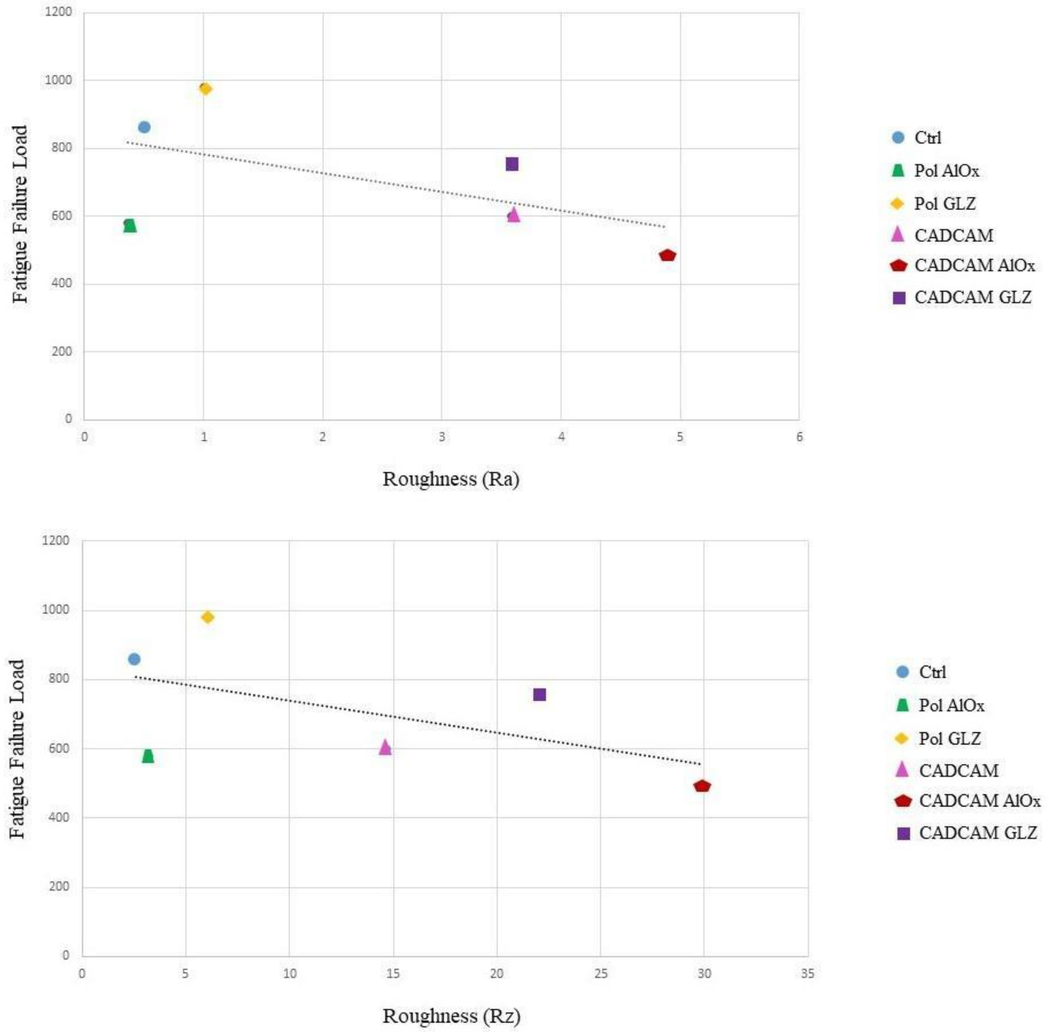

Figure 2. Relation between fatigue failure load and roughness parameters (Ra and Rz) according to each group.

<table>
<tr><th>Ctrl</th><th>Pol AlOx</th><th>Pol GLZ</th></tr>
<tr>
<td>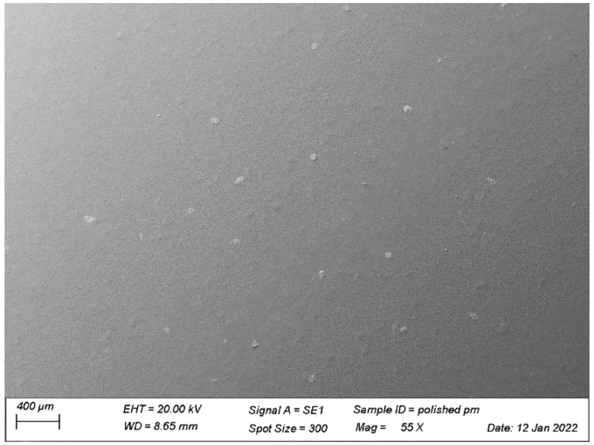</td>
<td>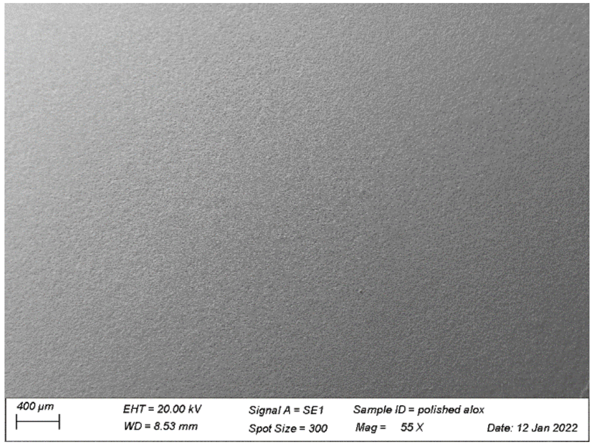</td>
<td>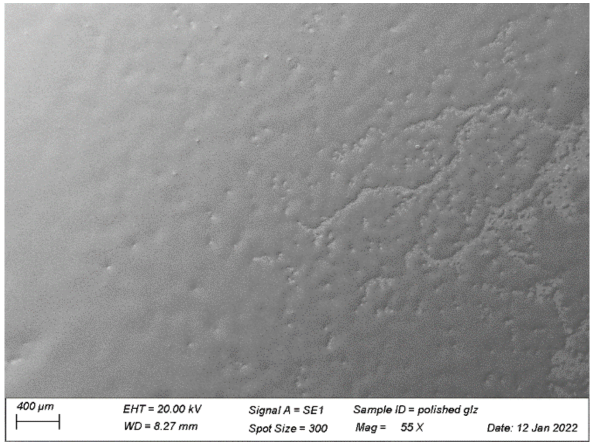</td>
</tr>
<tr>
<td>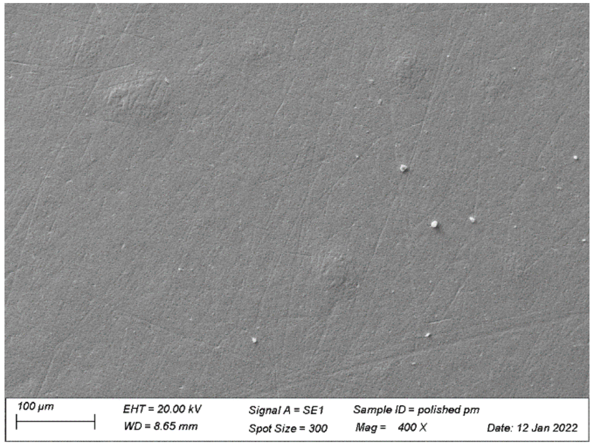</td>
<td>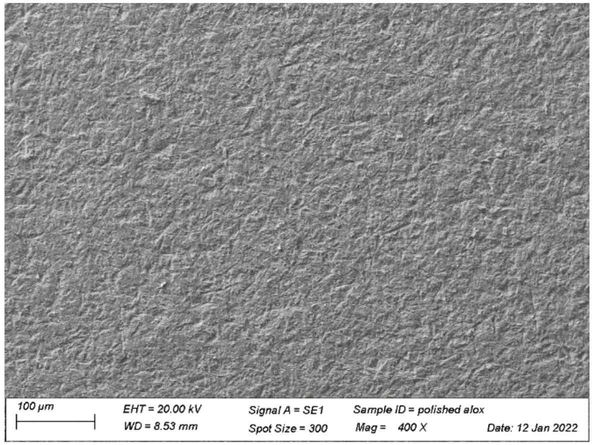</td>
<td>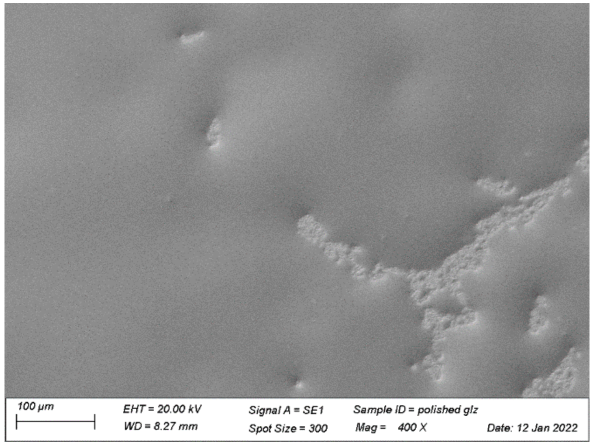</td>
</tr>
</table>

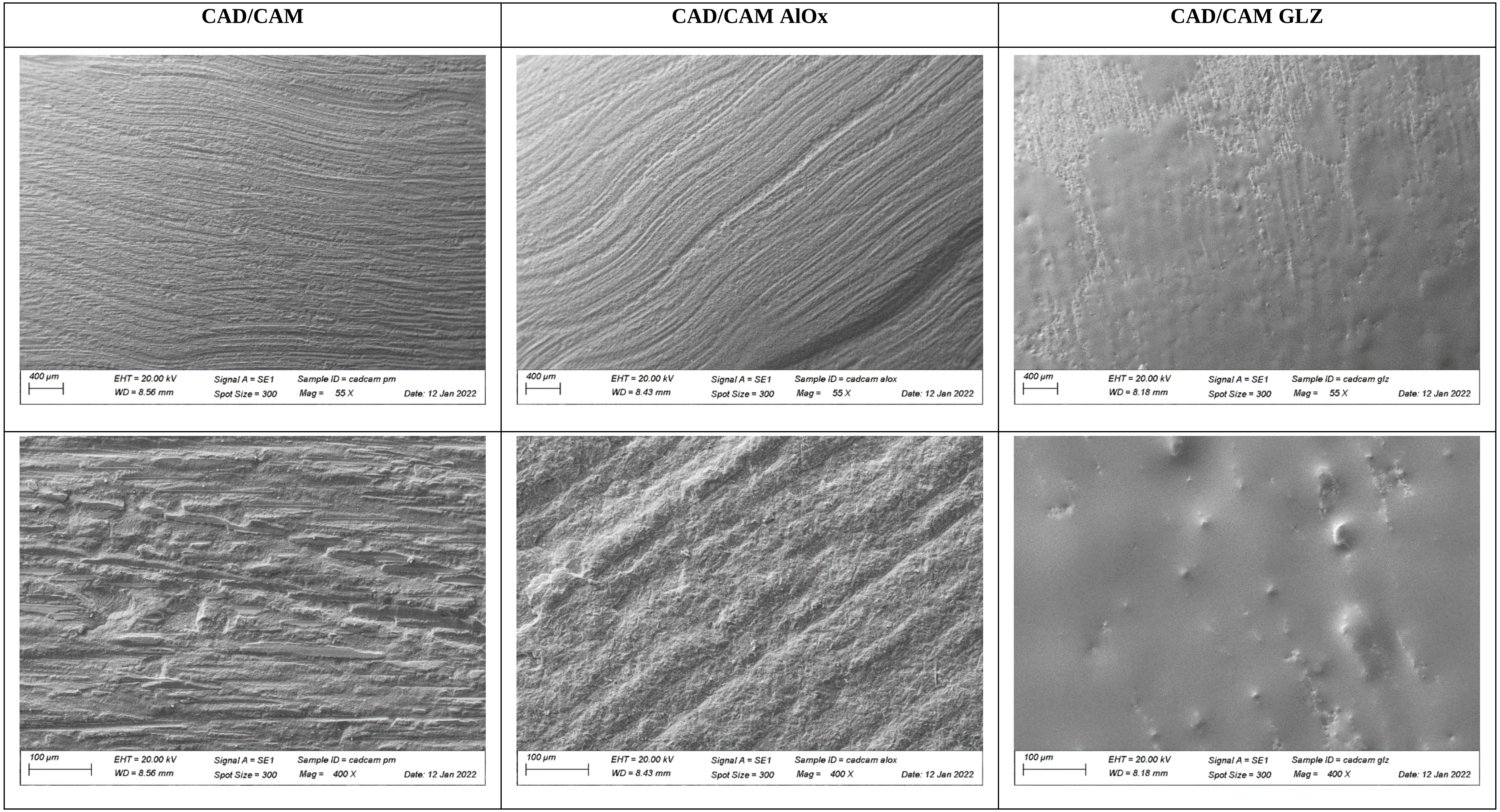

Figure 3. SEM micrographs of the ceramic surfaces according to each group at 55× (top) and 400× (bottom) magnifications.

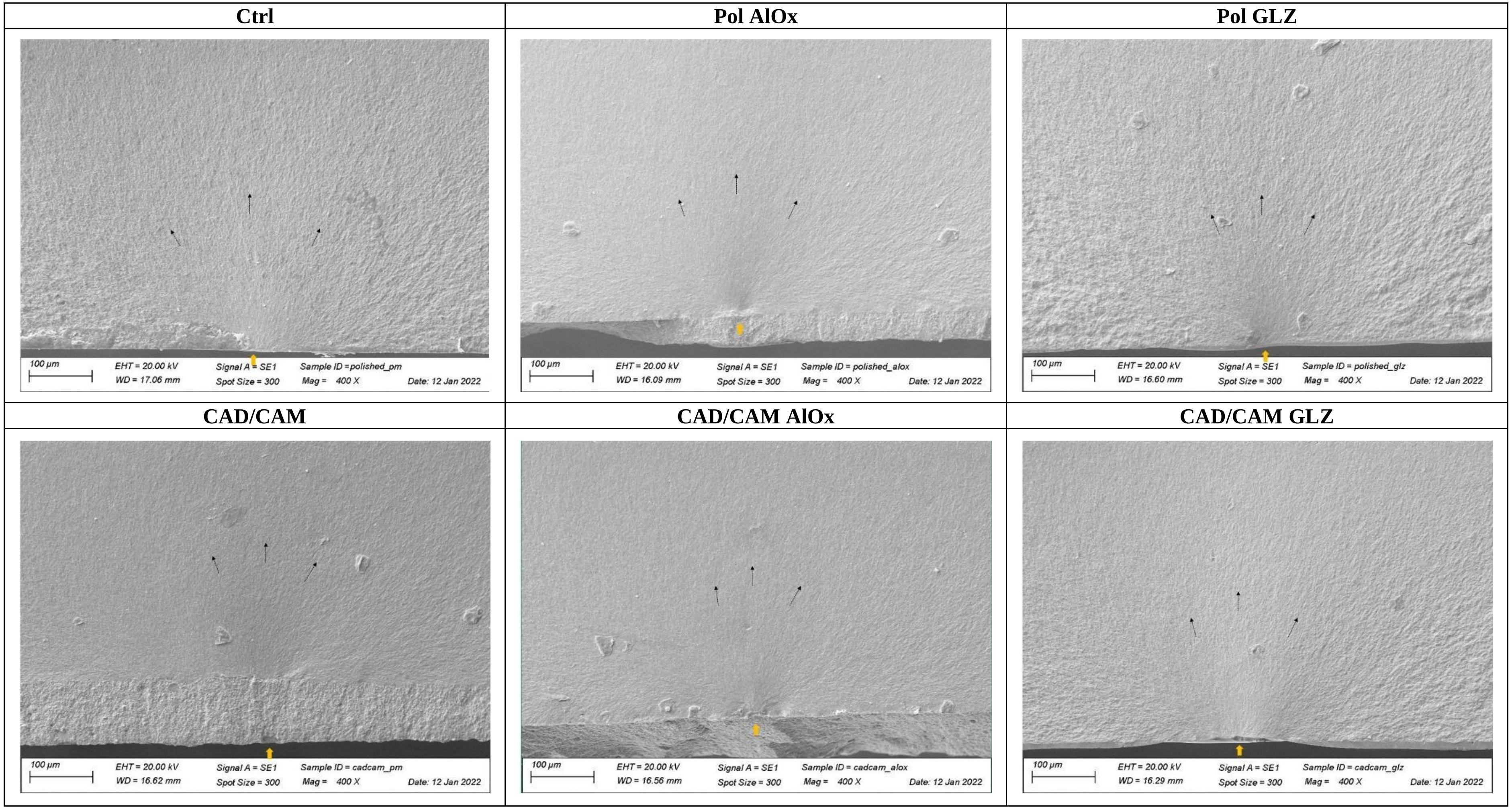

Figure 4. Representative SEM micrographs of fractured discs (fractographical examination) at 400× magnification. The yellow arrows indicate the crack origin and the dashed black arrows indicate the hackle lines characteristic of fracture marks.

N-ID	ID	ID-GLZ

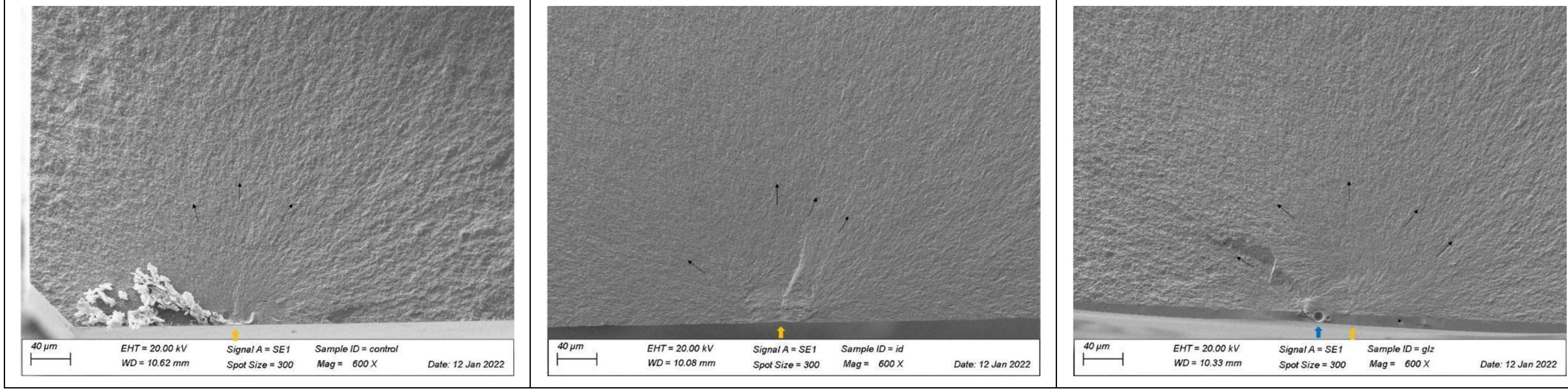

Figure 5. Representative SEM micrographs of fractured bars (fractographical examination) at 600× magnification. The yellow arrows indicate the crack origin and the dashed black arrows indicate the hackle lines. The blue arrow indicates a bubble in the ID-GLZ group, probably due to the glaze spray application.

5. CONSIDERAÇÕES FINAIS

As cerâmicas odontológicas são materiais de natureza friável, ou seja, suportam pouca ou nenhuma deformação plástica antes de fraturar, por isso são sensíveis à presença de defeitos e apresentam menor resistência à tração quando comparada à compressão (HONDRUM, 1992). A superfície de cimentação (região interna) da peça cerâmica concentra grande parte das tensões de tração responsáveis pelo início da maioria das falhas das restaurações cerâmicas (KELLY et al., 1990; THOMPSON et al., 1994). Desse modo, torna-se imprescindível a avaliação de procedimentos que afetam regiões de concentração de tensões de tração no comportamento em fadiga dos materiais cerâmicos, que é o principal fator para a fratura da restauração por meio do crescimento lento de trincas, no qual a trinca se propaga ao longo do material levando a diminuição de resistência ao longo do tempo (KELLY et al., 2017; SCHERRER et al., 2017).

Diversos procedimentos clínicos podem ser considerados preditores do comportamento mecânico das restaurações cerâmicas, tais como o desgaste realizado pelas brocas do CAD/CAM (*Computer Assisted Design/Computer Assisted Machining*) (FRAGA et al., 2017; GUILARDI et al., 2020; SINDEL et al., 1998) e tratamentos de superfície (CADORE-RODRIGUES et al., 2021; PROCHNOW et al., 2018), que foram avaliados na presente tese considerando zircônias de terceira geração com ≥4-5% mol de óxido de ítrio.

De acordo com o artigo 1 da presente tese, os diferentes tratamentos de superfície promovem rugosidades superficiais e alterações topográficas de forma distinta, e, por conseguinte, diferentes comportamentos mecânicos da zircônia de terceira geração. Dentre os jateamentos utilizados, as partículas modificadas por sílica (óxido de alumínio revestido por sílica e óxido de alumínio revestido com 7% de sílica) induzem um comportamento mecânico em fadiga similar a uma condição sem tratamento (controle). Enquanto as partículas de óxido de alumínio, por sua característica de partícula dura e afiada (ZHANG et al., 2006), apresentam um potencial de induzir efeitos deletérios no comportamento mecânico do material. A deposição de filmes de sílica é um tratamento que não promove alteração superficial por ser um método estritamente baseado em adesão química (DE QUEIROZ et al., 2011), não alterando as propriedades mecânicas da zircônia de terceira geração. Enquanto a aplicação de glaze de baixa fusão promove uma superfície mais homogênea, no qual a habilidade de infiltração do glaze em microporos e microtrincas confere ao material um efeito "cicatrizante" (ANUSAVICE; PHILLIPS, 2003) proporcionando melhor performance em fadiga da zircônia de terceira geração.

Os resultados apresentados no artigo 2 mostram que apesar dos tratamentos de superfície promoverem diferentes alterações superficiais, eles são fundamentais para manter um estável desempenho mecânico em fadiga do conjunto restaurador (cerâmica-cimento resinoso-substrato análogo de dentina) após envelhecimento, o que inclui também apenas aplicação de primer universal. Porém, quando a superfície da zircônia não recebe nenhum tipo de tratamento, a interface adesiva cimento resinoso/zircônia é mais suscetível a degradação causada pelo armazenamento em água e termociclagem, induzindo resultados instáveis.

Além disso, é importante considerar a topografia final pós processamento cerâmico ao explorar o desempenho mecânico das restaurações *in vitro*. Assim, de acordo com os resultados do artigo 3, a simulação em laboratório do desgaste realizado pelas brocas do CAD/CAM altera de forma expressiva a topografia da zircônia, diminuindo o desempenho à fadiga do conjunto restaurador. Além disso, a topografia gerada pelo desgaste altera a resposta aos tratamentos de superfície, onde apenas a aplicação de glaze em spray pode reverter os danos causados por meio da sua infiltração nos defeitos superficiais proporcionando melhor distribuição de tensões e consequentemente induzindo um melhor desempenho à fadiga da zircônia de terceira geração comparado com o jateamento com óxido de alumínio. O impacto das partículas do jateamento ocasiona extenso desgaste erosivo no substrato cerâmico (CHINTAPALLI et al., 2013; GUAZZATO et al., 2005), o que parece ter gerado uma superfície mais heterogênea para adesão prejudicando o comportamento em fadiga do conjunto. Ademais, existe uma relação inversa entre rugosidade superficial e carga para falha em fadiga da zircônia de terceira geração, quanto maior a rugosidade menor o comportamento mecânico em fadiga do conjunto restaurador.

Portanto, a partir desses achados podemos concluir que os tratamentos de superfície modificam de forma distinta a topografia de zircônias de terceira geração, sendo fundamentais para um estável desempenho à fadiga do conjunto restaurador cerâmica-cimento resinoso-substrato análogo de dentina. Entretanto, considerando uma topografia final pós processamento cerâmico, a simulação em laboratório do desgaste com as brocas do CAD/CAM promove um efeito deletério no comportamento em fadiga da zircônia de terceira geração, no qual a aplicação de glaze em spray induz uma melhor performance em fadiga do conjunto restaurador.

REFERÊNCIAS

ABOUSHELIB, M. N.; KLEVERLAAN, C. J.; FEILZER, A. J. Selective infiltration-etching technique for a strong and durable bond of resin cements to zirconia-based materials. **Journal of Prosthetic Dentistry**, v. 98, n. 5, p. 379–388, 2007.

ALGHAZZAWI, T. F. Advancements in CAD/CAM technology: Options for practical implementation. **Journal of Prosthodontic Research**, v. 60, n. 2, p. 72–84, 2016.

ANUSAVICE, K. J.; PHILLIPS, R. W. **Phillip's Science of Dental Materials**. 11. ed. St Louis: Elsevier, 2003.

BLATZ, M. B.; CONEJO, J. The Current State of Chairside Digital Dentistry and Materials. **Dental Clinics of North America**, v. 63, n. 2, p. 175–197, 2019.

BOTTINO, M. A. et al. Bonding of Y-TZP to dentin: Effects of Y-TZP surface conditioning, resin cement type, and aging. **Operative Dentistry**, v. 39, n. 3, p. 291–300, 2014.

CADORE-RODRIGUES, A. et al. Stable Resin Bonding to Y-TZP Ceramic with Air Abrasion by Alumina Particles Containing 7% Silica. v. 22, n. 2, p. 149–159, 2020a.

CADORE-RODRIGUES, A. C. et al. Air-abrasion using new silica-alumina powders containing different silica concentrations: Effect on the microstructural characteristics and fatigue behavior of a Y-TZP ceramic. **Journal of the Mechanical Behavior of Biomedical Materials**, v. 98, n. May, p. 11–19, 2019.

CADORE-RODRIGUES, A. C. et al. Fatigue performance of fully-stabilized zirconia polycrystals monolithic restorations: The effects of surface treatments at the bonding surface. **Journal of the Mechanical Behavior of Biomedical Materials**, v. 110, n. April, 2020b.

CADORE-RODRIGUES, A. C. et al. Surface treatments and its effects on the fatigue behavior of a 5% mol yttria partially stabilized zirconia material. **Journal of the Mechanical Behavior of Biomedical Materials**, v. 120, n. April, 2021.

CARELLI, M.; ANTUNES, F. Can low-fusing glass application affect the marginal misfit and bond strength of Y-TZP crowns ? v. 32, p. 1–10, 2018.

CATTELL, M. J. et al. The development and testing of glaze materials for application to the fit surface of dental ceramic restorations. **Dental Materials**, v. 25, n. 4, p. 431–441, 2009.

CHEN, B. et al. Effects of tribochemical silica coating and alumina-particle air abrasion on 3Y-TZP and 5Y-TZP: Evaluation of surface hardness, roughness, bonding, and phase transformation. **Journal of Adhesive Dentistry**, v. 22, n. 4, p. 373–382, 2020.

CHINTAPALLI, R. K. et al. Phase transformation and subsurface damage in 3Y-TZP after sandblasting. **Dental Materials**, v. 29, n. 5, p. 566–572, 2013.

CHUN, E. P. et al. Microstructural analysis and reliability of monolithic zirconia after simulated adjustment protocols. **Dental Materials**, v. 33, n. 8, p. 934–943, 2017.

CORAZZA, P. H. et al. Influence of CAD-CAM diamond bur deterioration on surface roughness and maximum failure load of Y-TZP-based restorations. **American Journal of Dentistry**, v. 28, n. 2, p. 95–99, 2015.

CURA, C. et al. Comparison of alternative adhesive cementation concepts for zirconia ceramic: Glaze layer vs zirconia primer. **Journal of Adhesive Dentistry**, v. 14, n. 1, p. 75–82, 2012.

DA SILVA, L. H. et al. Dental ceramics: A review of new materials and processing methods. **Brazilian Oral Research**, v. 31, p. 133–146, 2017.

DE KOK, P. et al. The effect of internal roughness and bonding on the fracture resistance and structural reliability of lithium disilicate ceramic. **Dental Materials**, v. 33, n. 12, p. 1416–1425, 2017.

DE QUEIROZ, J. R. C. et al. Deposition of SiOx thin films on Y-TZP by reactive magnetron sputtering: Influence of plasma parameters on the adhesion properties between Y-TZP and resin cement for application in dental prosthesis. **Materials Research**, v. 14, n. 2, p. 212–216, 2011.

DELLA BONA, A. et al. Effect of surface treatments on the bond strength of a zirconia-reinforced ceramic to composite resin. **Brazilian oral research**, v. 21, n. 1, p. 10–15, 2007.

DENRY, I. How and when does fabrication damage adversely affect the clinical performance of ceramic restorations? **Dental Materials**, v. 29, n. 1, p. 85–96, 2013.

DENRY, I.; KELLY, J. Emerging Ceramic-based Materials for Dentistry. p. 1235–1242, 2014.

DENRY, I.; KELLY, J. R. State of the art of zirconia for dental applications. **Dental Materials**, v. 24, n. 3, p. 299–307, 2008.

DRUCK, C. C. et al. Adhesion to Y-TZP ceramic: Study of silica nanofilm coating on the surface of Y-TZP. **Journal of Biomedical Materials Research - Part B Applied Biomaterials**, v. 103, n. 1, p. 143–150, 2015.

DUARTE, D. A. et al. Titanium dioxide thin films deposition by direct current hollow cathode magnetron sputtering. v. 13107, 2010.

FRAGA, S. et al. Impact of machining on the flexural fatigue strength of glass and polycrystalline CAD/CAM ceramics. **Dental Materials**, v. 33, n. 11, p. 1286–1297, 2017.

GIORDANO, R. Materials for chairside CAD/CAM-produced restorations. **Journal of the American Dental Association**, v. 137, n. 9 SUPPL., p. 14S-21S, 2006.

GONZAGA, C. et al. Slow crack growth and reliability of dental ceramics. **Dental Materials**, v. 27, n. 4, p. 394–406, 2010.

GUAZZATO, M. et al. Influence of surface and heat treatments on the flexural strength of Y-TZP dental ceramic. **Journal of Dentistry**, v. 33, n. 1, p. 9–18, 2005.

GUILARDI, L. F. et al. Fatigue performance of distinct CAD/CAM dental ceramics. **Journal of the Mechanical Behavior of Biomedical Materials**, v. 103, n. October 2019, p. 103540, 2020.

HO, G. W.; MATINLINNA, J. P. Insights on Ceramics as Dental Materials . Part II : Chemical Surface Treatments. p. 117–123, 2011.

HONDRUM, S. O. A review of the strength properties of dental ceramics. **The Journal of Prosthetic Dentistry**, v. 67, n. 6, p. 859–865, 1992.

KARLSEN, C. Å.; SCHRIWER, C.; ØILO, M. Damage tolerance of six dental zirconias with different translucencies. **Biomaterial Investigations in Dentistry**, v. 7, n. 1, p. 126–133, 2020.

KELLY, J. R. et al. Fracture surface analysis of dental ceramics: clinically failed restorations. **The International journal of prosthodontics**, v. 3, n. 5, p. 430–40, 1990.

KELLY, J. R. et al. ADM guidance-ceramics: Fatigue principles and testing. **Dental Materials**, v. 33, n. 11, p. 1192–1204, 2017.

KERN, M.; WEGNER, S. M. Bonding to zirconia ceramic : adhesion methods and their durability.

v. 5641, n. 98, p. 64–71, 1998.

KITAYAMA, S. et al. Effect of an internal coating technique on tensile bond strengths of resin cements to zirconia ceramics. **Dental Materials Journal**, v. 28, n. 4, p. 446–453, 2009.

KONSTANTINIDIS, I. et al. Clinical outcomes of monolithic zirconia crowns with cad/cam technology. A 1-year follow-up prospective clinical study of 65 patients. **International Journal of Environmental Research and Public Health**, v. 15, n. 11, 2018.

KONTONASAKI, E.; GIASIMAKOPOULOS, P.; RIGOS, A. E. Strength and aging resistance of monolithic zirconia: an update to current knowledge. **Japanese Dental Science Review**, v. 56, n. 1, p. 1–23, 2020.

MIYAZAKI, T.; HOTTA, Y. CAD/CAM systems available for the fabrication of crown and bridge restorations. **Australian Dental Journal**, v. 56, n. SUPPL. 1, p. 97–106, 2011.

MOON, J. E. et al. Effects of airborne-particle abrasion protocol choice on the surface characteristics of monolithic zirconia materials and the shear bond strength of resin cement. **Ceramics International**, v. 42, n. 1, p. 1552–1562, 2016.

ÖZCAN, M.; BERNASCONI, M. Adhesion to Zirconia Used for Dental Restorations: A Systematic Review and Meta-Analysis. **Journal of Adhesive Dentistry**, v. 17, n. 1, p. 7–26, 2015.

OZCAN, M.; PFEIFFER, P.; NERGIZ, I. A brief history and current status of metal-and ceramic surface-conditioning concepts for resin bonding in dentistry. **Quintessence international (Berlin, Germany : 1985)**, v. 29, p. 713–724, 1998.

ÖZCAN, M.; VALLITTU, P. K. Effect of surface conditioning methods on the bond strength of luting cement to ceramics. **Dental Materials**, v. 19, n. 8, p. 725–731, 2003.

PEREIRA, G. K. R. et al. Mechanical reliability, fatigue strength and survival analysis of new polycrystalline translucent zirconia ceramics for monolithic restorations. **Journal of the Mechanical Behavior of Biomedical Materials**, v. 85, n. May, p. 57–65, 2018.

PEUTZFELDT, A.; ASMUSSEN, E. Silicoating : evaluation of a new method of bonding composite resin to metal. n. 2, 1988.

PICONI, C.; MACCAURO, G. Zirconia as a ceramic biomaterial. **Biomaterials**, v. 20, n. 1, p. 1–25, 1999.

POZZOBON, J. L. et al. Mechanical behavior of yttria-stabilized tetragonal zirconia polycrystalline ceramic after different zirconia surface treatments. **Materials Science and Engineering C**, v. 77, p. 828–835, 2017.

PROCHNOW, C. et al. Hydrofluoric acid concentrations: Effect on the cyclic load to failure of machined lithium disilicate restorations. **Dental Materials**, v. 34, n. 9, p. e255–e263, 2018.

REKOW, D.; THOMPSON, V. P. Near-surface damage - A persistent problem in crowns obtained by computer-aided design and manufacturing. **Proceedings of the Institution of Mechanical Engineers, Part H: Journal of Engineering in Medicine**, v. 219, n. 4, p. 233–243, 2005.

RITZBERGER, C. et al. Properties and clinical application of three types of dental glass-ceramics and ceramics for CAD-CAM technologies. **Materials**, v. 3, n. 6, p. 3700–3713, 2010.

SAILER, I. et al. All-ceramic or metal-ceramic tooth-supported fixed dental prostheses (FDPs)? A systematic review of the survival and complication rates. Part I: Single crowns (SCs). **Dental Materials**, v. 31, n. 6, p. 603–623, 2015.

SCHERRER, S. S. et al. ADM guidance—Ceramics: guidance to the use of fractography in failure analysis of brittle materials. **Dental Materials**, v. 33, n. 6, p. 599–620, 2017.

SINDEL, J. et al. Evaluation of subsurface damage in CAD / CAM machined dental ceramics. **J Mater Sci Mater Med**, v. 9, p. 291–295, 1998.

SPAZZIN, A. O. et al. Strengthening of porcelain provided by resin cements and flowable composites. **Operative Dentistry**, v. 41, n. 2, p. 179–188, 2016.

SPAZZIN, A. O. et al. Ceramic strengthening by tuning the elastic moduli of resin-based luting agents. **Dental Materials**, v. 33, n. 3, p. 358–366, 2017.

STAWARCZYK, B. et al. Three generations of zirconia: From veneered to monolithic. Part I. **Quintessence international (Berlin, Germany : 1985)**, v. 48, n. 5, p. 369–380, 2017.

SULAIMAN, T. A. et al. Effect of different treatments on the flexural strength of fully versus partially stabilized monolithic zirconia. **Journal of Prosthetic Dentistry**, v. 118, n. 2, p. 216–220, 2017.

SULAIMAN, T. A. Materials in digital dentistry—A review. **Journal of Esthetic and Restorative Dentistry**, v. 32, n. 2, p. 171–181, 2020.

THOMPSON, J. Y. et al. Fracture Surface Characterization of Clinically Failed All-ceramic Crowns. **Journal of Dental Research**, v. 73, n. 12, p. 1824–1832, 1994.

VANDERLEI, A.; BOTTINO, M. A.; VALANDRO, L. F. Evaluation of resin bond strength to yttriastabilized tetragonal zirconia and framework marginal fit: Comparison of different surface conditionings. **Operative Dentistry**, v. 39, n. 1, p. 50–63, 2014.

WANG, H.; ABOUSHELIB, M. N.; FEILZER, A. J. Strength influencing variables on CAD/CAM zirconia frameworks. **Dental Materials**, v. 24, n. 5, p. 633–638, 2008.

WEGNER, S. M. et al. Effect of Different Artificial Aging Conditions on Ceramic- Composite Bond Strength. **The International Journal of Prosthodontics**, v. 15, n. 3, 2002.

WISKOTT, H. W.; NICHOLLS, J. I.; BELSER, U. C. Stress fatigue: basic principles and prosthodontic implications. **The International journal of prosthodontics**, v. 8, n. 2, p. 105–16, 1995.

ZARONE, F.; RUSSO, S.; SORRENTINO, R. From porcelain-fused-to-metal to zirconia: Clinical and experimental considerations. **Dental Materials**, v. 27, n. 1, p. 83–96, 2011.

ZHANG, G. .; SATISH, K. .; KO, W. . **The mechanics of material removal mechanisms in the machining of ceramics**. [s.l.] Institute for Systems Research, 1994.

ZHANG, Y. et al. Damage accumulation and fatigue life of particle-abraded ceramics. **The International journal of prosthodontics**, v. 19, n. 5, p. 442–8, 2006.

ZUCUNI, C. P. et al. CAD/CAM machining Vs pre-sintering in-lab fabrication techniques of Y-TZP ceramic specimens: Effects on their mechanical fatigue behavior. **Journal of the Mechanical Behavior of Biomedical Materials**, v. 71, p. 201–208, 2017a.

ZUCUNI, C. P. et al. Fatigue strength of yttria-stabilized zirconia polycrystals: Effects of grinding, polishing, glazing, and heat treatment. **Journal of the Mechanical Behavior of Biomedical Materials**, v. 75, n. May, p. 512–520, 2017b.

ZUCUNI, C. P. et al. Low-fusing porcelain glaze application does not damage the fatigue strength of Y-TZP. **Journal of the Mechanical Behavior of Biomedical Materials**, v. 99, n. July, p. 198–205, 2019.

ANEXO A – NORMAS PARA PUBLICAÇÃO NO PERIÓDICO JOURNAL OF THE MECHANICAL BEHAVIOR OF BIOMEDICAL MATERIALS

GUIDE FOR AUTHORS
We now differentiate between the requirements for new and revised submissions. You may choose to submit your manuscript as a single Word or PDF file to be used in the refereeing process. Only when your paper is at the revision stage, will you be requested to put your paper in to a 'correct format' for acceptance and provide the items required for the publication of your article.
To find out more, please visit the Preparation section below.
Authors are requested to submit a cover letter that clearly states the novelty of the work presented in their manuscript.

Types of Contributions

Research Paper: A full-length article describing original research. There is no limit on the number of words, figures etc but authors should be as succinct as possible.

Review Article: An article which reviews previous work in a given field. Reviews are written by invitation only but the editor would welcome suggestions.

Technical Note: A short article describing a new experimental technique or analytical approach.

Short Communication: An article presenting new work in reduced form, which for some reason is not suitable for a full research paper. For example a case study.

Opinion Piece: A short article presenting the author's opinion on a particular question. Normally shorter and less comprehensive than a review article, making use of published and/or unpublished results.

Tutorial: An article of an educational nature, explaining how to use a particular experimental technique or analytical method. Normally written by invitation only but the editor welcomes suggestions.

Please ensure that you select the appropriate article type from the list of options when making your submission. Authors contributing to special issues should ensure that they select the special issue article type from this list.

The journal also accepts letters, which should be sent directly to the editor in chief for consideration.

Submission checklist

You can use this list to carry out a final check of your submission before you send it to the journal for review. Please check the relevant section in this Guide for Authors for more details.

Ensure that the following items are present:

One author has been designated as the corresponding author with contact details:
• E-mail address
• Full postal address

All necessary files have been uploaded:
Manuscript:
• Include keywords
• All figures (include relevant captions)
• All tables (including titles, description, footnotes)
• Ensure all figure and table citations in the text match the files provided
• Indicate clearly if color should be used for any figures in print
Graphical Abstracts / Highlights files (where applicable)
Supplemental files (where applicable)

Further considerations
• Manuscript has been 'spell checked' and 'grammar checked'
• All references mentioned in the Reference List are cited in the text, and vice versa
• Permission has been obtained for use of copyrighted material from other sources (including the Internet)
• A competing interests statement is provided, even if the authors have no competing interests to declare
• Journal policies detailed in this guide have been reviewed
• Referee suggestions and contact details provided, based on journal requirements

For further information, visit our Support Center.

Ethics in publishing

Please see our information on Ethics in publishing.

Declaration of competing interest

All authors must disclose any financial and personal relationships with other people or organizations that could inappropriately influence (bias) their work. Examples of potential conflicts of interest include employment, consultancies, stock ownership, honoraria, paid expert testimony, patent applications/registrations, and grants or other funding. Authors should complete the declaration of competing interest statement using this template and upload to the submission system at the Attach/Upload Files step. Note: Please do not convert the .docx template to another file type. Author signatures are not required. If there are no interests to declare, please choose the first option in the template. More information.

Submission declaration and verification

Submission of an article implies that the work described has not been published previously (except in the form of an abstract, a published lecture or academic thesis, see 'Multiple, redundant or concurrent publication' for more information), that it is not under consideration for publication elsewhere, that its publication is approved by all authors and tacitly or explicitly by the responsible authorities where the work was carried out, and that, if accepted, it will not be published elsewhere in the same form, in English or in any other language, including electronically without the written consent of the copyright-holder. To verify originality, your article may be checked by the originality detection service Crossref Similarity Check.

Preprints
Please note that preprints can be shared anywhere at any time, in line with Elsevier's sharing policy. Sharing your preprints e.g. on a preprint server will not count as prior publication (see 'Multiple, redundant or concurrent publication' for more information).

Preprint posting on SSRN

In support of Open Science, this journal offers its authors a free preprint posting service. Preprints provide early registration and dissemination of your research, which facilitates early citations and collaboration.

During submission to Editorial Manager, you can choose to release your manuscript publicly as a preprint on the preprint server SSRN once it enters peer-review with the journal. Your choice will have no effect on the editorial process or outcome with the journal. Please note that the corresponding author is expected to seek approval from all co-authors before agreeing to release the manuscript publicly on SSRN.

You will be notified via email when your preprint is posted online and a Digital Object Identifier (DOI) is assigned. Your preprint will remain globally available free to read whether the journal accepts or rejects your manuscript.

For more information about posting to SSRN, please consult the SSRN Terms of Use and FAQs.

Use of inclusive language

Inclusive language acknowledges diversity, conveys respect to all people, is sensitive to differences, and promotes equal opportunities. Content should make no assumptions about the beliefs or commitments of any reader; contain nothing which might imply that one individual is superior to another on the grounds of age, gender, race, ethnicity, culture, sexual orientation, disability or health condition; and use inclusive language throughout. Authors should ensure that writing is free from bias, stereotypes, slang, reference to dominant culture and/or cultural assumptions. We advise to seek gender neutrality by using plural nouns ("clinicians, patients/clients") as default/wherever possible to avoid using "he, she," or "he/she." We recommend avoiding the use of descriptors that refer to personal attributes such as age, gender, race, ethnicity, culture, sexual orientation, disability or health condition unless they are relevant and valid. When coding terminology is used, we recommend to avoid offensive or exclusionary terms such as "master", "slave", "blacklist" and "whitelist". We suggest using alternatives that are more appropriate and (self-) explanatory such as "primary", "secondary", "blocklist" and "allowlist". These guidelines are meant as a point of reference to help identify appropriate language but are by no means exhaustive or definitive.

Author contributions

For transparency, we encourage authors to submit an author statement file outlining their individual contributions to the paper using the relevant CRediT roles: Conceptualization; Data curation; Formal analysis; Funding acquisition; Investigation; Methodology; Project administration; Resources; Software; Supervision; Validation; Visualization; Roles/Writing - original draft; Writing - review & editing. Authorship statements should be formatted with the names of authors first and CRediT role(s) following. More details and an example.

Changes to authorship

Authors are expected to consider carefully the list and order of authors before submitting their manuscript and provide the definitive list of authors at the time of the original submission. Any addition, deletion or rearrangement of author names in the authorship list should be made only before the manuscript has been accepted and only if approved by the journal Editor. To request such a change, the Editor must receive the following from the corresponding author: (a) the reason for the change in author list and (b) written confirmation (e-mail, letter) from all authors that they agree with the addition, removal or rearrangement. In the case of addition or removal of authors, this includes confirmation from the author being added or removed.

Only in exceptional circumstances will the Editor consider the addition, deletion or rearrangement of authors after the manuscript has been accepted. While the Editor considers the request, publication of the manuscript will be suspended. If the manuscript has already been published in an online issue, any requests approved by the Editor will result in a corrigendum.

Copyright

Upon acceptance of an article, authors will be asked to complete a 'Journal Publishing Agreement' (see more information on this). An e-mail will be sent to the corresponding author confirming receipt of the manuscript together with a 'Journal Publishing Agreement' form or a link to the online version of this agreement.

Subscribers may reproduce tables of contents or prepare lists of articles including abstracts for internal circulation within their institutions. Permission of the Publisher is required for resale or distribution outside the institution and for all other derivative works, including compilations and translations. If excerpts from other copyrighted works are included, the author(s) must obtain written permission from the copyright owners and credit the source(s) in the article. Elsevier has preprinted forms for use by authors in these cases.

For gold open access articles: Upon acceptance of an article, authors will be asked to complete a 'License Agreement' (more information). Permitted third party reuse of gold open access articles is determined by the author's choice of user license.

Author rights
As an author you (or your employer or institution) have certain rights to reuse your work. More information.

Elsevier supports responsible sharing
Find out how you can share your research published in Elsevier journals.

Role of the funding source

You are requested to identify who provided financial support for the conduct of the research and/or preparation of the article and to briefly describe the role of the sponsor(s), if any, in study design; in the collection, analysis and interpretation of data; in the writing of the report; and in the decision to submit the article for publication. If the funding source(s) had no such involvement, it is recommended to state this.

Open access

Please visit our Open Access page for more information.

Elsevier Researcher Academy
Researcher Academy is a free e-learning platform designed to support early and mid-career researchers throughout their research journey. The "Learn" environment at Researcher Academy offers several interactive modules, webinars, downloadable guides and resources to guide you through the process of writing for research and going through peer review. Feel free to use these free resources to improve your submission and navigate the publication process with ease.

Language (usage and editing services)
Please write your text in good English (American or British usage is accepted, but not a mixture of these). Authors who feel their English language manuscript may require editing to eliminate possible grammatical or spelling errors and to conform to correct scientific English may wish to use the English Language Editing service available from Elsevier's Author Services.

Submission

Our online submission system guides you stepwise through the process of entering your article details and uploading your files. The system converts your article files to a single PDF file used in the peer-review process. Editable files (e.g., Word, LaTeX) are required to typeset your article for final publication. All correspondence, including notification of the Editor's decision and requests for revision, is sent by e-mail.

Queries

For questions about the editorial process (including the status of manuscripts under review) or for technical support on submissions, please visit our Support Center.

NEW SUBMISSIONS

Submission to this journal proceeds totally online and you will be guided stepwise through the creation and uploading of your files. The system automatically converts your files to a single PDF file, which is used in the peer-review process.
As part of the Your Paper Your Way service, you may choose to submit your manuscript as a single file to be used in the refereeing process. This can be a PDF file or a Word document, in any format or lay-out that can be used by referees to evaluate your manuscript. It should contain high enough quality figures for refereeing. If you prefer to do so, you may still provide all or some of the source files at the initial submission. Please note that individual figure files larger than 10 MB must be uploaded separately.

References

There are no strict requirements on reference formatting at submission. References can be in any style or format as long as the style is consistent. Where applicable, author(s) name(s), journal title/book title, chapter title/article title, year of publication, volume number/book chapter and the article number or pagination must be present. Use of DOI is highly encouraged. The reference style used by the journal will be applied to the accepted article by Elsevier at the proof stage. Note that missing data will be highlighted at proof stage for the author to correct.

Formatting requirements
There are no strict formatting requirements but all manuscripts must contain the essential elements needed to convey your manuscript, for example Abstract, Keywords, Introduction, Materials and Methods, Results, Conclusions, Artwork and Tables with Captions.
If your article includes any Videos and/or other Supplementary material, this should be included in your initial submission for peer review purposes.
Divide the article into clearly defined sections.

Figures and tables embedded in text
Please ensure the figures and the tables included in the single file are placed next to the relevant text in the manuscript, rather than at the bottom or the top of the file. The corresponding caption should be placed directly below the figure or table.

Peer review

This journal operates a single anonymized review process. All contributions will be initially assessed by the editor for suitability for the journal. Papers deemed suitable are then typically sent to a minimum of two independent expert reviewers to assess the scientific quality of the paper. The Editor is responsible for the final decision regarding acceptance or rejection of articles. The Editor's decision is final. Editors are not involved in decisions about papers which they have written themselves or have been written by family members or colleagues or which relate to products or services in which the editor has an interest. Any such submission is subject to all of the journal's usual procedures, with peer review handled independently of the relevant editor and their research groups. More information on types of peer review.

REVISED SUBMISSIONS

Use of word processing software
Regardless of the file format of the original submission, at revision you must provide us with an editable file of the entire article. Keep the layout of the text as simple as possible. Most formatting codes will be removed and replaced on processing the article. The electronic text should be prepared in a way very similar to that of conventional manuscripts (see also the Guide to Publishing with Elsevier). See also the section on Electronic artwork.
To avoid unnecessary errors you are strongly advised to use the 'spell-check' and 'grammar-check' functions of your word processor.

LaTeX
You are recommended to use the Elsevier article class elsarticle.cls to prepare your manuscript and BibTeX to generate your bibliography.
Our LaTeX site has detailed submission instructions, templates and other information.

Article structure

Subdivision - numbered sections
Divide your article into clearly defined and numbered sections. Subsections should be numbered 1.1 (then 1.1.1, 1.1.2, ...), 1.2, etc. (the abstract is not included in section numbering). Use this numbering also for internal cross-referencing: do not just refer to 'the text'. Any subsection may be given a brief heading. Each heading should appear on its own separate line.

Introduction
State the objectives of the work and provide an adequate background, avoiding a detailed literature survey or a summary of the results.

Material and methods
Provide sufficient details to allow the work to be reproduced by an independent researcher. Methods that are already published should be summarized, and indicated by a reference. If quoting directly from a previously published method, use quotation marks and also cite the source. Any modifications to existing methods should also be described.

Theory/calculation
A Theory section should extend, not repeat, the background to the article already dealt with in the Introduction and lay the foundation for further work. In contrast, a Calculation section represents a practical development from a theoretical basis.

Results
Results should be clear and concise.

Discussion
This should explore the significance of the results of the work, not repeat them. A combined Results and Discussion section is often appropriate. Avoid extensive citations and discussion of published literature.

Conclusions

The main conclusions of the study may be presented in a short Conclusions section, which may stand alone or form a subsection of a Discussion or Results and Discussion section.

Appendices
If there is more than one appendix, they should be identified as A, B, etc. Formulae and equations in appendices should be given separate numbering: Eq. (A.1), Eq. (A.2), etc.; in a subsequent appendix, Eq. (B.1) and so on. Similarly for tables and figures: Table A.1; Fig. A.1, etc.

Essential title page information

• Title. Concise and informative. Titles are often used in information-retrieval systems. Avoid abbreviations and formulae where possible.
• Author names and affiliations. Please clearly indicate the given name(s) and family name(s) of each author and check that all names are accurately spelled. You can add your name between parentheses in your own script behind the English transliteration. Present the authors' affiliation addresses (where the actual work was done) below the names. Indicate all affiliations with a lower-case superscript letter immediately after the author's name and in front of the appropriate address. Provide the full postal address of each affiliation, including the country name and, if available, the e-mail address of each author.
• Corresponding author. Clearly indicate who will handle correspondence at all stages of refereeing and publication, also post-publication. This responsibility includes answering any future queries about Methodology and Materials. Ensure that the e-mail address is given and that contact details are kept up to date by the corresponding author.
• Present/permanent address. If an author has moved since the work described in the article was done, or was visiting at the time, a 'Present address' (or 'Permanent address') may be indicated as a footnote to that author's name. The address at which the author actually did the work must be retained as the main, affiliation address. Superscript Arabic numerals are used for such footnotes.

Highlights

Highlights are mandatory for this journal as they help increase the discoverability of your article via search engines. They consist of a short collection of bullet points that capture the novel results of your research as well as new methods that were used during the study (if any). Please have a look at the examples here: example Highlights.

Highlights should be submitted in a separate editable file in the online submission system. Please use 'Highlights' in the file name and include 3 to 5 bullet points (maximum 85 characters, including spaces, per bullet point).

Abstract

A concise and factual abstract is required. The abstract should state briefly the purpose of the research, the principal results and major conclusions. An abstract is often presented separately from the article, so it must be able to stand alone. For this reason, References should be avoided, but if essential, then cite the author(s) and year(s). Also, non-standard or uncommon abbreviations should be avoided, but if essential they must be defined at their first mention in the abstract itself.

Graphical abstract
A graphical abstract is mandatory for this journal. It should summarize the contents of the article in a concise, pictorial form designed to capture the attention of a wide readership online. Authors must provide images that clearly represent the work described in the article. Graphical abstracts should be submitted as a separate file in the online submission system. Image size: please provide an image with a minimum of 531 × 1328 pixels (h × w) or proportionally more. The image should be readable at a size of 5 × 13 cm using a regular screen resolution of 96 dpi. Preferred file types: TIFF, EPS, PDF or MS Office files. You can view Example Graphical Abstracts on our information site.
Authors can make use of Elsevier's Illustration Services to ensure the best presentation of their images also in accordance with all technical requirements.

Abbreviations
Define abbreviations that are not standard in this field in a footnote to be placed on the first page of the article. Such abbreviations that are unavoidable in the abstract must be defined at their first mention there, as well as in the footnote. Ensure consistency of abbreviations throughout the article.

Acknowledgements
Collate acknowledgements in a separate section at the end of the article before the references and do not, therefore, include them on the title page, as a footnote to the title or otherwise. List here those individuals who provided help during the research (e.g., providing language help, writing assistance or proof reading the article, etc.).

Formatting of funding sources
List funding sources in this standard way to facilitate compliance to funder's requirements:

Funding: This work was supported by the National Institutes of Health [grant numbers xxxx, yyyy]; the Bill & Melinda Gates Foundation, Seattle, WA [grant number zzzz]; and the United States Institutes of Peace [grant number aaaa].

It is not necessary to include detailed descriptions on the program or type of grants and awards. When funding is from a block grant or other resources available to a university, college, or other research institution, submit the name of the institute or organization that provided the funding.

If no funding has been provided for the research, it is recommended to include the following sentence:

This research did not receive any specific grant from funding agencies in the public, commercial, or not-for-profit sectors.

Units

Follow internationally accepted rules and conventions: use the international system of units (SI). If other quantities are mentioned, give their equivalent in SI. Authors wishing to present a table of nomenclature should do so on the second page of their manuscript.

Math formulae
Please submit math equations as editable text and not as images. Present simple formulae in line with normal text where possible and use the solidus (/) instead of a horizontal line for small fractional terms, e.g., X/Y. In principle, variables are to be presented in italics. Powers of e are often more conveniently denoted by exp. Number consecutively any equations that have to be displayed separately from the text (if referred to explicitly in the text).

Footnotes
Footnotes should be used sparingly. Number them consecutively throughout the article. Many word processors build footnotes into the text, and this feature may be used. Should this not be the case, indicate the position of footnotes in the text and present the footnotes themselves separately at the end of the article.

Artwork

Electronic artwork
General points
• Make sure you use uniform lettering and sizing of your original artwork.
• Preferred fonts: Arial (or Helvetica), Times New Roman (or Times), Symbol, Courier.
• Number the illustrations according to their sequence in the text.
• Use a logical naming convention for your artwork files.
• Indicate per figure if it is a single, 1.5 or 2-column fitting image.
• For Word submissions only, you may still provide figures and their captions, and tables within a single file at the revision stage.
• Please note that individual figure files larger than 10 MB must be provided in separate source files.

A detailed guide on electronic artwork is available.
You are urged to visit this site; some excerpts from the detailed information are given here.
Formats
Regardless of the application used, when your electronic artwork is finalized, please 'save as' or convert the images to one of the following formats (note the resolution requirements for line drawings, halftones, and line/halftone combinations given below):
EPS (or PDF): Vector drawings. Embed the font or save the text as 'graphics'.
TIFF (or JPG): Color or grayscale photographs (halftones): always use a minimum of 300 dpi.
TIFF (or JPG): Bitmapped line drawings: use a minimum of 1000 dpi.
TIFF (or JPG): Combinations bitmapped line/half-tone (color or grayscale): a minimum of 500 dpi is required.
Please do not:
• Supply files that are optimized for screen use (e.g., GIF, BMP, PICT, WPG); the resolution is too low.
• Supply files that are too low in resolution.
• Submit graphics that are disproportionately large for the content.

Color artwork
Please make sure that artwork files are in an acceptable format (TIFF (or JPEG), EPS (or PDF) or MS Office files) and with the correct resolution. If, together with your accepted article, you submit usable color figures then Elsevier will ensure, at no additional charge, that these figures will appear in color online (e.g., ScienceDirect and other sites) in addition to color reproduction in print. Further information on the preparation of electronic artwork.

Figure captions
Ensure that each illustration has a caption. A caption should comprise a brief title (not on the figure itself) and a description of the illustration. Keep text in the illustrations themselves to a minimum but explain all symbols and abbreviations used.

Tables

Please submit tables as editable text and not as images. Tables can be placed either next to the relevant text in the article, or on separate page(s) at the end. Number tables consecutively in accordance with their appearance in the text and place any table notes below the table body. Be sparing in the use of tables and ensure that the data presented in them do not duplicate results described elsewhere in the article. Please avoid using vertical rules and shading in table cells.

References

Citation in text
Please ensure that every reference cited in the text is also present in the reference list (and vice versa). Any references cited in the abstract must be given in full. Unpublished results and personal communications are not recommended in the reference list, but may

be mentioned in the text. If these references are included in the reference list they should follow the standard reference style of the journal and should include a substitution of the publication date with either 'Unpublished results' or 'Personal communication'. Citation of a reference as 'in press' implies that the item has been accepted for publication.

Reference links
Increased discoverability of research and high quality peer review are ensured by online links to the sources cited. In order to allow us to create links to abstracting and indexing services, such as Scopus, CrossRef and PubMed, please ensure that data provided in the references are correct. Please note that incorrect surnames, journal/book titles, publication year and pagination may prevent link creation. When copying references, please be careful as they may already contain errors. Use of the DOI is highly encouraged.

A DOI is guaranteed never to change, so you can use it as a permanent link to any electronic article. An example of a citation using DOI for an article not yet in an issue is: VanDecar J.C., Russo R.M., James D.E., Ambeh W.B., Franke M. (2003). Aseismic continuation of the Lesser Antilles slab beneath northeastern Venezuela. Journal of Geophysical Research, https://doi.org/10.1029/2001JB000884. Please note the format of such citations should be in the same style as all other references in the paper.

Web references
As a minimum, the full URL should be given and the date when the reference was last accessed. Any further information, if known (DOI, author names, dates, reference to a source publication, etc.), should also be given. Web references can be listed separately (e.g., after the reference list) under a different heading if desired, or can be included in the reference list.

Data references
This journal encourages you to cite underlying or relevant datasets in your manuscript by citing them in your text and including a data reference in your Reference List. Data references should include the following elements: author name(s), dataset title, data repository, version (where available), year, and global persistent identifier. Add [dataset] immediately before the reference so we can properly identify it as a data reference. The [dataset] identifier will not appear in your published article.

Preprint references
Where a preprint has subsequently become available as a peer-reviewed publication, the formal publication should be used as the reference. If there are preprints that are central to your work or that cover crucial developments in the topic, but are not yet formally published, these may be referenced. Preprints should be clearly marked as such, for example by including the word preprint, or the name of the preprint server, as part of the reference. The preprint DOI should also be provided.

References in a special issue
Please ensure that the words 'this issue' are added to any references in the list (and any citations in the text) to other articles in the same Special Issue.

Reference management software
Most Elsevier journals have their reference template available in many of the most popular reference management software products. These include all products that support Citation Style Language styles, such as Mendeley. Using citation plug-ins from these products, authors only need to select the appropriate journal template when preparing their article, after which citations and bibliographies will be automatically formatted in the journal's style. If no template is yet available for this journal, please follow the format of the sample references and citations as shown in this Guide. If you use reference management software, please ensure that you remove all field codes before submitting the electronic manuscript. More information on how to remove field codes from different reference management software.

Reference formatting
There are no strict requirements on reference formatting at submission. References can be in any style or format as long as the style is consistent. Where applicable, author(s) name(s), journal title/book title, chapter title/article title, year of publication, volume number/book chapter and the article number or pagination must be present. Use of DOI is highly encouraged. The reference style used by the journal will be applied to the accepted article by Elsevier at the proof stage. Note that missing data will be highlighted at proof stage for the author to correct. If you do wish to format the references yourself they should be arranged according to the following examples:

Reference style
Text: All citations in the text should refer to:
1. Single author: the author's name (without initials, unless there is ambiguity) and the year of publication;
2. Two authors: both authors' names and the year of publication;
3. Three or more authors: first author's name followed by 'et al.' and the year of publication.
Citations may be made directly (or parenthetically). Groups of references can be listed either first alphabetically, then chronologically, or vice versa.
Examples: 'as demonstrated (Allan, 2000a, 2000b, 1999; Allan and Jones, 1999)…. Or, as demonstrated (Jones, 1999; Allan, 2000)… Kramer et al. (2010) have recently shown …'
List: References should be arranged first alphabetically and then further sorted chronologically if necessary. More than one reference from the same author(s) in the same year must be identified by the letters 'a', 'b', 'c', etc., placed after the year of publication.
Examples:
Reference to a journal publication:
Van der Geer, J., Hanraads, J.A.J., Lupton, R.A., 2010. The art of writing a scientific article. J. Sci. Commun. 163, 51–59. https://doi.org/10.1016/j.Sc.2010.00372.

Reference to a journal publication with an article number:
Van der Geer, J., Hanraads, J.A.J., Lupton, R.A., 2018. The art of writing a scientific article. Heliyon. 19, e00205. https://doi.org/10.1016/j.heliyon.2018.e00205.
Reference to a book:
Strunk Jr., W., White, E.B., 2000. The Elements of Style, fourth ed. Longman, New York.
Reference to a chapter in an edited book:
Mettam, G.R., Adams, L.B., 2009. How to prepare an electronic version of your article, in: Jones, B.S., Smith , R.Z. (Eds.), Introduction to the Electronic Age. E-Publishing Inc., New York, pp. 281–304.
Reference to a website:
Cancer Research UK, 1975. Cancer statistics reports for the UK. http://www.cancerresearchuk.org/aboutcancer/statistics/cancerstatsreport/ (accessed 13 March 2003).
Reference to a dataset:
[dataset] Oguro, M., Imahiro, S., Saito, S., Nakashizuka, T., 2015. Mortality data for Japanese oak wilt disease and surrounding forest compositions. Mendeley Data, v1. https://doi.org/10.17632/xwj98nb39r.1.
Reference to software:
Coon, E., Berndt, M., Jan, A., Svyatsky, D., Atchley, A., Kikinzon, E., Harp, D., Manzini, G., Shelef, E., Lipnikov, K., Garimella, R., Xu, C., Moulton, D., Karra, S., Painter, S., Jafarov, E., & Molins, S., 2020. Advanced Terrestrial Simulator (ATS) v0.88 (Version 0.88). Zenodo. https://doi.org/10.5281/zenodo.3727209.

Journal abbreviations source
Journal names should be abbreviated according to the List of Title Word Abbreviations.

Video

Elsevier accepts video material and animation sequences to support and enhance your scientific research. Authors who have video or animation files that they wish to submit with their article are strongly encouraged to include links to these within the body of the article. This can be done in the same way as a figure or table by referring to the video or animation content and noting in the body text where it should be placed. All submitted files should be properly labeled so that they directly relate to the video file's content. In order to ensure that your video or animation material is directly usable, please provide the file in one of our recommended file formats with a preferred maximum size of 150 MB per file, 1 GB in total. Video and animation files supplied will be published online in the electronic version of your article in Elsevier Web products, including ScienceDirect. Please supply 'stills' with your files: you can choose any frame from the video or animation or make a separate image. These will be used instead of standard icons and will personalize the link to your video data. For more detailed instructions please visit our video instruction pages. Note: since video and animation cannot be embedded in the print version of the journal, please provide text for both the electronic and the print version for the portions of the article that refer to this content.

Data visualization

Include interactive data visualizations in your publication and let your readers interact and engage more closely with your research. Follow the instructions here to find out about available data visualization options and how to include them with your article.

Supplementary material

Supplementary material such as applications, images and sound clips, can be published with your article to enhance it. Submitted supplementary items are published exactly as they are received (Excel or PowerPoint files will appear as such online). Please submit your material together with the article and supply a concise, descriptive caption for each supplementary file. If you wish to make changes to supplementary material during any stage of the process, please make sure to provide an updated file. Do not annotate any corrections on a previous version. Please switch off the 'Track Changes' option in Microsoft Office files as these will appear in the published version.

Research data

This journal encourages and enables you to share data that supports your research publication where appropriate, and enables you to interlink the data with your published articles. Research data refers to the results of observations or experimentation that validate research findings. To facilitate reproducibility and data reuse, this journal also encourages you to share your software, code, models, algorithms, protocols, methods and other useful materials related to the project.

Below are a number of ways in which you can associate data with your article or make a statement about the availability of your data when submitting your manuscript. If you are sharing data in one of these ways, you are encouraged to cite the data in your manuscript and reference list. Please refer to the "References" section for more information about data citation. For more information on depositing, sharing and using research data and other relevant research materials, visit the research data page.

Data linking
If you have made your research data available in a data repository, you can link your article directly to the dataset. Elsevier collaborates with a number of repositories to link articles on ScienceDirect with relevant repositories, giving readers access to underlying data that gives them a better understanding of the research described.

There are different ways to link your datasets to your article. When available, you can directly link your dataset to your article by providing the relevant information in the submission system. For more information, visit the database linking page.

For supported data repositories a repository banner will automatically appear next to your published article on ScienceDirect.

In addition, you can link to relevant data or entities through identifiers within the text of your manuscript, using the following format: Database: xxxx (e.g., TAIR: AT1G01020; CCDC: 734053; PDB: 1XFN).

Mendeley Data

This journal supports Mendeley Data, enabling you to deposit any research data (including raw and processed data, video, code, software, algorithms, protocols, and methods) associated with your manuscript in a free-to-use, open access repository. During the submission process, after uploading your manuscript, you will have the opportunity to upload your relevant datasets directly to Mendeley Data. The datasets will be listed and directly accessible to readers next to your published article online.

For more information, visit the Mendeley Data for journals page.

Data in Brief

You have the option of converting any or all parts of your supplementary or additional raw data into a data article published in Data in Brief. A data article is a new kind of article that ensures that your data are actively reviewed, curated, formatted, indexed, given a DOI and made publicly available to all upon publication (watch this video describing the benefits of publishing your data in Data in Brief). You are encouraged to submit your data article for Data in Brief as an additional item directly alongside the revised version of your manuscript. If your research article is accepted, your data article will automatically be transferred over to Data in Brief where it will be editorially reviewed, published open access and linked to your research article on ScienceDirect. Please note an open access fee is payable for publication in Data in Brief. Full details can be found on the Data in Brief website. Please use this template to write your Data in Brief data article.

MethodsX

You have the option of converting relevant protocols and methods into one or multiple MethodsX articles, a new kind of article that describes the details of customized research methods. Many researchers spend a significant amount of time on developing methods to fit their specific needs or setting, but often without getting credit for this part of their work. MethodsX, an open access journal, now publishes this information in order to make it searchable, peer reviewed, citable and reproducible. Authors are encouraged to submit their MethodsX article as an additional item directly alongside the revised version of their manuscript. If your research article is accepted, your methods article will automatically be transferred over to MethodsX where it will be editorially reviewed. Please note an open access fee is payable for publication in MethodsX. Full details can be found on the MethodsX website. Please use the methods template or protocol template to prepare your MethodsX article.

Data statement

To foster transparency, we encourage you to state the availability of your data in your submission. This may be a requirement of your funding body or institution. If your data is unavailable to access or unsuitable to post, you will have the opportunity to indicate why during the submission process, for example by stating that the research data is confidential. The statement will appear with your published article on ScienceDirect. For more information, visit the Data Statement page.

Online proof correction

To ensure a fast publication process of the article, we kindly ask authors to provide us with their proof corrections within two days. Corresponding authors will receive an e-mail with a link to our online proofing system, allowing annotation and correction of proofs online. The environment is similar to MS Word: in addition to editing text, you can also comment on figures/tables and answer questions from the Copy Editor. Web-based proofing provides a faster and less error-prone process by allowing you to directly type your corrections, eliminating the potential introduction of errors.

If preferred, you can still choose to annotate and upload your edits on the PDF version. All instructions for proofing will be given in the e-mail we send to authors, including alternative methods to the online version and PDF.

We will do everything possible to get your article published quickly and accurately. Please use this proof only for checking the typesetting, editing, completeness and correctness of the text, tables and figures. Significant changes to the article as accepted for publication will only be considered at this stage with permission from the Editor. It is important to ensure that all corrections are sent back to us in one communication. Please check carefully before replying, as inclusion of any subsequent corrections cannot be guaranteed. Proofreading is solely your responsibility.

Offprints

The corresponding author will, at no cost, receive a customized Share Link providing 50 days free access to the final published version of the article on ScienceDirect. The Share Link can be used for sharing the article via any communication channel, including email and social media. For an extra charge, paper offprints can be ordered via the offprint order form which is sent once the article is accepted for publication. Both corresponding and co-authors may order offprints at any time via Elsevier's Author Services. Corresponding authors who have published their article gold open access do not receive a Share Link as their final published version of the article is available open access on ScienceDirect and can be shared through the article DOI link.